Title
Development and Application of Technologies to Study Individual Kinase Substrate Relationships

Author
Allen, Jasmina Josie

Publication Date
2008-09-15

Peer reviewed|Thesis/dissertation

Development and Application of Technologies to Study Individual Kinase Substrate Relationships

by

Jasmina J. Allen

DISSERTATION

Submitted in partial satisfaction of the requirements for the degree of

DOCTOR OF PHILOSOPHY

in

Chemistry and Chemical Biology

in the

GRADUATE DIVISION

of the

Acknowledgments and Dedication

I thank Kevan Shokat for guiding me through an impactful project, Alma Burlingame for his support, Jim Wells and Dustin Maly for mentorship, and Valerie Ohman for excellent administrative assistance. This thesis is dedicated to my family.

Portions of this work were published elsewhere. The equation in Chapter 1 was developed with the assistance of Morris Feldman. Chapter two was published in the Journal of the American Chemical Society, 2004, volume 126. Scott E. Lazerwith synthesized hapten **(4)** and prepared Supplementary Scheme S1. Chapter 3 was published in Nature Methods 2007, volume 4. ManquingLi, performed Erk2 substrate labelling reactions, Craig Brinkworth, performed mass spectrometry of modified peptides, Jennifer Paulson, expressed Cdc5, Dan Wang, provided technical assistance for PKCδ experiments, Annette Hubner, constructed JNK1 plasmids, Wen-Hai Chou, constructed PKCδ plasmids, and Carol Katayama, created the AS Erk2 mouse. Mass Spectrometry in Chapter 4 was conducted by Shenheng Guan and Terry Zhang. In Chapter 5, furfuryl ATP was synthesized by Beatrice Wang and Christopher McClendon performed molecular modeling and docking analysis.

With these exceptions, the remainder of this work was performed by Jasmina J. Allen, under the direction of Kevan M. Shokat.

Development and Application of Technologies to Study Individual Kinase Substrate Relationships

by

Jasmina J. Allen

Abstract

The ubiquitous nature of protein phosphorylation makes it challenging to map kinase substrate relationships, which is a necessary step towards defining signaling network architecture. To trace the activity of individual kinases, in complex biological contexts, we developed a semi-synthetic reaction scheme which affords affinity tagged substrates of a kinase in question. A kinase, engineered to utilize a bio-orthogonal ATPγS analog, catalyzes thiophosphorylation of its direct substrates. Alkylation of thiophosphorylated residues creates an epitope for thiophosphate ester specific antibodies. A primary sequence context independent, high affinity rabbit monoclonal antibody was elicited against a hapten which presented the modification on a simple alkyl linker. The generality of semi-synthetic epitope construction was demonstrated with diverse in collaboration with multiple researchers. Labelled kinase substrates were analyzed with a number immunoassays and could be immunopurified and identified. By incorporating an isotopic label, at the step of thiophosphate alkylation, we were able to quantify phosphorylation events with mass spectrometry. To improve this methodology and discover new biological targets of ATP analogs, which are naturally occurring derivatives of plant hormones, we identified casein kinase 2 as an endogenous ATP analog utilizing enzyme. The tools we developed and insights we discovered advance field of kinase-substrate and kinase-ATP interactions.

Table of Contents

List of Tables

Chapter 1

Chapter 2

Chapter 3

Chapter 4

Chapter 5

List of Figures and Illustrations

Chapter 1

Chapter 2

Chapter 3

Chapter 4

Chapter 5

Appendix I

Chapter 1

Kinase Substrate Network Analysis: an Updated Perspective on the Pending Challenges and Available Techniques

In the 1950's Kennedy and Burnett discovered the first protein kinase activity(Kennedy 1992). Their *tour de force* strategy was based on tracking an enzymatic activity capable of radio-labeling casein in the presence of γ-^{32}P-ATP. Sequential rounds of biochemical fractionation and screening enabled isolation of an enzyme they termed casein kinase. They concluded, "The great biological reactivity of the phosphoproteins of a wide variety of tissues, particularly tumors, as evidenced by the very high rate of renewal of phosphoprotein phosphorus appears to point to some role of importance". Now, in 2008, we realize kinases are a ubiquitous class of signal transducing enzymes which regulate processes from circadian rhythms to metabolic sensing to oncogenesis. As which, kinases have emerged as essential members of our genome and are one of the most pursued class of drug targets(Manning et al. 2002). However, we only have realized a small fraction of the capabilities of kinase mediated signal transduction and there are still significant challenges towards realizing the true scope and *function* of protein phosphorylation.

In most cases, mammalian kinases exert their biological effects by transferring the γ-phosphate of ATP to hydroxyl phosphoacceptors on protein substrate serine, threonine, or tyrosine residues. Protein phosphatases counteract kinases, by hydrolyzing phosphorylated residues back to their native state(Jiang et al. 2008). Phosphorylated proteins may differ from their non-phosphorylated counterparts in their sub-cellular localization(Obsil et al. 2008), protein-protein interactions(Pieroni et al. 2008), enzymatic activity(Agius 2008), and stability(Virshup et al. 2007). In this manner, activation of a single kinase can result in dynamic signal amplification by modulating the functions of several, up to hundreds of, effector substrates. Thousands of researchers in multiple

scientific disciplines are working to understand protein phosphorylation because of the myriad biological and therapeutic consequences of kinase activation and inhibition. From the view of basic science, this knowledge enables a more thorough understanding of how signaling networks are "wired". From a drug development perspective, more sophisticated models may lead to improved drug target selection and validation.

A key component of kinase and phosphoprotein research is development and application of technologies which enable this growing field, and are the subject of several excellent reviews(Johnson et al. 2005; Sopko et al. 2008). Here, we aim to parameterize some of the challenges of constructing a comprehensive map of kinase substrate relationships and relate these parameters to available techniques. At the heart of this challenge is the ubiquitous phosphorylation reaction, catalyzed by kinase super-family members with highly conserved ATP binding pockets. Of the thousands of protein substrates, each protein isoform contains dozens to hundreds of potential phosphoacceptors. The *complexity* of the potential kinase-substrate network is dizzying. Once phosphate is transferred to a protein substrate it is difficult to distinguish from the reaction products of all other kinases, raising the question of how kinase-substrate *specificity* can be measured and tracked. Technologically, phosphorylation events are often difficult to identify because of low *abundance* and stoichiometry. Dozens of techniques are available to researchers, and each strategy has unique capabilities which are suited to study kinase-substrate interactions at varying levels of complexity, specificity and abundance. Select representative techniques for kinase and phosphoprotein research are outlined in **Box 1**.

Complexity

It is often cited that one third of the proteins in a cell may be phosphorylated(de la Fuente van Bentem et al. 2008). Given the massive amount of phosphoprotein and proteomic research conducted in recent years an updated perspective on the magnitude of possible phosphorylation events is due. For example, even a single protein in a single synchronized cell type, may contain dozens of phosphorylated residues (Olsen et al. 2006). Further, the definition of a protein is a moving target. For example, each transcript may be further specialized through alternative splicing and start/stop site utilization. A given polypeptide may exist in one of hundreds of potential post-translationally modified states. In some cases it is clear that phosphorylation at one residue primes phosphorylation at another(Al-Khouri et al. 2005). Other post-translational modifications including methylation, glycosylation, and ubiquitylation can also influence phosphorylation levels(Garcia et al. 2005). In most cases it is unknown which ensemble of modifications co-exist on a single polypeptide, as identifications are most always made at the peptide level. Top-down mass spectrometry based proteomics(Jungblut et al. 2008)aims to address this question.

Currently, nearly 50,000 phosphorylation events have been mapped (http://www.phosphosite.org). The vast majority of phosphorylation sites have been mapped using unbiased *in vivo* phosphopeptide enrichment coupled with mass spectrometric identification. Each new large scale study typically reports the vast majority of sites identified were previously unknown(Beausoleil et al. 2004), indicating we are just beginning to delve into the complexity of phosphorylation. The number of potential kinase substrate connections possible in an organism can be calculated as

below. For example the eukaryotic model organism, *S. cerevisiae*, encodes approximately 100 kinases, and approximately 6000 potential substrates, excluding spliceoforms and alternatively transcribed versions. Assuming each substrate may be modified twice, leads to ~$60x10^6$ possible outcomes. It has been estimated a single kinase phosphorylates an average of approximately 50 substrates(Ptacek et al. 2005), and some substrates are phosphorylated by a number of kinases(Kinoshita et al. 2008) indicating number of possibilities could be orders of magnitude larger.

$$\#\text{ kinase-substrate outcomes} = (\#\text{ kinases}+1)^{(\#\text{ residues modified/substrate})}(\#\text{ protein substrates})$$

Further, proteins in different cells, tissues, and intracellular environments may have differential phosphorylation states. Phosphoproteins in a liver(Han et al. 2008) are largely different than the phosphoproteins in a brain(Trinidad et al. 2008), and phosphoprotein levels in the mitochondria or nucleus may be markedly different than in the cytosol(Bijur et al. 2003). Quantitative mass spectrometry, combined with phospho-enrichment strategies, is beginning to reveal complex widespread changes in global phosphorylation as cells respond to stimuli(Paradela et al. 2008). Different sites may display differential kinetics and fold changes(Olsen et al. 2006), revealing additional layers of complexity as the time variable is included. Studies that enable such measurements typically incorporate stable isotopes into target cell populations, and the measured biological responses reflect *in vivo* network responses. However, in many cases we wish to study how a signal was transduced, to understand how the networks may be connected with the roles of individual kinases.

Network Level Kinase Substrate Connectivity

The connectivity of kinase-substrate networks is interlinked within the complexity, as all the possible connections give rise to the complexity. Deciphering connectivity within such a network is extremely difficult as the end products of kinase reactions are phosphoproteins, and the phosphate transferred from one kinase is chemically indistinguishable from all other cellular phosphorylation. Also, many kinases are situated within signaling cascades, such that activation of one kinase activates other kinases and ultimately results in a sea induced phosphorylation. Even a single site on a single substrate may be phosphorylated to differential stoichiometries by different kinases, depending on the stimulus. Techniques which unambiguously address questions of connectivity between kinases and substrates are conducted *in vitro*, to enable tracking of individual phosphate atoms. This knowledge comes at the cost of eliminating the variables which give rise to complexities discussed above. Similarly, unbiased *in vivo* techniques which can reveal complexity in real time are largely unsuited to address the direct connectivity of kinases and substrates.

Kinase to Substrate Connectivity

Multiple established techniques and strategies exist for researchers wishing to identify substrates that are phosphorylated by a kinase of interest. The most straight forward technique to address questions about a single kinase-substrate pair is the classic *in vitro* kinase assay, where a single kinase is incubated with a single kinase. Protein kinase assays conducted on arrays imprinted with candidate substrates is a high throughput format for *in vitro* kinase assays, and has been applied extensively to yeast kinases(Ptacek et al. 2005). A lack of comprehensive protein expression libraries for

mammalian proteins has limited the number of human kinase-substrate pairs identified with protein chips.

Instead, screens for substrates of mammalian kinases often involve introducing a kinase of interest to a mixture of cellular proteins under conditions which maximize activity from the kinase of interest. Kinase substrate tracking and elucidation (KESTREL) accomplishes this by optimizing reaction conditions to suit the kinase being studied, such that the labeling of that kinases substrates rise above the background phosphorylation of all other kinases in the mixture(Cohen et al. 2006).

Another way to raise the signal of the kinase of interest above background phosphorylation is to create an orthogonal kinase ATP analog pair. ATP analogs, which can be radio-labeled(Shah et al. 1997) or contain a γ-sulfur atom(Allen et al. 2007; Blethrow et al. 2008) enable tracking and purification of ATP analog specific kinase reaction products. Because cells are impermeable to ATP and ATP analogs, due to the presence of multiple negative charges on these molecules, these techniques are currently limited to cell extracts or permeabilized cells.

In vivo techniques have the obvious advantage of increased biological specificity, however at the cost of confidence that the events are direct. For example, antibodies have been developed that recognize phosphorylated kinase substrate consensus motifs. However, many kinases share similar preferred phosphorylation motifs. Genetic or chemical genetic techniques are other *in vivo* approaches to study kinase substrate relationships, however changes in phenotype or phosphorylation status could be indirect consequences of kinase inhibition or deletion. Ideally we would like to measure the connectivity of kinase substrate reactions *in vivo* with a single technique. However,

techniques which address *in vivo* complexity often leave the connections unknown. Similarly, techniques which unambiguously reveal kinase substrate network connections are often conducted under conditions which do not address many of the biological complexities.

Substrate to Kinase Connectivity

An abundance of high quality *in vivo* data demonstrating specific phosphorylation sites on many proteins of interest raises the next logical question, which kinase phosphorylated this site? Unfortunately, a paucity of techniques address this question. One strategy utilizes a mechanism based cross-linker to trap kinase-substrate interactions, which are typically transient and low affinity. A cysteine residue in introduced in place of the phosphorylated residue of interest, which is then cross-linked to lysine residues of the cognate kinase *in vitro*(Maly et al. 2004). Second generation cross-linkers with improved specificity are being developed,(Liu et al. 2008; Statsuk) although this appealing strategy is still being optimized to enable identification of substrate-kinase interactions in biologically complex samples.

Bioinformatic approaches utilize preferred kinase consensus motifs to predict which kinase(s) are likely responsible for phosphorylation events of interest(Obenauer et al. 2004). This approach can also predict exact sites of phosphorylation after a kinase-substrate pair has been identified. A more integrated approach incorporated several other network data types to increase the predicting power of the consensus algorithm(Linding et al. 2007). A suite of web based tools enable researchers to rapidly query such databases, Box 2.

Substrate to Phosphatase Connectivity

The reversal of phosphorylation, catalyzed by protein phosphatases, is equally important although much less studied than phosphorylation. Technology plays a role in this unbalance, as very few techniques are available to study this process. Phosphatases were first identified by using non-hydrolyzable thiophosphorylated substrates which can be used to purify cognate phosphatases(Mei et al. 1991). Phosphatase mutants which bind but do not dephosphoryate their substrates(Flint et al. 1997), can be used to purify cognate substrates. A recent study systematically examined genetic interactions between kinases and phosphatases. Growth phenotypes resulted when kinases and phosphatases in the same signaling networks are perturbed(Fiedler), revealing known and novel kinase-substrate-phosphatase interactions. As phosphorylation stoichiometry is delicately balanced by the activity of kinases and phosphatases, an understanding of which phosphatases act on which sites is key information which may be more easily and comprehensively obtained with new technologies.

Kinase and Nucleotide Connectivity?

Typically, only two thirds of the components of the forward phosphorylation reaction is considered, the kinase and the substrate. The third component, the nucleotide, may also play a role in specifying this reaction(Shugar 1996). Nucleotide levels are dynamic and can allosterically regulate kinase activity(Jorgensen et al. 2008), however the regulation could be more direct through utilization of alternative nucleotide donors. For example, the protein substrate specificity of PKCδ changes depending on weather ATP or GTP is utilized as a phosphodonor(Gschwendt et al. 1995). Modified nucleobases are prevalent in nature(Nishimura et al. 2006) and are also formed upon

DNA damage or through chemical processes(Wyszko et al. 2003). We recently discovered the mammalian kinase CK2 recognizes plant hormone derived N^6 alkylated ATPs as phosphodonors and inhibitors(Allen). The biological significance of alternative nucleotide utilization has not yet been discovered; although there is an exciting possibility it could add another dimension to the field of phosphorylation research.

Abundance

Mapping new interactions requires a means to identify phosphorylation events. Inherent to this challenge is the amount of material needed, the efficiency of the process, and the sensitivity of the detection method. Many interesting signaling proteins are present at low cellular copy numbers and only a percentage of the protein population may be phosphorylated. Phosphorylation visualization techniques such as radioactivity are extremely sensitive; however the identity of the protein must typically be obtained in another way. For example, protein arrays couple the identity and the phosphorylation status by spatially recognizing proteins, based on their pre-determined position on the array, and radioactive spots indicate which proteins are phosphorylated. Genetic techniques such as yeast synthetic growth phenotype screens and two-hybrid analysis are also extremely sensitive and have the advantage of making *in vivo* measurements, although follow up assays are necessary to confirm the effects are direct.

Many techniques are designed to aid in purifying and identifying phosphoproteins and phosphopeptides from cell preparations. Table 1 illustrates theoretical amounts of total protein necessary to purify components of varying abundance. However, the actual amounts necessary are larger due to the incomplete stoichiometry of a phosphorylation event and the efficiency purification processes. Mass

spectrometry is often the final readout, which typically requires low femtomole amounts of protein. Further, mass spectrometry techniques require the percentage of a given protein in a mixture to be considered, as instruments have limited dynamic range. These considerations form the impetus for the many affinity purification techniques which are often coupled to mass spectrometric readouts.

Future Perspectives

The intense progression of this field in recent years suggests even more rapid advances in those to come. We can expect more sophisticated, sensitive, and high throughput technologies will reveal connections between kinases and substrates in increasing numbers and more biologically informative ways. The knowledgebase is already overwhelming, and as more data accumulates organizing and integrating the data will likely be as important or more important as discovering new events. Box 2 provides links to a number of web-based tools and databases that organize and make predictions based upon experimental data from a number of sources.

Mapping kinase-substrate interactions is a first step towards understanding the biological significance and function of a given event. The classical way to test the importance of phosphorylation is to mutate the residue to a non-phosphorylatable or phosphomimetic residue and measure an altered phenotype. Placing kinases and substrates in integrated biological networks lends hypothesis about the possible functional importance of phosphorylation cascades and may help construct testable hypotheses concerning these functions. However, a single kinase may phosphorylated hundreds(Ubersax et al. 2003) even thousands of proteins(Meggio et al. 2003) and a single phosphorylation event may only transducer a fraction of the signal from a given

kinase. New techniques that link phosphorylation events with their functions will be necessary, particularly in a global way, will be particularly informative.

Table 1. Theoretical amounts of protein and cells necessary to identify proteins of varying cellular copy number, adapted from Gygi et.al.(Gygi et al. 2000) It is assumed that 1 ng (20 fmol) of a 50 KDa protein is purified in 100% yield. We estimate 200 mg of protein is obtained from $1x10^9$ HeLa cells.

copy number	protein amount	number of cells
1	1 g	5×10^9
10	100 mg	5×10^8
100	10 mg	5×10^7
1,000	1 mg	5×10^6
10,000	100 µg	5×10^5
100,000	10 µg	5×10^4

Box 1

Protein Arrays

Recombinant kinases phosphorylate substrates, which are arrayed on microchips(Ptacek et al. 2005). Targets are visualized through autoradiography.

KESTREL

Kinase substrate tracking and elucidation (KESTREL) identifies kinase substrates by adding purified kinases and radioactive ATP(Cohen & Knebel 2006). Assay conditions are tuned to reveal kinase specific phosphorylation events.

Analog Sensitive Kinases

The gatekeeper residue in a kinase of interest is engineered to create an allele that utilizes ATP analogs(Shah et al. 1997). Substrates of such analog specific (*AS*) kinases become specifically labeled and can be purified using conventional or thiophosphate specific approaches(Allen et al. 2007; Blethrow et al. 2008).

Synthetic Genetic Arrays

Yeast deletion mutants are mated pair-wise and knockout strains which exhibit significantly altered growth phenotypes are said suppress or buffer each other depending if growth is synthetically inhibited or enhanced in the double mutant(Ihmels et al. 2007). Kinase-substrate double mutants tend to have buffered growth rates(Fiedler).

Kinase Substrate Motifs

Peptide libraries are utilized to determine a kinases optimal phosphorylation consensus motifs(Hutti et al. 2004). Substrates and sites of phosphorylation can then be predicted bio-informatically(Obenauer & Yaffe 2004). Phosphorylation sites can also be queried against kinase consensus motifs to predict candidate kinases.

Antibodies

- Phosphotyrosine specific antibodies can detect and enrich phosphotyrosine containing proteins and peptides(Bergstrom Lind et al. 2008).
- General phosphoserine/threonine antibodies are typically lower affinity(Gronborg et al. 2002). Thiophosphorylated residues may be alkylated for recognition by a thiophosphate ester specific antibody(Allen et al. 2007).
- Phosphorylation motif antibodies are specific for kinase consensus motifs(Zhang et al. 2002) or phosphoprotein recognition motifs(Shen et al. 2003).
- SDS-PAGE gels containing phosphate chelating groups can induce dramatic phospho-shifts(Kinoshita et al. 2006), shifted proteins can then be detected by conventional methods.
- Site specific antibodies enable studies of individual phosphorylation sites.

Phosphopeptide Enrichment Strategies and Phosphoproteomics

Techniques include immobilized affinity chromatography (IMAC), chemical conversions, strong cation exchange and hydrophilic interaction chromatography, among other strategies, reviewed elsewhere(Paradela & Albar 2008).

Mass Spectrometry

Tandem mass spectrometry is a general enabling technology which provides hypothesis free identification of phosphoproteins and phosphopeptides. Electron capture/transfer disassociation technologies are particularly suited for phosphorylation site determination(Mikesh et al. 2006).

Box 2: Web-Based Resources for Kinase Substrate Research

http://www.humanproteinpedia.org/

Portal for sharing and searching data integrated from multiple MS and proteomic studies.

http://networkin.info/search.php

NetworKin predicts kinase substrate relationships using consensus motifs within the context of protein and genetic networks.

http://scansite.mit.edu/

Predicts phosphorylation sites based on input kinase consensus motifs and other tools.

http://www.phosphosite.org

Protein modification resource with culminated phosphorylation data from MS data and other sources, searches can be oriented with respect to the kinase or substrate of interest.

http://www.uniprot.org/

Universal protein knowledgebase useful for querying individual kinases or substrates for general information regarding sequence, function, complexes, and post-translational modifications.

http://interactome-cmp.ucsf.edu/

Search databases for yeast physical and genetic interactions, which may indicate kinase-substrate or substrate-phosphatase interactions.

https://portal.biobase-international.com/

Integrated protein and genomic databases for several organisms, requires subscription.

REFERENCES

Agius L. Glucokinase and molecular aspects of liver glycogen metabolism. Biochem J 2008; 414 (1):1-18.

Al-Khouri AM, Ma Y, Togo SH et al. Cooperative phosphorylation of the tumor suppressor phosphatase and tensin homologue (PTEN) by casein kinases and glycogen synthase kinase 3beta. J Biol Chem 2005; 280 (42):35195-202.

Allen JA, McClendon, C.L., Wang, B., Chalkley, R.J., Burlingame, A.L., Jacobsen, M.P., Shokat, K.M. Casein Kinase 2 Recognizes Plant Hormone Derived Nucleotide Triphosphates. in preparation.

Allen JJ, Li M, Brinkworth CS et al. A semisynthetic epitope for kinase substrates. Nat Methods 2007; 4 (6):511-6.

Beausoleil SA, Jedrychowski M, Schwartz D et al. Large-scale characterization of HeLa cell nuclear phosphoproteins. Proc Natl Acad Sci U S A 2004; 101 (33):12130-5.

Bergstrom Lind S, Molin M, Savitski MM et al. Immunoaffinity enrichments followed by mass spectrometric detection for studying global protein tyrosine phosphorylation. J Proteome Res 2008; 7 (7):2897-910.

Bijur GN, Jope RS. Glycogen synthase kinase-3 beta is highly activated in nuclei and mitochondria. Neuroreport 2003; 14 (18):2415-9.

Blethrow JD, Glavy JS, Morgan DO et al. Covalent capture of kinase-specific phosphopeptides reveals Cdk1-cyclin B substrates. Proc Natl Acad Sci U S A 2008; 105 (5):1442-7.

Cohen P, Knebel A. KESTREL: a powerful method for identifying the physiological substrates of protein kinases. Biochem J 2006; 393 (Pt 1):1-6.

de la Fuente van Bentem S, Anrather D, Dohnal I et al. Site-specific phosphorylation profiling of Arabidopsis proteins by mass spectrometry and peptide chip analysis. J Proteome Res 2008; 7 (6):2458-70.

Fiedler F, Braberg, H., Cagney, G., Mukherjee, P., Chechik, G., Collins, S.R., Shales, M., Wageningen, S., Kemmeren, P., Holstege, F., Christopher-Keogh, M., Weissman, J.S., Koller, D., Shokat, K.M., Krogan, N.J. Functional Organization of the S. cerevisiae Phosphorylation Network.submitted.

Flint AJ, Tiganis T, Barford D et al. Development of "substrate-trapping" mutants to identify physiological substrates of protein tyrosine phosphatases. Proc Natl Acad Sci U S A 1997; 94 (5):1680-5.

Garcia BA, Barber CM, Hake SB et al. Modifications of human histone H3 variants during mitosis. Biochemistry 2005; 44 (39):13202-13.

Gronborg M, Kristiansen TZ, Stensballe A et al. A mass spectrometry-based proteomic approach for identification of serine/threonine-phosphorylated proteins by enrichment with phospho-specific antibodies: identification of a novel protein, Frigg, as a protein kinase A substrate. Mol Cell Proteomics 2002; 1 (7):517-27.

Gschwendt M, Kittstein W, Kielbassa K et al. Protein kinase C delta accepts GTP for autophosphorylation. Biochem Biophys Res Commun 1995; 206 (2):614-20.

Gygi SP, Corthals GL, Zhang Y et al. Evaluation of two-dimensional gel electrophoresis-based proteome analysis technology. Proc Natl Acad Sci U S A 2000; 97 (17):9390-5.

Han G, Ye M, Zhou H et al. Large-scale phosphoproteome analysis of human liver tissue by enrichment and fractionation of phosphopeptides with strong anion exchange chromatography. Proteomics 2008; 8 (7):1346-61.

Hutti JE, Jarrell ET, Chang JD et al. A rapid method for determining protein kinase phosphorylation specificity. Nat Methods 2004; 1 (1):27-9.

Ihmels J, Collins SR, Schuldiner M et al. Backup without redundancy: genetic interactions reveal the cost of duplicate gene loss. Mol Syst Biol 2007; 3:86.

Jiang ZX, Zhang ZY. Targeting PTPs with small molecule inhibitors in cancer treatment. Cancer Metastasis Rev 2008; 27 (2):263-72.

Johnson SA, Hunter T. Kinomics: methods for deciphering the kinome. Nat Methods 2005; 2 (1):17-25.

Jorgensen SB, Rose AJ. How is AMPK activity regulated in skeletal muscles during exercise? Front Biosci 2008; 13:5589-604.

Jungblut PR, Holzhutter HG, Apweiler R et al. The speciation of the proteome. Chem Cent J 2008; 2:16.

Kennedy EP. Sailing to Byzantium. Annu Rev Biochem 1992; 61:1-28.

Kinoshita E, Kinoshita-Kikuta E, Matsubara M et al. Separation of phosphoprotein isotypes having the same number of phosphate groups using phosphate-affinity SDS-PAGE. Proteomics 2008; 8 (15):2994-3003.

Kinoshita E, Kinoshita-Kikuta E, Takiyama K et al. Phosphate-binding tag, a new tool to visualize phosphorylated proteins. Mol Cell Proteomics 2006; 5 (4):749-57.

Linding R, Jensen LJ, Ostheimer GJ et al. Systematic discovery of in vivo phosphorylation networks. Cell 2007; 129 (7):1415-26.

Liu K, Kalesh KA, Ong LB et al. An improved mechanism-based cross-linker for multiplexed kinase detection and inhibition in a complex proteome. Chembiochem 2008; 9 (12):1883-8.

Maly DJ, Allen JA, Shokat KM. A mechanism-based cross-linker for the identification of kinase-substrate pairs. J Am Chem Soc 2004; 126 (30):9160-1.

Manning G, Whyte DB, Martinez R et al. The protein kinase complement of the human genome. Science 2002; 298 (5600):1912-34.

Meggio F, Pinna LA. One-thousand-and-one substrates of protein kinase CK2? Faseb J 2003; 17 (3):349-68.

Mei L, Huganir RL. Purification and characterization of a protein tyrosine phosphatase which dephosphorylates the nicotinic acetylcholine receptor. J Biol Chem 1991; 266 (24):16063-72.

Mikesh LM, Ueberheide B, Chi A et al. The utility of ETD mass spectrometry in proteomic analysis. Biochim Biophys Acta 2006; 1764 (12):1811-22.

Nishimura S, Watanabe K. The discovery of modified nucleosides from the early days to the present: a personal perspective. J Biosci 2006; 31 (4):465-75.

Obenauer JC, Yaffe MB. Computational prediction of protein-protein interactions. Methods Mol Biol 2004; 261:445-68.

Obsil T, Obsilova V. Structure/function relationships underlying regulation of FOXO transcription factors. Oncogene 2008; 27 (16):2263-75.

Olsen JV, Blagoev B, Gnad F et al. Global, in vivo, and site-specific phosphorylation dynamics in signaling networks. Cell 2006; 127 (3):635-48.

Paradela A, Albar JP. Advances in the analysis of protein phosphorylation. J Proteome Res 2008; 7 (5):1809-18.

Pieroni E, de la Fuente van Bentem S, Mancosu G et al. Protein networking: insights into global functional organization of proteomes. Proteomics 2008; 8 (4):799-816.

Ptacek J, Devgan G, Michaud G et al. Global analysis of protein phosphorylation in yeast. Nature 2005; 438 (7068):679-84.

Shah K, Liu Y, Deirmengian C et al. Engineering unnatural nucleotide specificity for Rous sarcoma virus tyrosine kinase to uniquely label its direct substrates. Proc Natl Acad Sci U S A 1997; 94 (8):3565-70.

Shen YH, Godlewski J, Bronisz A et al. Significance of 14-3-3 self-dimerization for phosphorylation-dependent target binding. Mol Biol Cell 2003; 14 (11):4721-33.

Shugar D. The NTP phosphate donor in kinase reactions: is ATP a monopolist? Acta Biochim Pol 1996; 43 (1):9-23.

Sopko R, Andrews BJ. Linking the kinome and phosphorylome--a comprehensive review of approaches to find kinase targets. Mol Biosyst 2008; 4 (9):920-33.

Statsuk AV, Maly, D.J., Seeliger, M.A., Zarrinkar, P.P., Kuriyan, J., Shokat, K.M. Development of an optimized three component intermolecular reaction between protein kinases and their substrates.submitted.

Trinidad JC, Thalhammer A, Specht CG et al. Quantitative analysis of synaptic phosphorylation and protein expression. Mol Cell Proteomics 2008; 7 (4):684-96.

Ubersax JA, Woodbury EL, Quang PN et al. Targets of the cyclin-dependent kinase Cdk1. Nature 2003; 425 (6960):859-64.

Virshup DM, Eide EJ, Forger DB et al. Reversible protein phosphorylation regulates circadian rhythms. Cold Spring Harb Symp Quant Biol 2007; 72:413-20.

Wyszko E, Barciszewska MZ, Markiewicz M et al. "Action-at-a distance" of a new DNA oxidative damage product 6-furfuryl-adenine (kinetin) on template properties of modified DNA. Biochim Biophys Acta 2003; 1625 (3):239-45.

Zhang H, Zha X, Tan Y et al. Phosphoprotein analysis using antibodies broadly reactive against phosphorylated motifs. J Biol Chem 2002; 277 (42):39379-87.

Chapter 2

Bio-orthogonal Affinity Purification of Direct Kinase Substrates

Bio-orthogonal Affinity Purification of Direct Kinase Substrates

Jasmina J. Allen[1], Scott E. Lazerwith[†], and Kevan M. Shokat[2]

[1]Graduate Program in Chemistry and Chemical Biology

[†] Current Address: Pfizer Inc. Ann Arbor, MI

[2]Departments of Cellular and Molecular Pharmacology and Howard Hughes Medical Institute, University of California, San Francisco, CA

Abstract

Protein phosphorylation is a major mechanism of post-translational protein modification used to control cellular signalling. A challenge in phosphoproteomics is to identify the direct substrates of each protein kinase. Herein we describe a chemical strategy for delivery of a bio-orthogonal affinity tag to the substrates of an individual protein kinase. The kinase of interest is engineered to transfer a phosphorothioate moiety to phosphoacceptor hydroxyl groups on direct substrates. In a second non-enzymatic step, the introduced phosphorothioate is alkylated with *p*-nitrobenzylmesylate (PNBM). Antibodies directed against the modified phosphorothioate epitope recognize these labelled substrates, but not alkylation products of other cellular nucleophiles. This strategy is demonstrated with Cdk1/cyclinB substrates using ELISA, western blotting, and immunoprecipitation in the context of a whole cell lysate.

Protein kinases mediate signal transduction through phosphorylation of their protein substrates.[1] Up to one-third of proteins in a cell are phosphorylated,[2] and a major goal of phosphoproteomics is to characterize phosphorylation mediated signaling cascades by identifying phosphorylated proteins. This feat is analytically challenging because most phosphoproteins are of low abundance and sub-stoichiometrically phosphorylated. Further, once a phosphoprotein is identified, it is difficult to integrate the role of the phosphorylation event into signal transduction networks without knowledge of the upstream kinase. Affinity purification techniques such as strong cation exchange (SCX),[3] immobilized metal ion affinity chromatography (IMAC),[4] chemical tagging of phosphorylated residues with biotin[5] and phospho-motif specific antibodies[6] can enrich for phosphopeptides or proteins, but the information regarding the kinase responsible for phosphate transfer is uncoupled from the phosphorylation event. We previously have described methodology that allows selective labelling of direct kinase substrates, using analog specific (*as*) kinases and orthogonal unnatural nucleotides (A*TP and A*TPγS)[7], however it remains challenging to biochemically isolate the labelled substrates, impeding their identification.

Here we report a technique that combines direct substrate labelling with immunoaffinity purification (**Schemes 1 and 2**). To label the substrates of a given kinase an *as* allele is used to enzymatically label substrates with A*TPγS. The selectively introduced thiophosphate is then chemically derivitized to construct a bio-orthogonal affinity tag. This approach is similar to other bio-orthogonal tagging strategies using ketones[8] or azides,[9] except thiophosphate cannot be selectively tagged in a single

Scheme 1. Tandem approach for creating bio-orthogonal affinity tagged kinase substrates. Ser R=H, Thr R=Me

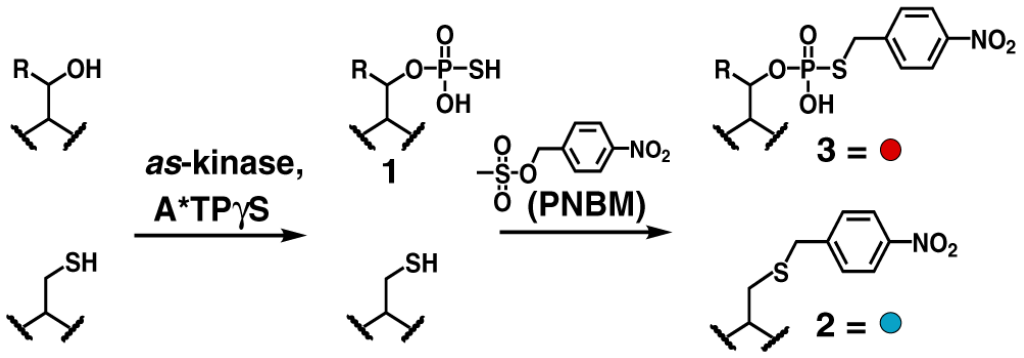

Scheme 2. Immunoaffinity Purification Stragegy

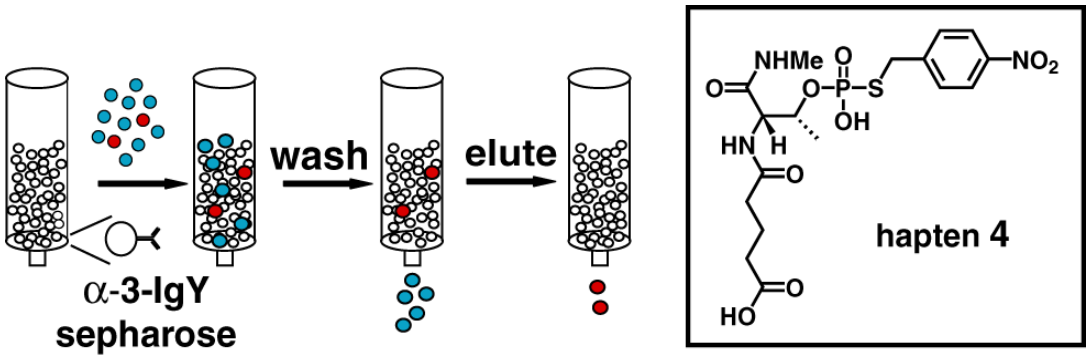

chemical step. For example an alkylating agent will label both thiophosphate and other cellular nucleophiles, but we envisioned an antibody could discriminate the thiophosphate alkylation products from other undesired alkylation products. The alkylating agent *p*-nitrobenzylmesylate (PNBM) was selected to construct the epitope because we predicted antibodies could recognize the product of thiophosphate alkylation over other nitrobenzyl alkylated amino acid residues, based on unique size and charge. Also several high affinity antibodies have been raised against haptens containing *p*-nitrophenyl moieties,[10] increasing the chances of eliciting an antibody capable of immunoprecipitation. Antibodies raised against hapten **4** are likely to be sequence independent because the binding determinants are relatively distant from the peptide backbone.

Utilizing hapten **4**, polyclonal antibodies (IgY and IgG) were raised in chickens and rabbits, respectively.[11] To enrich for specific binders, immune antibodies were purified on an affinity column containing immobilized hapten **4**. Chicken IgY antibodies (α-**3**-IgY) performed best in immunoprecipitations and were used in subsequent experiments. To investigate α-**3**-IgY binding requirements, cyclin dependant kinase 1 (Cdk1)[12] substrates Histone H1 (H1) and Swe1 were derivatized and tested in immunoassays. The α-**3**-IgY antibodies only successfully recognized H1 that had been thiophosphorylated and PNBM alkylated. In control experiments, untreated H1, PNBM alkylated H1, or thiophosphorylated H1 were not detected by ELISA (**Supplemental Figure S2**). Similarly, α-**3**-IgY recognition of the substrate Swe1[13] also required both thiophosphorylation and alkylation (**Figure 1**, lanes 1-4). Cell lysates contain abundant free thiols and other nucleophiles, which can react with PNBM, producing close

Figure 1. Recognition determinants for α-**3**-IgY immunoreactivity measured by western blotting. 25 ng of Swe1 or Swe1-P^S was treated with DMSO (lanes 1 and 3) or 2.5 mM PNBM in DMSO (lanes 2 and 4). 15 μg of WCL was treated with DMSO (lane 5), 2.5 mM PNBM in DMSO (lane 6), and 25 ng Swe1-P^S plus 2.5 mM PNBM in DMSO (lane 7). Lanes 8 and 9 show coomassie staining of samples identical to 6 and 7 respectively.

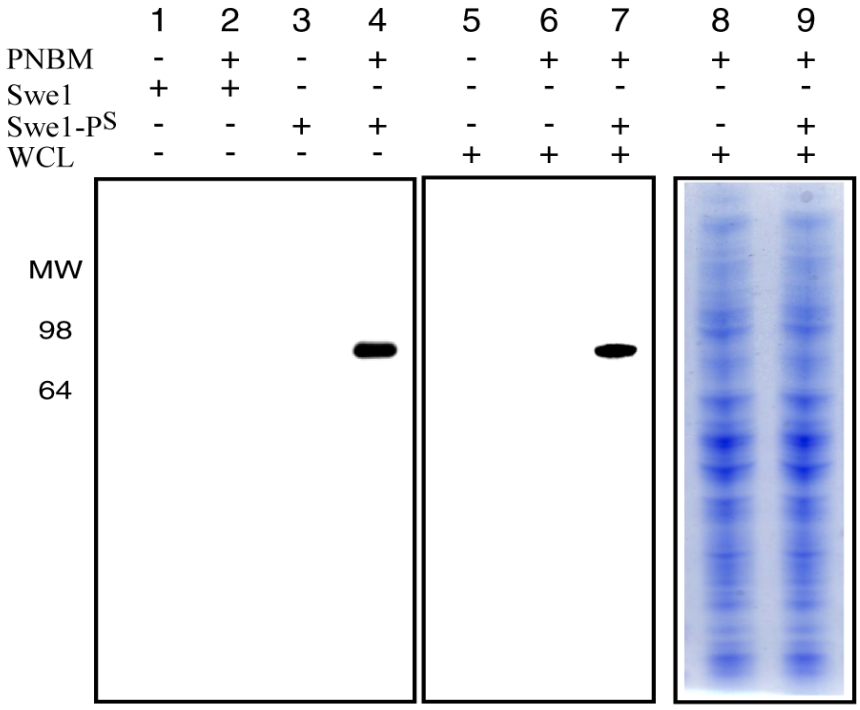

structural variants of **3**. Therefore, one of the most demanding requirements of α-**3**-IgY is the ability to discriminate phosphorothioate **3** from thioether **2** and other undesired alkylation products. To address this point, whole HeLa cell lysate (WCL) was treated with PNBM and analyzed by western blot. WCL was not recognized by α-**3**-IgY irrespective of treatment with PNBM, (Lanes 5 and 6, **Figure 1**). However, if Swe1 thiophosphate (Swe1-P^S) was added to the WCL in the presence of PNBM, Swe1-P^S+PNBM was readily detected (**Figure 1**, lane 7), indicating α-**3**-IgY exhibits the desired specificity for **3** in the context of whole cell lysate. Similar results were obtained with another Cdk1 substrate, Mob1 (**Supplemental Figure S3**). These results demonstrate that alkylation of thiophosphate with PNBM produces an epitope that can be specifically recognized in a complex protein mixture, validating this approach.

Because many antibodies do not recognize their targets with sufficient affinity for immunoprecipitation,[14] it was important to determine if α-3-IgY could immunopurify an epitope tagged substrate from a complex protein mixture. To enable rapid analysis and quantitation of immunoprecipitation experiments we prepared rhodamine labeled versions of the kinase substrate Histone H1 (Rh-H1-P^S and Rh-H1-P^S+PNBM). α-**3**-IgY or preimmune IgY, immobilized on sepharose beads, were incubated with the rhodamine-labeled proteins, washed extensively,and the bound proteins sepearated by SDS-PAGE and the in-gel fluorescence imaged. Rh-H1-P^S+PNBM bound to α-3-IgY sepharose beads but not to preimmune IgY; Rh-H1-P^S did not bind to either of the antibody conjugated beads, verifying that successful immunoprecipitation requires both the phosphorothioate modification and α-3-IgY (**Supplemental Figure S4**).

To examine the dynamic range of the immunoprecipitation, we assayed the efficiency of Rh-H1-P^S+PNBM recovery in the presence of varying concentrations of PNBM alkylated cellular proteins. α-**3**-IgY or preimmune IgY conjugated beads were incubated with increasing concentrations of PNBM alkylated WCL and a constant amount of Rh-H1-P^S+PNBM. Recovery of the Rh-H1-P^S+PNBM was still possible in the presence of up to 20 mg WCL (**Figure 2**, lane 3), although increasing WCL concentrations lowered the yield. The amount of Rh-H1-P^S+PNBM present in lane 3, Figure 3, is approximately 800 fmol (~30 ng), a quantity suitable for identification by mass spectrometry, indicating this technique can isolate kinase substrates in cases where the epitope tagged protein represents approximately 0.00005% of total protein. As the dynamic range of protein abundance in cells is ~10^6,[15] and most proteins are substoichiometrically phosphorylated, our results suggest α-**3**-IgY can enrich for moderately abundant substrates in WCL or less abundant substrates within partially purified fractions.

We have described a new affinity purification method based on sequential chemical labeling and conjugate specific antibody recognition. Large scale purification of unknown *as*-kinase substrates from whole cell lysates will likely require production of anti-**3** specific monoclonal antibodies, which is currently underway. The method we report here requires a kinase to utilize ATPγS as a phosphodonor, and although it is unclear what percentage of the kinome can utilize ATPγS, several kinases have been shown thiophosphorylate their substrates (see Supplementary Table S5 for a partial list). Combining this purification method with *as* kinase substrate labeling should provide a general route to the identification of direct kinase substrates. Other biological questions

Figure 2. Immunoprecipitation of Rh-H1-P^S+PNBM measured by fluorescence of the SDS-PAGE resolved immunoprecipitates. WCL* indicates treatment with PNBM. Lanes 1-3 were treated with α-**3**-IgY sepharose, and lanes 4-5 with preimmune-IgY sepharose.

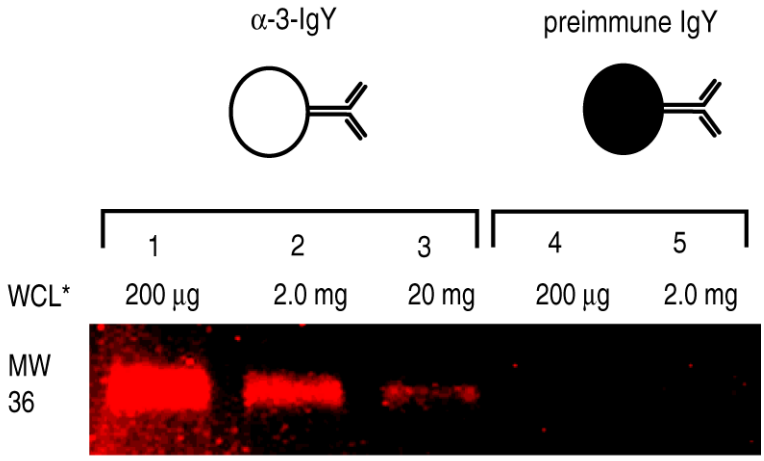

may be approached with tandem chemical/immunological strategies,[16] which are providing new routes to interrogate the proteome.

Acknowledgements

The authors are thankful to Mart Loog for providing Mob1 and Swe1, and Justin Blethrow for Cdk1F80G/cyclinB and assistance with early histone labeling experiments. HeLa cells were generously provided by the NCCC. This work was supported by a grant from the NIH (RO1 EB001987), Scott Lazerwith was supported by a NIH grant (1 F32 GM63312-01A1). We acknowledge Dustin Maly, Matthew Simon, and Zachary Knight for helpful comments on this manuscript. This work was supported by a grant from the NIH (RO1 EB001987), Scott Lazerwith was supported by a NIH grant (1 F32 GM63312-01A1). Mass spectra were provided by the Center for Mass Spectrometry at UC-San Francisco, supported by the NIH Division of Research Resources.

References

(1) Manning, G.; Whyte, D. B.; Martinez, R.; Hunter, T.; Sudarsanam, S. *Science* 2002, *298*, 1912-1934.

(2) Hubbard, M. J.; Cohen, P. *Trends Biochem Sci* 1993, *18*, 172-177.

(3) Beausoleil, S. A.; Jedrychowski, M.; Schwartz, D.; Elias, J. E.; Villen, J.; Li, J.; Cohn, M. A.; Cantley, L. C.; Gygi, S. P. *Proc Natl Acad Sci U S A* 2004, *101*, 12130-12135.

(4) Ficarro, S. B.; McCleland, M. L.; Stukenberg, P. T.; Burke, D. J.; Ross, M. M.; Shabanowitz, J.; Hunt, D. F.; White, F. M. *Nat Biotechnol* 2002, *20*, 301-305.

(5) (a) Zhou, H.; Watts, J. D.; Aebersold, R. *Nat Biotechnol* 2001, *19*, 375-378. (b) Oda, Y.; Nagasu, T.; Chait, B. T. *Nat Biotechnol* 2001, *19*, 379-382.

(6) (a) Zhang, H.; Zha, X.; Tan, Y.; Hornbeck, P. V.; Mastrangelo, A. J.; Alessi, D. R.; Polakiewicz, R. D.; Comb, M. J. *J Biol Chem* 2002, *277*, 39379-39387. (b) Kane, S.; Sano, H.; Liu, S. C.; Asara, J. M.; Lane, W. S.; Garner, C. C.; Lienhard, G. E. *J Biol Chem* 2002, *277*, 22115-22118.

(7) (a) Polson, A. G.; Huang, L.; Lukac, D. M.; Blethrow, J. D.; Morgan, D. O.; Burlingame, A. L.; Ganem, D. *J Virol* 2001, *75*, 3175-3184. (b) Eblen, S. T.; Kumar, N. V.; Shah, K.; Henderson, M. J.; Watts, C. K.; Shokat, K. M.; Weber, M. J. *J Biol Chem* 2003, *278*, 14926-14935. (c) Habelhah, H.; Shah, K.; Huang, L.; Burlingame, A. L.; Shokat, K. M.; Ronai, Z. *J Biol Chem* 2001, *276*, 18090-18095. (d) Shah, K.; Liu, Y.; Deirmengian, C.; Shokat, K. M. *Proc Natl Acad Sci U S A* 1997, *94*, 3565-3570.

(8) (a) Mahal, L. K.; Yarema, K. J.; Bertozzi, C. R. *Science* 1997, *276*, 1125-1128. (b) Khidekel, N.; Arndt, S.; Lamarre-Vincent, N.; Lippert, A.; Poulin-Kerstien, K. G.; Ramakrishnan, B.; Qasba, P. K.; Hsieh-Wilson, L. C. *J Am Chem Soc* 2003, *125*, 16162-16163.

(9) Saxon, E.; Bertozzi, C. R. *Science* 2000, *287*, 2007-2010.

(10) (a) Gigant, B.; Charbonnier, J. B.; Eshhar, Z.; Green, B. S.; Knossow, M. *J Mol Biol* 1998, *284*, 741-750. (b) Patten, P. A.; Gray, N. S.; Yang, P. L.; Marks, C. B.; Wedemayer, G. J.; Boniface, J. J.; Stevens, R. C.; Schultz, P. G. *Science* 1996, *271*, 1086-1091.

(11) Mouse immune responses were weak (unpublished data).

(12) Ubersax, J. A.; Woodbury, E. L.; Quang, P. N.; Paraz, M.; Blethrow, J. D.; Shah, K.; Shokat, K. M.; Morgan, D. O. *Nature* 2003, *425*, 859-864.

(13) McMillan, J. N.; Theesfeld, C. L.; Harrison, J. C.; Bardes, E. S.; Lew, D. J. *Mol Biol Cell* 2002, *13*, 3560-3575.

(14) Gronborg, M.; Kristiansen, T. Z.; Stensballe, A.; Andersen, J. S.; Ohara, O.; Mann, M.; Jensen, O. N.; Pandey, A. *Mol Cell Proteomics* 2002, *1*, 517-527.

(15) Gygi, S. P.; Corthals, G. L.; Zhang, Y.; Rochon, Y.; Aebersold, R. *Proc Natl Acad Sci U S A* 2000, *97*, 9390-9395.

(16) (a) Moore, L. L.; Fulton, A. M.; Harrison, M. L.; Geahlen, R. L. *J Proteome Res* 2004, *3*, 1184-1190. (b) Dickerson, T. J.; Yamamoto, N.; Ruiz, D. I.; Janda, K. D. *J Am Chem Soc* 2004, *126*, 11446-11447.

Supporting Information

Supplemental Scheme S1. Synthesis of Hapten **4**

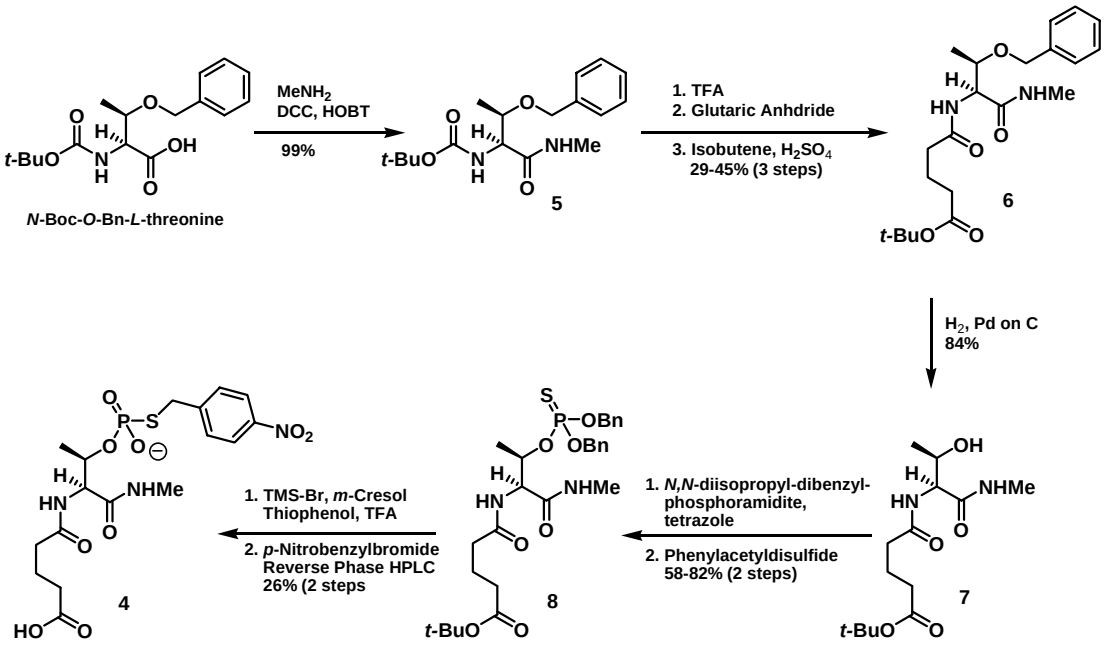

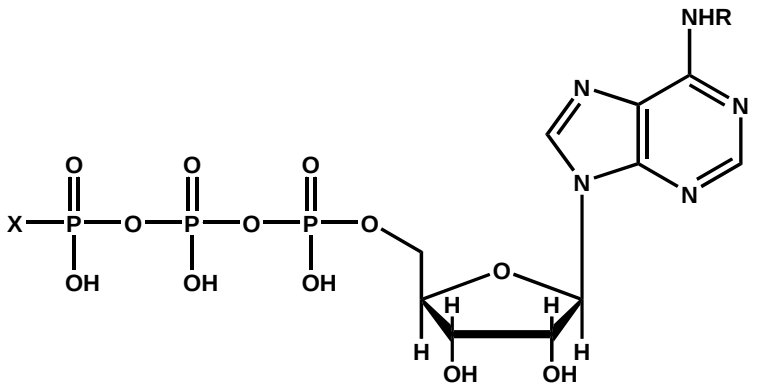

Supplemental Figure S1. Definitions of A*TP and A*TPγS

Compound	X	R
ATP	OH	H
N^6-benzyl ATP[1,2] (A*TP)	OH	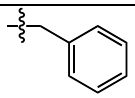
ATPγS	SH	H
N^6-benzyl ATPγS[3] (A*TPγS)	SH	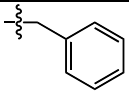

Supplemental Figure S2. ELISA Demonstrating α-**3**-IgY Recognition Determinants. Each protein antigen was coated in a 96 well plate and assayed by indirect ELISA, with colorimetric determination at 405 nm, reactions were done in triplicate.

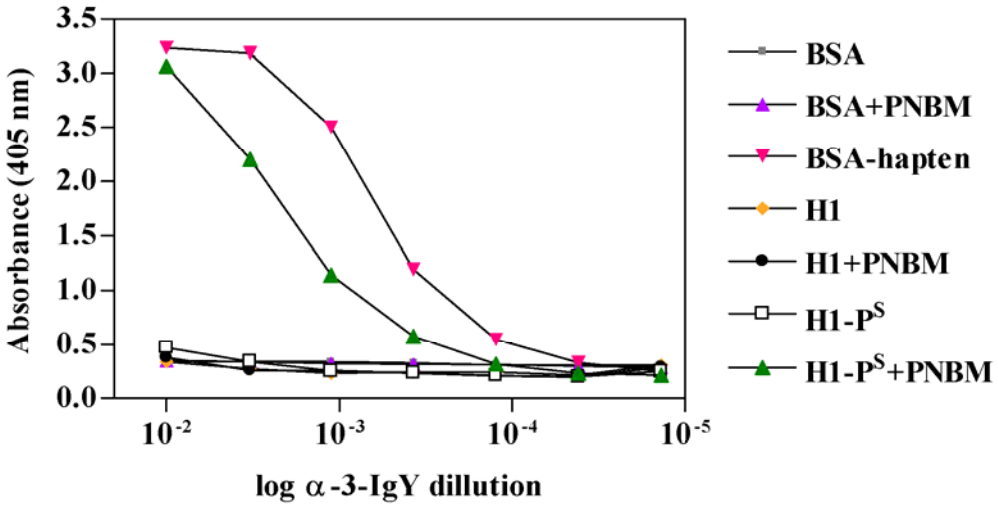

Supplemental Figure S3. Western Blot analysis of Mob1 and WCL. 25 ng of Mob1 or Mob1-P^S was treated with DMSO (lanes 1 and 3) or 2.5 mM PNBM in DMSO (lanes 2 and 4). 15 µg WCL was treated with DMSO (lane 5), 2.5 mM PNBM in DMSO (lane 6), and 25 ng Mob1-P^S plus 2.5 mM PNBM in DMSO (lane 7). Lanes 8 and 9 show coomassie staining of samples identical to 6 and 7 respectively.

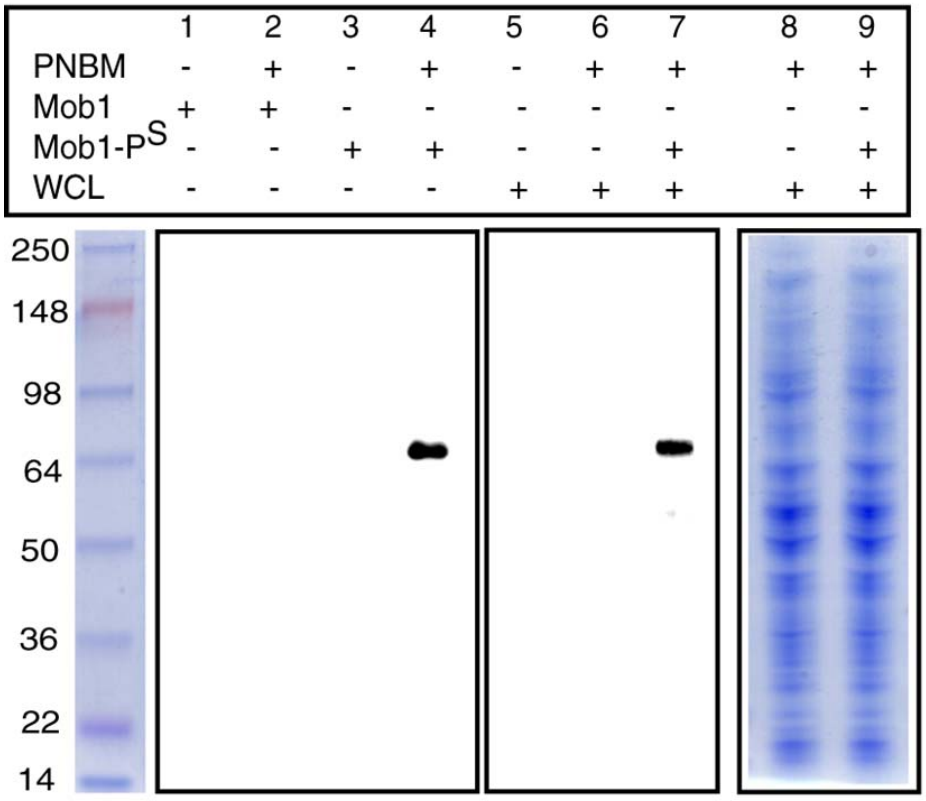

Supplemental Figure S4. Immunoprecipitation of Rh-H1-P^S, Requirement for PNBM and Immune Antibodies. 1 μg of Rh-H1-P^S treated with either 2.5 mM PNBM in DMSO or DMSO and then immunoprecipitations were attempted with preimmune or α-**3**-IgY sepharose beads. After gel electrophoresis, immoprecipitated proteins were visualized by in-gel fluorescence scanning (excitation at 523 nm, emission collected with a 580 nm band pass filter).

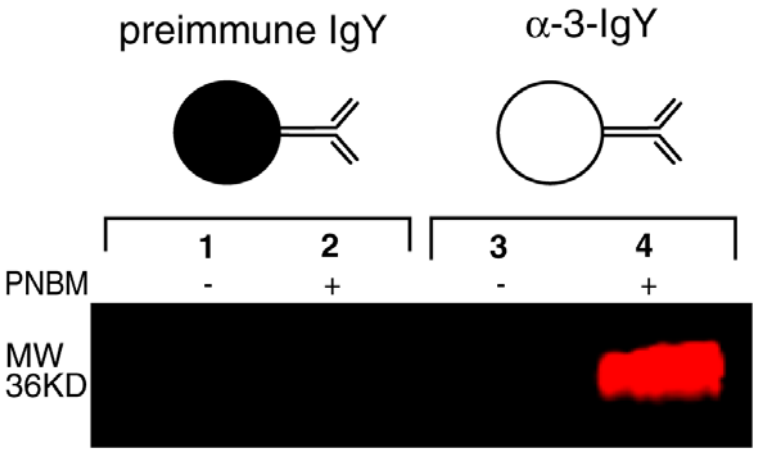

Supplemental Table 1. Kinases that have been shown to thiophosphorylate their substrates. The kinases listed below have been shown to thiophosphorylate defined substrates *in vitro*. Several other examples exist where proteins have been thiophosphorylated in crude preparations.[4,5]

Kinase	**Reference**
MAP kinase (p38α)	[6]
cyclin dependant kinase 1 (Cdk1)	[3] and this study
cyclin dependant kinase 2 (Cdk2)	[3]
phosphoinositide dependant kinase 1 (PDK1)	[7]
casein kinase 1 (CK1)	[8]
myosin light chain kinase (MLCK)	[8]
protein kinase A (PKA)	[9-11]
protein kinase B (Akt, PKB)	[12]
protein kinase C (PKC)	[13]
integrin linked kinase (ILK)	[14]
calcium/calmodulin dependent protein kinase II (CAMIIK)	[15]
C-terminal Src kinase (Csk)	[16]
cyclic nucleotide dependant protein kinase (PKG Iα)	[17]
Rho associated kinase (ROC)	[18]
MEK2	[19]
phosphorylase kinase	[11]

General Methods

Unless noted, chemical reagents and solvents were used unpurified from commercial sources. Reaction mixtures were magnetically stirred. Thin layer chromatography was performed on Merck precoated silica gel F-254 plates (0.25 mm). Concentration *in vacuo* was generally performed using a Büchi rotary evaporator. Flash column chromatography was performed on Baker 230-400 mesh silica gel.

Nuclear magnetic resonance spectra were recorded on a Varian 400 MHz instrument. Proton NMR spectra were recorded in ppm using the residual solvent signal as an internal standard: $CDCl_3$ (7.26 ppm), C_6D_6 (7.15 ppm) or d_6-DMSO (2.49 ppm). Carbon NMR were recorded in ppm relative to solvent signal: $CDCl_3$ (77.07 ppm), C_6D_6 (128.0 ppm) or d_6-DMSO (39.5 ppm). High resolution electron impact mass spectra were recorded on a MicroMass VG70E spectrometer by Sun Yuequan at the University of California-San Francisco Center for Mass Spectrometry.

Protected Threonine 5. A solution of N-Boc-O-Benzyl-(L)-threonine (3.00 g, 9.70 mmol) in THF (24 mL) was treated with hydroxybenzotriazole (HOBT) (1.378 g, 10.2 mmol) and methylamine (2.0 M in THF, 6.00 mL, 10.7 mmol) and cooled to 0 °C. Dicyclohexycarbodiimide (DCC) (2.105 g, 10.2 mmol) was added and the solution was allowed to warm to ambient temperature. After stirring for 16 h, ether (100 mL) was added and a white precipitate was removed by filtration through celite. The precipitate was washed with ether, and the filtrate was concentrated. Flash chromatography (hexanes-EtOAc-MeOH, 40:60:0.5) afforded 3.10 g (99%) of desired **4** as a white

powder: R_f = 0.29 (hexane-EtOAc, 33:66). Analytical data was consistent with the literature.[20]

***t*-Butyl Ester 6.** A solution of protected threonine **4** (3.10 g, 9.62 mmol) in CH_2Cl_2 (27 mL) was cooled to 0 °C and treated with trifluoroacetic acid (3.0 mL, 38.5 mmol). The solution was allowed to warm to ambient temperature and stirred for 48 h. Toluene (10 mL) was added and the reaction mixture was concentrated to a pink oil. An additional 10 mL of toluene was added and the solution was concentrated again. The crude deprotected amine was carried on without further purification: R_f = 0.13 (EtOAc-MeOH, 90:10).

Crude amine in MeOH (20 mL) was treated with glutaric anhydride (2.75 g, 24.1 mmol) and 2,6-lutidine (4.5 mL, 38.5 mmol). The solution was stirred at ambient temperature for approximately 4 days. 1M HCl was added and the mixture was extracted with EtOAc three times and with CH_2Cl_2 once. The combined organic layers were dried over Na_2SO_4 (anhyd), filtered and concentrated. The crude acid was carried on without further purification: R_f = 0.29 (EtOAc-MeOH, 90:10).

Crude acid in CH_2Cl_2 (20 mL) was treated with concentrated sulfuric acid (0.050 mL, 0.96 mmol), cooled to 0 °C and sealed with a rubber septum. The solution was charged with isobutylene by bubbling through the stirring solution via a needle (with a second needle as an outlet). After approximately 1 hour the isobutylene bubbling was stopped, the two needles were removed and the reaction mixture stirred while allowing to warm to ambient temperature. After 16 hours, additional concentrated sulfuric acid (0.100 mL, 1.92 mmol) was added and the solution was recharged with isobutylene at 0

°C for 1 h. The reaction mixture was sealed with a rubber septum and stirred at ambient temperature for approximately 7 days. 10% sat. $NaHCO_3$ was added and the mixture was extracted 3 times with EtOAc. The combined organic layers were washed once with $NaHCO_3$ (sat aq), dried over Na_2SO_4, filtered and concentrated. Flash chromatography (CH_2Cl_2-EtOAc, 50:50 to 30:70 to 10:90) afforded 1.09 g (29%, 3 steps) *t*-butyl ester **5** as a glassy solid: R_f = 0.27 (EtOAc); ^{1}H NMR (400 MHz, $CDCl_3$) δ 7.35 (m, 5H), 6.59 (m, 1H), 6.51 (br d, *J* = 6.6 Hz 1H), 4.64 (d, *J* = 11.5 Hz, 1H), 4.60 (d, *J* = 11.5 Hz, 1H), 4.53 (dd, *J* = 6.6, 3.0 Hz, 1H), 4.16 (dq, *J* = 6.3, 2.9 Hz, 1H), 2.81 (d, *J* = 4.9 Hz, 3H), 2.28 (m, 4H), 1.93 (m, 2H), 1.43 (s, 9H), 1.11 (d, *J* = 6.3 Hz, 3H); ^{13}C NMR (100 MHz, $CDCl_3$) δ 172.6, 172.5, 170.0, 138.0, 128.5, 127.93, 127.85, 80.5, 74.2, 71,7, 56.1, 35.4, 34.6, 28.1, 26.3, 20.9, 15.5; HRMS calcd for $[C_{21}H_{32}N_2O_5 - O\text{-}t\text{Bu}]^+$: 319.165782, found: 319.166378.

Alcohol 7. 10% palladium on carbon (approx 0.1 g) was placed in a round bottom flask under argon. *t*-Butyl ester **5** (0.97 g) in MeOH (25 mL) was added. The mixture was evacuated and placed under hydrogen with a balloon. The mixture was stirred under hydrogen, refilling the balloon with hydrogen every 24 h. After 72 h the reaction mixture was carefully evacuated and purged with argon several times and filtered through celite. The filter cake was washed several times with CH_2Cl_2 and the filtrate was concentrated to afford 0.630 g (84%) of alcohol **6** as a white powder: R_f = 0.13 (EtOAc); ^{1}H NMR (400 MHz, $CDCl_3$) δ 6.93 (br s, 1H), 6.66 (br s, 1H), 4.34 (m, 2H), 4.01 (br s, 1H), 2.79 (d, *J* = 4.4 Hz, 3H), 2.32 (m, 2H), 2.26 (t, *J* = 7.1 Hz, 2H), 1.92 (m, 2H), 1.43 (s, 9H), 1.14 (d,

J = 6.1 Hz, 3H); ^{13}C NMR (100 MHz, $CDCl_3$) δ 173.6, 172.5, 171.9, 80.6, 66.4, 56.6, 35.3, 34.5, 28.1, 26.2, 21.0, 18.2; HRMS calcd for $[C_{10}H_{17}N_2O_5]^+$ (M-O*t*-Bu): 229.118832, found: 229.118403.

Dibenzyloxyphosphorthioate 8. **A**lcohol **6** (0.200 g, 0.661 mmol) and dibenzyl-diisopropylphosphoramidite (0.280 mL, 0.827 mmol) were azeotropically dried by the evaporation of 2 mL dioxane, and redissolved in dioxane (6.5 mL). Tetrazole (0.070 g, 0.992 mmol) was added and the reaction mixture was stirred at 23 °C. After 2 h TLC showed complete coupling and phenylacetyl disulfide (0.459 g, 1.65 mmol) was added. The reaction mixture was at 23 °C for an addition 2 h. The mixture was concentrated and partitioned between ethyl acetate and water. The organic layer was separated and the aqueous layer was extracted again with ethyl acetate. The combined organic layers were washed with brine, dried over Na_2SO_4, filtered and concentrated. Flash chromatography (EtOAc-hexanes, 50:50 to 60:40 to 75:25) afforded 0.314 (82%) of desired dibenzylphosphorthioate **7** as a white powder: R_f = 0.47 (EtOAc-hexanes, 75:25); ^{1}H NMR (400 MHz, $CDCl_3$) δ 7.33 (br s, 8H), 6.51 (m, 2H), 5.05 (m, 5 H), 4.54 (m, 1H), 2.72 (d, J = 4.4 Hz, 3H), 2.24 (m, 4H), 1.90 (m, 2H), 1.43 (s, 9H), 1.24 (d, J = 6.4 Hz, 3H); ^{13}C NMR (100 MHz, $CDCl_3$) δ 172.55, 172.50, 168.8, 135.72, 135.68, 135.6, 128.60, 128.59, 128.57, 128.2, 128.1, 80.5, 74.94, 74.88, 70.13, 70.08, 70.02, 56.85, 56.79, 35.2, 34.6, 28.1, 26.3, 20.8, 17.79, 17.77; 31P NMR (162 MHz) δ 68.6; ESIMS 601.93 (M+Na).

***p*-Nitrobenzylphosphorthioate 4 (hapten 4).** A mixture of dibenzyloxyphosphorothioate **7** (0.027 g, 0.0467 mmol), *m*-cresol (0.097 mL, 0.93 mmol), and thiophenol (0.095 mL, 0.93 mmol) was cooled to 0 °C and treated with trifluoroacetic acid (0.60 mL) and bromotrimethylsilane (0.123 mL, 0.93 mmol). The reaction mixture was stirred at 0 °C for 1.5 h, diluted with toluene and concentrated in vacuo. Additional toluene was added and the mixture was concentrated again. The resulting oil was dissolved in $NaHCO_3$ (sat aq, 5 mL) and washed once with pentane (5 mL). The aqueous layer (containing deprotected phosphorothioate) was treated with a solution of *p*-nitrobenzyl bromide (0.020 g, 0.093 mmol) in ethanol (1 mL). The reaction mixture was stirred at ambient temperature for 2 hours. After washing with a small amount of pentane, the aqueous mixture was purified by reverse-phase preparative HPLC (^{18}C prep column, 30 min gradient, H_2O-CH_3CN 90:10 to H_2O-CH_3CN 40:60, 254 nm). A peak at 22.8 min was collected and concentrated to afford 0.0135 g (61%, 2 steps) of desired phorphorthioate **3** as a white powder: ^{1}H NMR (400 MHz, DMSO) δ 8.17 (d, J = 8.5 Hz, 2H), 8.02 (br d, J = 8.3 Hz, 1H), 7.91 (m, 1H), 7.65 (d, J = 8.5 Hz, 2H), 4.60 (m, 1H), 4.30 (m, 1H), 4.04 (m, 2H), 2.57 (d, J = 4.2 Hz, 3H), 2.22 (q, J = 7.3 Hz, 4H), 1.71 (quint, J = 7.3 Hz, 2H), 1.14 (d, J = 6.1 Hz, 3H); ^{31}P NMR (162 MHz) δ 20.2; ESIMS (negative mode) 476.028 (M-H); Extinction coefficient = 6300 M^{-1} cm^{-1}.

***Para*-nitrobenzylmesylate (PNBM).** *Para*-nitrobenzyl alcohol (1.00 g, 6.53 mmol) in THF (10 mL) was treated with triethylamine (1.83 mL, 13.1 mmol), cooled to –10 °C and treated dropwise with methanesulfonyl chloride (0.610 mL, 7.84 mmol). After stirring for 30 min, 10% HCl (25 mL) was added. An additional 10 ml of water was added and the

mixture was extracted twice with ethyl acetate. The combined organic layers were dried over Na_2SO_4 (anhyd), filtered and concentrated to afford an off-white powder. Analytical data was consistent with the literature.[21]

Preparation of Hapten-KLH Conjugate. Hapten **4** (10 mg, 0.021 mmol) in DMF (0.5 mL) was treated with dicyclohexylcarbodiimide (4.3 mg, 0.021 mmol) and *N*-hydroxysuccinimide (2.4 mg, 0.021 mM) and stirred 5 h. The cloudy mixture was centrifuged and the clear supernatant was added to a solution of keyhole limpet hemocyanin (KLH, Pierce, 10 mg) in 0.1 M borate buffer (pH = 8). After stirring for several hours, NaOH (30 μL, 1.0 M aqueous) was added to maintain neutral pH, and the mixture was stirred an additional 16 hours. The reaction mixture was purified over a prepacked Sephadex G-25 gel filtration column (PD-10). Fractions containing hapten-KLH conjuagate **8** were determined by Bradford assay, and the coupling efficiency was estimated by determining the absorption at 280 nm. Three fractions containing between 1 and 2.5 mg/mL of protein were collected, and coupling efficiency was determined to be 120 haptens/KLH. BSA-Hapten **4** was prepared in the same manner, coupling efficiency was 11 haptens/BSA.

Purification of polyclonal sera. An affinity purification column was prepared as follows: Diaminodipropyl amine gel (2 mL, 16-20 uMole/mL, Pierce) was placed in a small fritted column. Buffer was allowed to drain off and the remaining solid was washed with PBS (6 mL). Hapten **3** (7.2 mg, 0.021 mmol) in conjugation buffer (2 mL, 0.1 M MES, 0.9% NaCl, pH= 7.4) was added, followed by EDC (120 mg) in conjugation

buffer (0.75 mL). The ends of the column were capped and the column was placed on a rotator for 16 hours. The column was drained and washed with 1 M NaCl. Coupling efficiency was estimated by measuring the absorbance of the wash fractions at 280 nm. Approximately 5.2 mg of hapten was recovered, for a coupling efficiency of 26%. The affinity column was washed with PBS (10 mL), and 12 mL of total immune IgY (Aves Labs) was added. The column was drained until the anti-sera had fully entered the beads, and the column was capped and incubated at ambient temperature for 1.5 h. Unbound antibodies were washed from the column with 150 mL PBS and bound antibodies were eluted with acidic elution buffer (0.1 M glycine, pH=2.8), followed by basic elution buffer (0.1 M triethylamine pH 11). Individual fractions (1 mL) were immediately neutralized with 50 μL 1M TRIS, pH= 9.5 or 50 μL 1M TRIS, pH= 3.5. Fractions were pooled, concentrated, and exchanged into coupling buffer (0.1 M $NaHCO_3$, 0.5 M NaCl pH 8.3) with an Amicon centrifugal 10,000 MWCO filter as per the manufacturers instructions to afford α-**3**-IgY at 5 mg/ml.

Preparation of Antibody Coated Sepharose Beads. Sepharose-CNBr (Amersham Biosciences), 1.0 ml hydrated volume, was washed extensively with ice cold 1.0 mM HCl, then α-**3**-IgY or preimmune IgY (500 μl, 5 mg/ml in coupling buffer (0.1 M $NaHCO_3$, 0.5 M NaCl pH 8.3)) was added and allowed to react for 3 hours with rotation at ambient temperature. Coupling efficiency was calculated to be 75% based on absorbance at 280 nm. Antibody binding supernatant was removed, the beads were washed with additional coupling buffer, and unreacted sites on the beads were blocked by overnight incubation at 4 ˚C with 1.0 ml 0.1 M Tris-HCl pH 8.0. The beads were then

washed extensively with alternating 0.1 M acetate, 0.5 M NaCl, pH= 3.5 and 0.1 M Tris-HCl, 0.5 M NaCl, pH=8.0. After one final wash with PBS the beads were stored at 4 ˚C until further use.

Preparation of histone H1-nitrobenzylthiophosphate. Histone-H1 (Calbiochem, 500 μg) in kinase buffer (10 mM HEPES, 150 mM NaCl, 5 mM $MgCl_2$, 100 μM ATPγS pH **= 7.5**, 500 μL final volume) was treated with Cdk1(F80G)/CycB (5 μg) and incubated for 16 hours at 30˚C . The kinase reaction was purified through Micro Bio-Spin P6 columns (Bio-Rad Laboratories) to afford Histone thiophosphate (H1-P^S). H1-P^S (240 μL, approx 240 μg) in TRIS buffer (10 mM TRIS-HCl, pH = 7.4) was treated with a 12 μL of 50 mM PNBM in DMSO. The reaction was incubated for 2 hours at ambient temperature to afford histone nitrobenzylthiophosphate (H1-P^S+PNBM).

Rhodamine labelling of H1-nitrobenzylthiophosphate. Rhodamine-NHS ester was prepared by treatment of 5(6)-carboxytetramethylrhodamine (2.5 mg, 5.8 μmol) with N-hydroxysuccinimide (3.6 mg, 31 μmol), and diisopropylcarbodiimine (7 μl, 47 μmol) in DMF (90 μl) for 18 hours at ambient temperature. The reaction mixture was then diluted three fold with DMSO (to afford an estimated 20 mM Rh-NHS). H1-P^S+PNBM, or H1-P^S was treated with Rh-NHS (0.5 μl of 20 mM Rh-NHS per 100 μl of 0.3 mg/ml H1-P^S+PNBM) for 10 minutes at ambient temperature. The proteins were immediately purified into TRIS buffer (10 mM TRIS-HCl, pH = 7.4) with Micro Bio-Spin P6 columns. Protein concentration was estimated by comparison with know amounts of H1 on coomassie stained SDS-PAGE gels. The extent of rhodamine labeling was quantitated

(0.2 rhodamine/H1) by fluorescence gel imaging of the prepared conjugates as compared to a monorhodamine labeled protein Histone H2A (120C).

Preparation of Mob1 and Swe1 nitrobenzylthiophosphate conjugates. Bacterially expressed Mob1 (maltose binding protein fusion) and Swe1 (glutathione transferase fusion) were kindly provided by Mart Loog, Morgan Lab. Solutions of each protein (30 μL, 0.5 mg/ml) were treated with Cdk1(F80G)/cyclinB (1 μg) in kinase buffer, the total reaction volume was 150 μL. Thiophosphorylation reactions proceeded overnight at 30˚C to afford Mob1-P^S and Swe1-P^S. Without further purification and in the same buffer the proteins were alkylated with 7.5 μL of 50 mM PNBM in DMSO for 2 hours at ambient temperature to afford the protein nitrobenzylthiophosphate esters (Mob1-P^S+PNBM and Swe1-P^S+PNBM).

ELISA. 96-well plates (Nunc Immunosorb) were coated with 50 μL/well antigen (2.5 μg/mL in PBS) and incubated at 4 °C overnight. After washing three times with PBS, the wells were blocked with 200 μL BSA (10 mg/mL in PBS-T (PBS with 0.05% Tween-20)) for 2 h at ambient temperature. The plates were washed four times with PBS-T, then 50 μL serial dilutions of affinity purified polyclonal IgY (100 μg/mL diluted from 1:100 to 1: 100,000 in PBS-T containing 0.1% BSA) were added to the wells, and the plates were incubated at 4 °C overnight. After washing four times with PBS-T and twice with PBS, the plates were treated with 100 μL/well Anti-Chicken IgY (IgG)-Alkaline Phosphatase antibody (Sigma) and incubated at ambient temperature for 1 h. After washing three times with PBS-T and twice with PBS, the plates were developed by

treatment with 100 μL/well of ABTS (Southern Biotechnology, Birmingham, AL) solution (0.3 mg/mL ABTS in 65 mM citrate, 90 mM Na_2HPO_4, pH=4.0 containing 0.1% hydrogen peroxide). After 10 minutes the absorbance at 405 nm was read with a microplate reader.

Immunoblot Analyis. Proteins were resolved by SDS-PAGE and transferred to nitrocellulose paper. The blots were blocked with 5% BSA in TBS-T (Tris-buffered saline, pH=7, with 0.05% Tween-20) for 1 h at ambient. The blots were next incubated with a solution of α-3-IgY (2000:1 dilution (100 μg/ml starting concentration) in TBS-T containing 5% BSA at 4°C overnight. After washing 4 times (10 min each) with TBS-T. The blots were treated with a solution anti-Chicken IgY (IgG)-Alkaline Phosphatase antibody (Sigma) (5000:1 dilution in TBS-T containing 5% BSA), and washed again 4 times (10 min each) with TBS-T. The blots were developed with Pico SuperSignal (Pierce), and chemiluminescence was imaged on an Alpha Innotech.

Immunoprecipitation of Rh-H1-P^S+PNBM. HeLa-S3 cells (NCCC) were lysed in RIPA buffer ((50 mM Tris-HCl, 2 mM EGTA, 150 mM NaCl, 1% SDS, and 1% NP-40, pH=8.0) with Roche complete mini protease tablet, and 1 μM PMSF) for 15 min at 4 ˚C, and then centrifuged at 14,000 rcf for 10 min at 4 ˚C. Soluble lysates were treated with 2.6 mM PNBM for 2 hours at ambient temperature, then purified through PD-10 Sephadex column. Alkylated lysates were precleared with preimmune IgY-sepharose beads (50 μl beads per 1.0 ml lysate) for 15 min at 4 ˚C, and protein concentration was measured using a Bradford assay. Sepharose beads coated with α-3-IgY or preimmune

IgY were preblocked with BSA (200 µl of a 50% suspension, 200 µg BSA in 1.0 ml RIPA lysis buffer). For each experiment 1 µg of Rh-H1-P^S-PNBN, or Rh-H1-P^S, was mixed with either 200 µg of BSA, or increasing amounts of precleared HeLa lysate. Total volume was adjusted to 1.3 ml with RIPA buffer, and 50 ul of BSA blocked α-3-IgY or preimmune IgY Sepharose beads were added, immunoprecipitations were incubated with rotation at 4 ˚C overnight. Following removal of the binding supernatant the beads were washed 4X with 1.0 ml RIPA wash buffer (50 mM Tris-HCl, 2 mM EGTA, 150 mM NaCl, and 1% NP40, pH=7.5). Bound proteins were eluted with 2X SDS-PAGE sample buffer, electrophoresed, and Rhodamine imaged on a Typhoon (Amersham Biosciences), excitation at 523 nM, emission collected with a 580 nM band pass filter.

Supplemental References

(1) Shah, K.; Liu, Y.; Deirmengian, C.; Shokat, K. M. *Proc Natl Acad Sci U S A* **1997**, *94*, 3565-3570.

(2) Ulrich, S. M.; Kenski, D. M.; Shokat, K. M. *Biochemistry* **2003**, *42*, 7915-7921.

(3) Polson, A. G.; Huang, L.; Lukac, D. M.; Blethrow, J. D.; Morgan, D. O.; Burlingame, A. L.; Ganem, D. *J Virol* **2001**, *75*, 3175-3184.

(4) Joubert, S.; Labrecque, J.; De Lean, A. *Biochemistry* **2001**, *40*, 11096-11105.

(5) Cassel, D.; Glaser, L. *Proc Natl Acad Sci U S A* **1982**, *79*, 2231-2235.

(6) Chen, G.; Porter, M. D.; Bristol, J. R.; Fitzgibbon, M. J.; Pazhanisamy, S. *Biochemistry* **2000**, *39*, 2079-2087.

(7) Zou, K.; Cheley, S.; Givens, R. S.; Bayley, H. *J Am Chem Soc* **2002**, *124*, 8220-8229.

(8) Kwon, S. W.; Kim, S. C.; Jaunbergs, J.; Falck, J. R.; Zhao, Y. *Mol Cell Proteomics* **2003**, *2*, 242-247.

(9) Che, F. Y.; Xia, Q. C. *Sheng Wu Hua Xue Yu Sheng Wu Wu Li Xue Bao (Shanghai)* **2000**, *32*, 69-73.

(10) Gergely, P.; Vereb, G.; Bot, G. *Biochim Biophys Acta* **1976**, *429*, 809-816.

(11) Gratecos, D.; Fischer, E. H. *Biochem Biophys Res Commun* **1974**, *58*, 960-967.

(12) Our Unpublished Observations.

(13) Giambalvo, C. T.; Price, L. H. *Synapse* **2003**, *50*, 212-222.

(14) Deng, J. T.; Sutherland, C.; Brautigan, D. L.; Eto, M.; Walsh, M. P. *Biochem J* **2002**, *367*, 517-524.

(15) McGlade-McCulloh, E.; Yamamoto, H.; Tan, S. E.; Brickey, D. A.; Soderling, T. R. *Nature* **1993**, *362*, 640-642.

(16) Cole, P. A.; Burn, P.; Takacs, B.; Walsh, C. T. *J Biol Chem* **1994**, *269*, 30880-30887.

(17) Peshenko, I. V.; Olshevskaya, E. V.; Dizhoor, A. M. *J Biol Chem* **2004**, *279*, 50342-50349.

(18) Feng, J.; Ito, M.; Ichikawa, K.; Isaka, N.; Nishikawa, M.; Hartshorne, D. J.; Nakano, T. *J Biol Chem* **1999**, *274*, 37385-37390.

(19) Khokhlatchev, A. V.; Canagarajah, B.; Wilsbacher, J.; Robinson, M.; Atkinson, M.; Goldsmith, E.; Cobb, M. H. *Cell* **1998**, *93*, 605-615.

(20) Akaji, K.; Kiso, Y. *Tetrahedron* **1999**, *55*, 10685-10694.

(21) Dietze, P.; Jencks, W. P. *J Am Chem Soc* **1989**, *111*, 5880-5886.

Chapter 3

A Semi-Synthetic Epitope forKinsase Substrates

A Semi-Synthetic Epitope for Kinase Substrates

Jasmina J. Allen[1], Manqing Li[2], Craig S. Brinkworth[3,†], Jennifer L. Paulson[3‡], Dan Wang[4], Anette Hübner[5], Wen-Hai Chou[4], Roger J. Davis[5], Alma L. Burlingame[3], Robert O. Messing[4], Carol D. Katayama[2], Stephen M. Hedrick[2] & Kevan M. Shokat[6]

[1]Graduate Program in Chemistry and Chemical Biology, University of California San Francisco, San Francisco, California 94143, USA. [2]Divisions of Biological Sciences and Cellular and Molecular Medicine, University of California, San Diego, California 92093, USA. [3]University of California San Francisco, San Francisco, California 94143, USA. [4]Ernest Gallo Clinic and Research Center, University of California San Francisco, Emeryville, CA 94608. [5]Howard Hughes Medical Institute and Program in Molecular Medicine, University of Massachusetts Medical School, Worcester, Massachusetts, 01605, USA. [6]Howard Hughes Medical Institute, Department of Cellular and Molecular Pharmacology, University of California, San Francisco, California 94143, USA. [†]Current Address: Defense Science and Technology Organisation, Fishermans Bend, VIC 3207, Australia. [‡]Current Address: Oregon Health and Science University, Portland, Oregon 97239 USA.

Abstract

The ubiquitous nature of protein phosphorylation makes it challenging to map kinase substrate relationships, which is a necessary step towards defining signaling network architecture. To trace the activity of individual kinases we have developed a semi-synthetic reaction scheme which affords affinity tagged substrates of the kinase in question. First a kinase, engineered to utilize a bio-orthogonal ATPγS analog, catalyzes thiophosphorylation of its direct substrates. Second, alkylation of thiophosphorylated serine, threonine, or tyrosine residues creates an epitope for thiophosphate ester specific antibodies. The generality of semi-synthetic epitope construction was demonstrated with 13 diverse kinases: JNK1, p38α MAPK, Erk1, Erk2, Akt1, PKCδ, PKCε, Cdk1/cyclinB, CK1, Cdc5, GSK3β, Src, and Abl. Application of this approach, in cells isolated from a mouse which expressed endogenous levels of an analog specific kinase (Erk2), enabled purification of direct Erk2 substrates.

Introduction

Kinase substrate interactions transduce extracellular signals into appropriate intracellular responses, and mapping these relationships is fundamental to understanding how signaling network connectivity results in distinct biological outcomes. Yet, due to a paucity of techniques that enable association of an individual kinase with its direct substrates, a great many connections remain to be defined[1,2]. Shared enzymology among protein kinase family members makes it difficult to follow the activity of a single kinase in the presence of all other cellular kinases. Protein chips[3] circumvent this challenge by isolating a kinase and potential substrates from cellular complexity. However, cellular components that impede substrate identification can also impose specificity, as kinase fidelity is often enforced through scaffolds[4], cofactors, and priming of nearby residues with phosphorylation[5]. Our goal is to develop bio-orthogonal chemical reactions, unique from the natural repertoire of cellular enzymology, to enable individual kinase substrates to be traced in the presence of signaling components which contribute to physiological specificity.

Specific kinase substrate labeling is achieved by engineering the kinase of interest to accept bio-orthogonal ATP analogs that are not utilized by the remainder of the kinome[6]. For example, analog specific (AS) kinases utilize bulky [γ-^{32}P]ATP analogs[7] to produce radiolabeled substrates of a single kinase. Application of this strategy to yeast GST or TAP-tagged libraries has yielded hundreds of Cdc28[8] and Pho85[9] substrate pairs. In these screens AS kinases were added to yeast extracts containing candidate substrates, which can be purified by virtue of their genetically encoded affinity handles. However such libraries are not available for mammalian proteins and, without the aid of an affinity

handle, identification of mammalian AS kinase substrates faces the same challenges as other phosphoproteomic studies including the dynamic range of protein abundance and sub-stoichiometric substrate phosphorylation[10]. In studies of mammalian AS kinase substrates this challenge has typically been addressed by immunoprecipitating the kinase followed by identification of bound substrates. For example AS ERK2 substrates can be identified by performing kinase assays on immune complexes[11], which provides a necessary pre-enrichment of ERK2 binding proteins. However, many kinase substrate interactions are of low affinity and are not amenable to this approach. Further, in all previous studies of AS kinase substrates the kinase was either overexpressed or purified and added to cell extracts. Here we report two key advances towards the goal of unbiased identification of endogenous kinase substrates: substrate labelling in cells derived from a "gene knock in" AS kinase mouse[12-14] and development of a method for affinity purification of AS kinase substrates.

To convert the phosphate, delivered specifically by an AS kinase into an affinity handle we developed a semi-synthetic reaction scheme (**Fig 1a**). First, an AS kinase (magenta) utilizes N-6-alkylated ATPγS (A*TPγS) to thiophosphorylate its substrates. Because all other kinases (slate) will instead transfer phosphate to their substrates, substituting a reactive sulphur in place of oxygen provides a unique starting point from which to differentiate AS kinase substrates from all other phosphoproteins. However, reactions which can functionalize thiophosphate containing proteins, facilitating their purification, will also modify other cellular nucleophiles. For example, alkylation of thiophosphate with the electrophilic tag *p*-nitrobenzylmesylate (PNBM) is concomitant with formation of undesired alkylation products resulting from derivatization of cysteine

thiols. To specifically detect and purify thiophosphate reaction products, we have developed polyclonal and monoclonal antibodies which discriminate thiophosphate esters from cysteine alkylation products (thioethers).

In our first report[15], we used this approach to detect substrates of the serine-threonine kinase, Cdk1. To further develop this strategy, and expand the portion of the kinome tractable with this approach, each of the reaction steps in **Figure 1a** was analyzed for specificity and applicability to many kinase substrate pairs. Diverse kinases were screened for the ability to thiophosphorylate their protein substrates and the vast majority of kinases utilized ATPγS as a phosphodonor. Orthogonal A*TPγS analogs were synthesized and found to be preferred substrates for AS kinases, enabling delivery of thiophosphate to individual kinase substrates. The resulting panel of labelled kinase substrates, which contained modified serine, threonine, and tyrosine residues in the context of diverse kinase consensus motifs, were all recognized by new thiophosphate ester specific antibodies. Our initial hapten design presents the thiophosphate ester modification on a threonine backbone[15]; however, the elicited hapten specific antibodies suffer from either low yield of specific antibody or low affinity and are not expected to recognize modified tyrosine residues. Here, we designed a new hapten (**Fig. 1b**) containing only the minimal desired epitope in an effort to focus the immune response on the thiophosphate ester moiety. The elicited rabbit polyclonal and monoclonal antibodies are thiosphosphate ester specific, context independent, and capable of immunoprecipitation. Application of this semi-synthetic immunoaffinity approach enabled purification of the direct substrates of an AS kinase (Erk2) which was expressed at endogenous levels.

Results

Generation of thiophosphate ester specific IgG

Rabbit α-hapten-IgG was elicited with a hapten conjugate, consisting of a *p*-nitrobenzylthiophosphate ester with a three carbon linker to keyhole limpet hemocyanin (KLH) (**Fig. 1b**). Affinity purified polyclonal antibodies only recognized c-Jun-GST containing both thiophosphorylation and PNBM modifications (**Fig. 1c**), verifying that the antibodies discriminate thiophosphate alkylation products from all other possible alkylation products. In contrast, antibodies raised in chicken (α-hapten-IgY) recognized PNBM alkylated proteins whether or not they had been thiophosphorylated (**Supplementary Fig. 1**) and were not used in any further experiments. α-hapten-IgG comprised approximately 3% of total serum IgG, yielding milligrams of antibody for western blot and kinetic experiments. Meanwhile, cells from this rabbit were used to generate hybridomas. Forty eight hybridoma supernatants were immunoreactive against a BSA-hapten conjugate and forty had modest to excellent specificity for thiophosphate esters over thioethers (**Supplementary Fig. 2a**). Several of these clones immunoprecipitated affinity tagged histone H1 (**Supplementary Fig. 2b**). Clones with the strongest signal also specifically recognized thiophosphate alkylation products in the context of a whole cell lysate (**Supplementary Fig. 2c**), each of these hybridomas were further subcloned. The subclone with the strongest signal in these assays (51-8) was used for large scale rabbit monoclonal antibody (RmAb) production.

Specificity and Yield of PNBM alkylation

Proteins contain several functional groups which could potentially react with PNBM and hinder automated database searching and identification of AS kinase

Figure 1. Strategy for labeling individual kinase substrates (**a**) Reaction sequence for affinity tagging analog specific (AS) kinase substrates. First, an AS kinase (magenta) utilizes N-6-alkylated-ATPγS (A*TPγS) to thiophosphorylate its substrates (pale magenta). In a second step, alkylation with *p*-nitrobenzylmesylate (PNBM) yields thiophosphate esters and thioethers. Only AS kinase substrates are recognized by α-hapten-IgG. (**b**) Structure of the hapten conjugate used to elicit thiophosphate ester specific antibodies (KLH = keyhole limpet hemocyanin). (**c**) JNK1 was incubated with c-Jun-GST and combinations of ATPγS and PNBM, reaction products were analyzed with α-hapten-IgG western blot analysis. α-GST-IgG confirms equal loading.

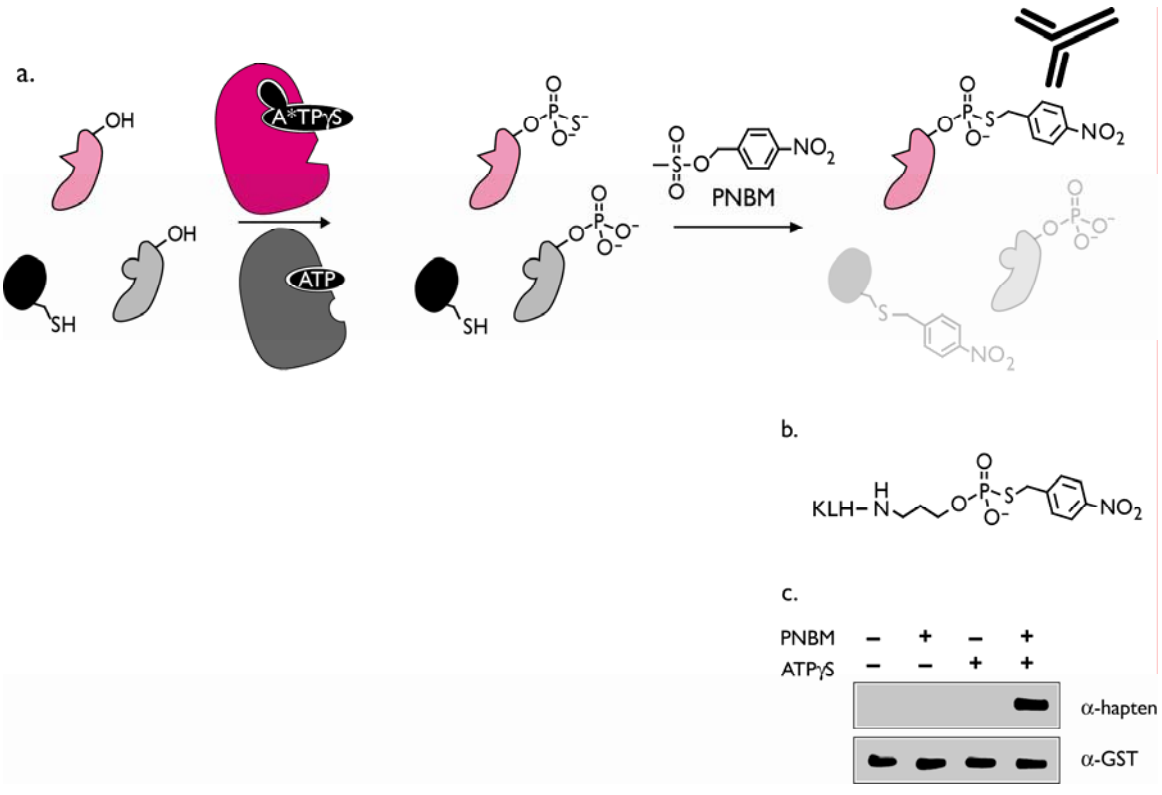

substrates from mass spectrometric data. To determine the extent of PNBM alkylation of proteogenic amino acids c-Jun-GST was thiophosphorylated and alkylated as in **Figure 1c**, digested with trypsin, and analyzed with tandem mass spectrometry. Following standard MASCOT based sequencing software analysis, c-Jun-GST was readily identified with 56% sequence coverage (darkened residues, **Fig. 2a**); indicating PNBM does not modify alcohol, amine, or carboxylic acid functional groups. Manual sequencing of unassigned tandem mass spectra yielded peptides that contained alkylated cysteine and thiophosphorylated serine residues. Sites of cysteine alkylation were localized by inspection of the y-ion series (**Fig. 2b**). Initial MS-MS spectra of thiophosphate ester containing peptides contained few sequence ions; lowering the collision induced disassociation (CID) energy produced the more informative spectra shown in **Figure 2c**. A prominent 169 Dalton mass shift, corresponding to elimination of *p*-nitrobenzyl thiol, was observed from the molecular ion and produced an additional y-ion series.

To determine the yield of thiophosphate alkylation, a model thiophosphopeptide was synthesized and PNBM alkylation was monitored with HPLC (**Supplementary Fig. 3a-3c** online). The reaction was complete after a one-hour treatment with 2.5 mM PNBM. Only one product was observed in the HPLC chromatogram and mass spectrometric analysis confirmed this to be the monoalkylated peptide (**Supplementary Fig. 3d)**.

Generality of ATPγS utilization and antibody recognition

To determine the general applicability of this labelling strategy, each of the reaction steps was tested with a diverse set of kinase substrate pairs. Several kinases have been

Figure 2. Mass spectrometric analysis of thiophosphorylated and alkylated c-Jun-GST. (**a**) Sequence coverage of c-Jun-GST: residues in black were identified by automated database searching of the unmodified peptides, blue indicates peptides that contain a modified cysteine, red indicate thiophosphate ester containing peptides, and residues in grey were not observed. (**b**) Tandem mass spectrum of a thioether containing peptide. (**c**) Tandem mass spectrum of a peptide containing a modified serine, which corresponds to a site of JNK1 phosphorylation. A 169 Dalton loss, consistent with the depicted elimination, was observed from the doubly charged molecular ion and also gave rise to an additional *y*-ion series. Ions that have undergone this loss are labeled in red.

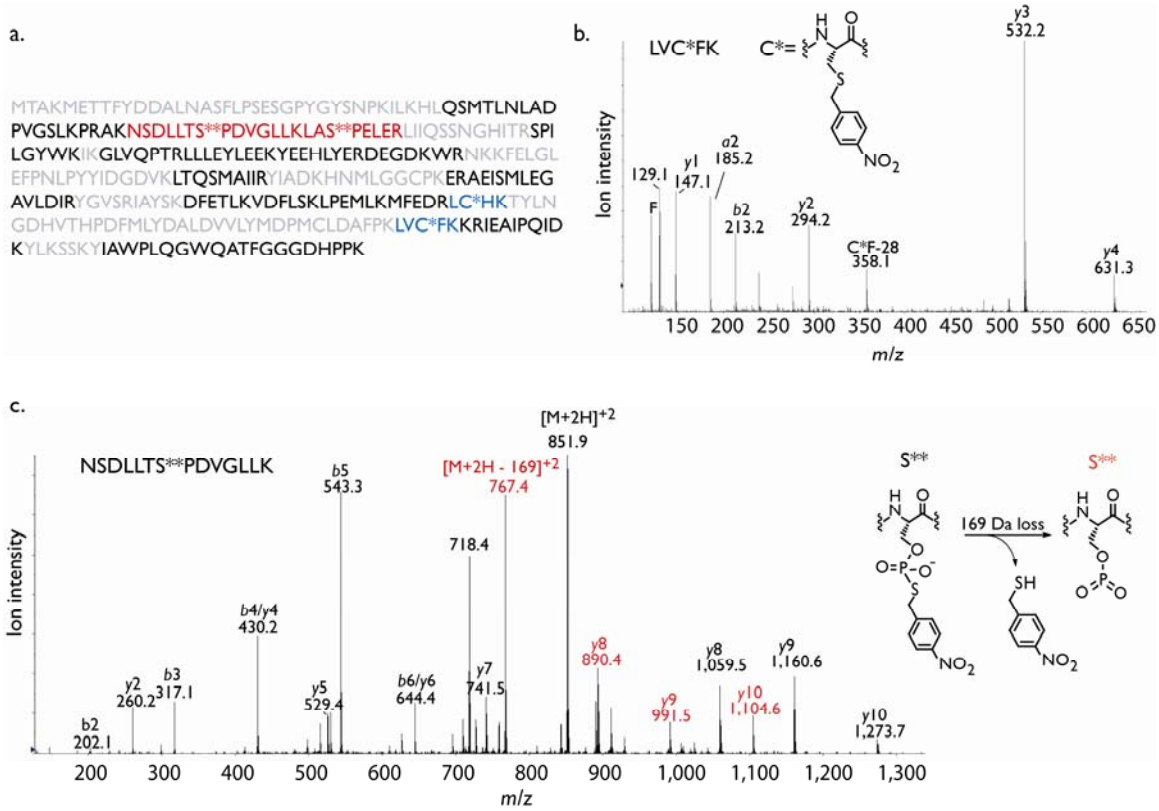

reported to utilize ATPγS as a phosphodonor (for a partial list see[15]), although often with a reduced k_{cat}[16]. However, the generality of thiophosphate transfer among kinases remains unclear. We screened 15 kinases for the ability to thiophosphorylate protein substrates, and all but two (GRK2 and JNK2, data not shown) accepted ATPγS as a phosphodonor. Thiophosphorylated substrates from the remaining 13 kinases were alkylated with PNBM and analyzed for antibody recognition in the context of different kinase consensus phosphorylation motifs[17] (**Fig 3. and Fig. 4**). The polyclonal antibodies recognized each labeled substrate regardless of the modified residue (serine, threonine, or tyrosine) and the amino acid residues surrounding the site of phosphorylation. When the monoclonal antibody became available we tested a diverse subset of labelled kinase substrates (PKCδ, JNK1, GSK3β, Src and CK1) and in every case the 51-8 antibody selectively recognized the modified substrate (**Supplementary Fig. 2**).

A*TPγS synthesis and utilization by AS kinases

A*TPγS contains two permutations from the natural kinase substrate ATP, an N-6 appendage and substitution of the terminal oxygen of the γ-phosphate with sulfur (**Fig. 4a**). The N-6 modification was introduced to the adenosine riboside, followed by diphosphorylation[18] to afford N-6 alkylated ADPs. A*TPγS analogs were synthesized by condensation of the N-6 alkylated ADPs with an S-protected phosphodiester[19], to ensure that the sulphur on the γ-phosphate is non-bridging. Previous work in our laboratory has demonstrated that N-6-benzyl and N-6-phenethyl ATP are consistently selected, from a diverse panel of N-6 modified ATP analogs, as efficient substrates for AS kinases. Based on these data we synthesized N-6-benzyl and N-6-phenethyl ATPγS.

Figure 3. α-hapten-IgG detection of thiophosphate esterified kinase substrates. Each panel is labeled with the corresponding kinase and its' preferred phosphorylation consensus motif. A description of the conditions for each kinase reaction is provided in the **Supplementary Methods** online, full length western blots are presented in **Supplementary Figure 1**.

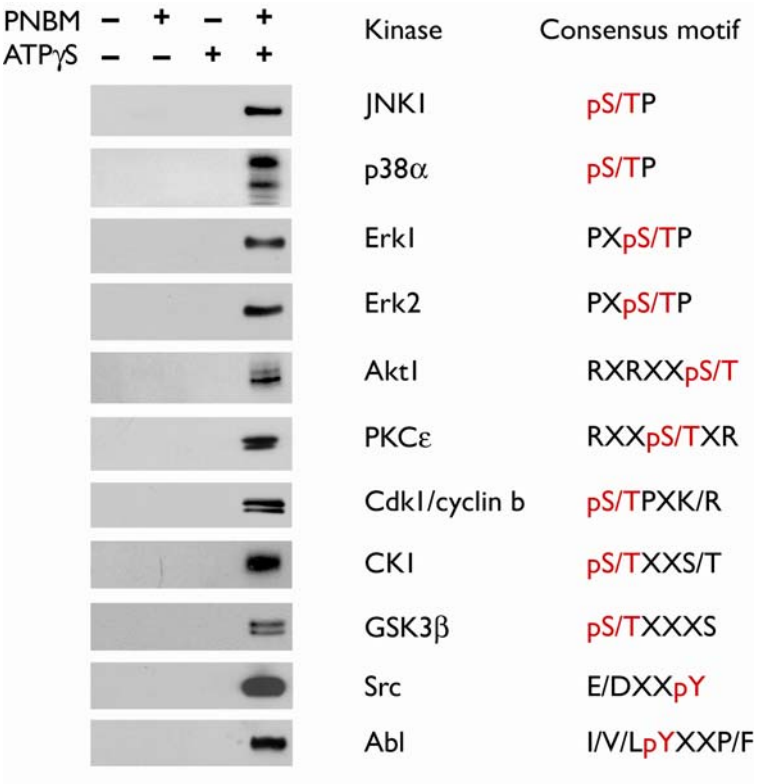

We asked if these A*TPγS analogs were bio-orthogonal (not accepted by wild-type enzymes) and if the unnatural analogs could be accepted by AS kinases. Wild type and AS alleles of kinases with diverse roles in cellular signalling were tested for their ability to utilize ATPγS and A*TPγS as thiophosphate donors: PKCδ, a second messenger activated kinase[20], Cdc5, the yeast polo-kinase which regulates cell division[21], and JNK1, a stress activated MAP kinase[22]. The assay for thiophosphorylation was based on alkylating the *in vitro* kinase reactions with PNBM, followed by western blot analysis (**Fig. 4b**). Importantly, wild-type kinases accepted ATPγS and could not utilize A*TPγS analogs. Each of the AS kinases were able to utilize ATPγS and one or both of the A*TPγS analogs: AS PKCδ favored N-6-benzyl-ATPγS, AS Cdc5 favored N-6-phenethyl-ATPγS, and AS JNK1 used both analogs to a similar extent. Western blot analysis provides a rapid assessment of the preferred nucleotides but does not allow quantitative analysis of the thiophosphorylation reaction. To obtain relative kinetic parameters for unnatural A*TPγS analog usage we developed a disassociation enhanced lanthanide fluorescence immunoassay (DELFIA)[23], employing europium labeled α-hapten-IgG (**Supplementary Fig. 4a-b**). The AS kinases typically had a lower specificity (k_{cat}/K_m) for ATPγS than the corresponding wt kinase, but an increase in k_{cat}/K_m was observed when the AS kinase utilized its preferred A*TPγS analog (**Supplementary Fig. 4c**). In each case the magnitude of k_{cat}/K_m correlated with the intensity of the corresponding band on the western blot.

Labelling, Immunoprecipitation, and Identification of Erk2 Substrates

To explore the utility of this technique to affinity label and immunoprecipitate kinase substrates in a cellular context we utilized cells expressing endogenous levels of

Figure 4. A*TPγS analog orthogonality and acceptance by AS kinases. (**a**) Chemical structure of A*TPγS, R indicates the site of N-6 modification. (**b**) Kinase reactions with ATPγS and A*TPγS analogs. Following PNBM alkylation, the labeled substrates were detected with α-hapten-IgG western blot analysis, full length western blots are presented in **Supplementary Figure 1.**

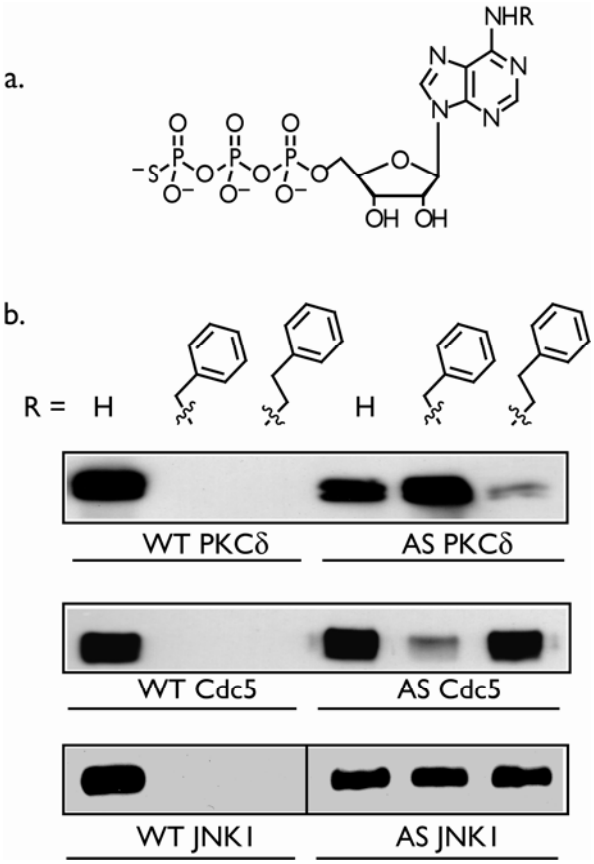

AS Erk2. Mouse embryonic fibroblasts (MEFs) were prepared from 13.5-day old embryos of *Erk1* $^{-/-}$ *Erk2*$^{+/+}$ and *Erk1*$^{-/-}$ *Erk2*$^{AS/AS}$ (AS allele is Q103G) mice. To establish that A*TPγS analogs were accepted by AS Erk2 but not WT Erk2 we immunoprecipitated Erk2 from each of these cell lines and tested each allele with A*TPγS analogs. N-6-phenethyl-ATPγS was found to be a preferred nucleotide substrate for AS Erk2 and was not utilized by WT Erk2 (data not shown). Concentrations of A*TPγS and GTP, a competitor for any general nucleotidases or non-specific phophotransferases, that yielded specifically labelled AS Erk2 substrates were optimized by adding varying concentrations of the nucleotides to digitonin permeabilized MEFs. Alkylation and western blot analysis of cells permeabilized in the presence of 100 μM A*TPγS and 1 mM GTP revealed several proteins that were selectively labelled in the AS Erk2 expressing cells (**Fig. 5a**). Immunoprecipitation of these samples with the 51-8 monoclonal antibody yielded many specifically enriched proteins (**Fig. 5b**). Following silver staining of the immunoprecipiates, a set of bands at 200 kDa were observed (**Fig. 5c**). The entire length of the gel (both WT and AS lanes) was cut into approximately 1 mm slices and digested with trypsin. Mass spectrometry and database searching identified each of the high molecular weight bands as the nucleoporin translocated promoter region (Tpr), which is a reported Erk2 substrate[11]. Forty-five peptides, matching Tpr, were sequenced from LC MS-MS analysis of these gels bands – one of which is shown in **Figure 5d**. None of the other selectively immunoprecipitated substrates were present at a level sufficient for mass spectrometric identification.

Discussion

Currently 40 kinases have been rendered analog specific (**Supplementary Table 1** online) and it is expected that most protein kinases will be amenable to this approach[24]. The use of AS kinases in combination with bio-orthogonal ATP analogs has enabled the identification of several AS kinases substrates, yet the vast majority of such pairs remain to be identified. Here we report a unified technique for AS kinase substrate labelling and phosphoprotein affinity purification, which is applicable to all three common types of phosphorylation. Additionally, the suite of immunoassays described here allow for detection, quantification, and purification of wild type kinase substrates.

A further advance, towards our goal of physiologically relevant assays of individual kinases, is labelling substrates in gently permeabilized cells expressing endogenous levels of an AS kinase, Erk2. Immunoprecipitation of these samples, prepared from a modest amount of material (15 $x10^6$ cells), enriched a sufficient quantity of Tpr for mass spectrometric identification. Currently we are extending this study to identify additional kinase substrates in tissues isolated from AS kinase expressing mice. We are also exploring the possibility of immunoprecipitating modified peptides to identify the sites of phosphorylation, this approach was recently applied to identify tyrosine phosphorylation sites[25].

High affinity serine and threonine phosphospecific antibodies typically rely on residues or motifs[26] flanking the site of phosphorylation, whereas anti phosphotyrosine antibodies can recognize tyrosine phosphorylated sites independent of context[25]. Using this semi-synthetic approach we are able to convert each of these phospho-amino acids into an epitope that can be recognized by a single antibody— a new concept in the area of

Figure 5. Labeling, immunoprecipitation, and identification of AS kinase substrates. (**a**) MEFs expressing either WT or AS Erk2 were permeabilized, incubated with A*TPγS, alkylated, and analyzed by western blot (RmAb α-hapten-IgG). (b) Western blot analysis of the same samples (in panel **5a**) after immunoprecipitation. (c) Silver stain of immunoprecipitates from panel **5b**. (d) LC MS-MS spectrum of a tryptic peptide, FEVAQVESLR, from the indicated band in panel **5c**. Full length western blots and silver stained gel are presented in **Supplementary Figure 1**.

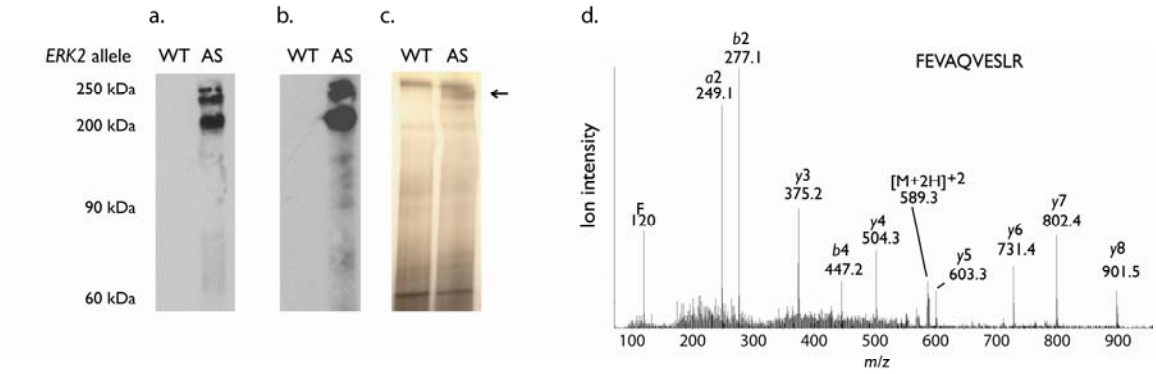

modification specific antibodies. A key feature of the epitope construction strategy is discrimination of closely related reaction products i.e. specificity for thioesters over thioethers. The ability to provide a second filter that distinguishes desired from undesired reaction products rather than relying on a single completely bio-orthogonal reaction, such as click chemistry, oxime formation, or the Staudinger ligation[27], may prove to be a general approach to broaden the scope of chemical functionalities and modification strategies used in bio-orthogonal tagging schemes.

Methods

Antibody generation and Purification

Hapten (**Supplementary Fig. 5**) was conjugated to succinylated KLH, using EDCI and Sulfo-NHS overnight at pH 8, purified with a PD-10 gel filtration column (Amersham) and used immunize rabbits (Epitomics) and chickens (Aves Labs). Polyclonal antibodies were purified on an affinity column (Diaminodipropyl amine gel, Pierce) containing immobilized hapten. After elution, the antibodies were concentrated using a 10 KDa MWCO Amicon ultra centrifugal filter. For DELFIA the antibodies were labelled with Eu^{3+} according the manufacturer's instructions (Perkin Elmer). Monoclonal antibodies were produced by Epitomics (South San Francisco, CA), and screened in ELISA, western blot, and immunoprecipitation assays as described in **Supplementary Methods** online.

A*TPγS analog synthesis

The overall synthetic scheme is illustrated in **Supplementary Figure 6**. N-6-modified ribosides[28] were converted to the N-6-modified-ADP molecules by reaction with $POCl_3$, followed by phosphoric acid and 1,8-diazabicyclo[5.4.0]undec-7-ene

(DBU)[18]. The reactions were quenched with 0.1 M triethylammonium bicarbonate (TEAB) and purified with strong cation exchange chromatography (0.1M to 1M of TEAB) on a Hi-Prep QFF column (Amersham Biosciences). Fractions containing the diphosphates were pooled, lyophilized, and analyzed by mass spectrometry. Yields ranged from 25-30%. A*TPγS analogs were synthesized as described for ATPγS[19], the purification and analysis were performed as described above for the ADP analogs. The lyophilized solids were obtained in 6-8% yield.

***in vitro* Kinase Reactions followed by Antibody Detection**

Kinases were incubated with their respective substrates in appropriate kinase buffers (see **Supplementary Methods** online for details). For screens of analog preference and orthogonality using western blot analysis ATPγS or A*TPγS analogs were used at 1 mM. For kinetic measurements ATPγS or A*TPγS analog concentration varied from 0.1 μM to 250 μM. Proteins were alkylated with 2.5 mM PNBM for two hours at room temperature, and analyzed by western blotting or DELFIA. For western blotting the antibodies were diluted 1:15,000 in Tris-buffered saline containing 0.5% Tween 20 (TBST) and 5% Milk. The blots were rocked overnight at 4°C, followed by incubation with goat-anti-IgG HRP (Promega) or rabbit-anti-IgY HRP (Sigma) and imaged with chemiluminescence on film.

Mice

All experiments involving live animals were approved by The University of California San Diego Institutional Animal Care and Use Committee (IACUC). *Erk2*$^{AS/AS}$ knockin mice were produced using standard techniques of gene targeting by homologous recombination. A 2.7 kb short arm including exon 2 and a 6.4 kb long arm containing

exon 3 were cloned into pfloxΔTK. Exon 3 was modified by site-directed mutagenesis to change the CAG glutamine codon at position 102 to GGC glycine. This eliminated an *Eco*0109t restriction site that was used for screening. The targeting vector was sent to the UCSD Cancer Center Transgenic facility to produce transfected R1 mouse embryonic stem cells. Two clones that tested position for homologous recombination and retention of the codon mutation were used to produce chimeric mice by blastocyst injection. Upon breeding the targeted allele was transmitted to offspring and further transmitted at a Mendelian frequency.

Erk2$^{AS/AS}$ mice retaining the neomycin resistance gene were bred to EIIA-cre mice[29] and offspring were selected for successful recombination. *Erk2*$^{AS/AS}$ mice were then crossed with *Erk1*$^{-/-}$ mice generously provided by Drs. G. Pages and J Pouyssegur (Centre National de la Recherche Scientifique, Nice, France). The resulting mice were intercrossed and selected for an *Erk1* $^{-/-}$ *Erk2*$^{+/+}$ or *Erk1*$^{-/-}$ *Erk2*$^{AS/AS}$ genotype. Embryonic fibroblasts were derived as described in the **Supplementary Methods**.

Cell Permeablization and Erk2 substrate labeling

15 x10^6 WT or AS *Erk2* MEFs cells were trypsinized, pelleted (200 x G at 4°C), and resuspended with DMEM to afford 5x10^6 cells/ml. Phorbol 12-myristate 13-acetate (PMA) (20 ng/ml) and ionomycin (1 μM) were added for 5 minutes at 37°C and then the cells were pelleted. Permeabilization proceeded for 5 min on ice in 1X Dulbecco's phosphate buffered saline (DPBS) and 1X kinase buffer (Cell Signaling) containing complete protease inhibitor cocktail (Roche), phosphatase inhibitor cocktails I and II (Calbiochem), and 50 μg/ml digitonin (Sigma). Cells were pelleted and resuspended in the same buffer with the following exceptions, digitonin was omitted and 100 μM N-6-

phenethyl ATPγS and 1 mM GTP were included. The kinase reaction proceeded at 30°C for 30 minutes with gentle rocking. The cells were then pelleted and lysed on ice for 15 min in 0.5 ml RIPA buffer (50 mM Tris pH 8, 150 mM NaCl, 1.0% NP-40, 0.1% SDS) containing 25 μM EDTA. Lysates were cleared by centrifugation, alkylated, and stored at -80°C.

Immunoprecipitation of Erk2 Substrates with 51-8 antibody

PNBM, which potentially inhibits immunoprecipitation, was removed using size exclusion chromatography. PD-10 columns (Amersham Biosciences) were equilibrated with RIPA, and 0.5 ml of alkylated proteins were applied to the column and eluted with RIPA containing protease inhibitors. Fractions (0.5 ml) were collected and the protein containing fractions (7-9) were pooled and pre-cleared with 100 μl of 50% rProtG agarose (Invitrogen) for 5 hours at 4°C. Meanwhile 20 μg of 51-8 RmAb was bound to 100 μl of 50% rProtG agarose in 1.0 ml RIPA containing 0.5 mg/ml BSA for 5 hours at 4°C. After removal of the beads from the lysate, the antibody bound beads were added. Immunoprecipitation proceeded overnight at 4°C, and the samples were then washed 4X with 1.0 ml RIPA. Bound proteins were eluted with SDS-PAGE sample buffer and analyzed by western blotting and silver staining.

Mass Spectrometry

Bands were excised from either a coomassie stained gel (c-Jun-GST) or a silver stained gel (Tpr) and subjected to in-gel tryptic digestion. Peptides were separated with nano-HPLC and sequenced by tandem mass spectrometry on a QSTAR-XL (Applied Biosystems). The spectra were submitted to the Mascot search engine to identify unmodified peptides and PNBM modified peptides were sequenced manually.

Additional methods

Detailed descriptions of all experiments are available in the **Supplementary Methods**.

ACKNOWLEDGEMENTS

The authors are thankful to D. Randle and D. Morgan for wild type Cdc5, D. Kenski for performing GRK2 kinase assays, H. Luecke for helpful suggestions, D. Maly for helpful comments on the manuscript, and V. Ohman for excellent administrative assistance. HeLa cells were provided by the NCCC. Supported by National Institute of Health (NIH) (NIBIB) R01 EB001987, and in part by NIH grant AA013588 and funds provided by the State of California for medical research on alcohol and substance abuse through the University of California at San Francisco (to R. Messing). J. Allen was funded by ARCS, Genentech, and the Sandler Foundation. Mass spectrometry was made possible by NIH grants NCRR RR015804 and NCRR RR001614.

Author Contributions

J.A., and K.S., wrote the manuscript. J.A., performed all experiments except those mentioned below. M. L., performed Erk2 substrate labelling reactions, C. B., performed mass spectrometry of modified peptides, J. P., expressed Cdc5, D. W., provided technical assistance for PKCδ experiments, A. H., constructed JNK1 plasmids, W. C., constructed PKCδ plasmids, A. B., advised C.B., R. M., advised D.W., W. C., and assisted in manuscript revision, C. K., constructed the AS Erk2 mouse, S. H., advised M. L. and C.K., K.S. advised J.A.

References

1. D. C. Berwick and J. M. Tavare, *Trends Biochem. Sci.* **29** (5), 227 (2004).
2. J. Ptacek and M. Snyder, *Trends Genet.* **22** (10), 545 (2006).
3. J. Ptacek, G. Devgan, G. Michaud et al., *Nature* **438** (7068), 679 (2005).
4. D. K. Morrison and R. J. Davis, *Annu. Rev. Cell Dev. Biol.* **19**, 91 (2003).
5. R. M. Biondi and A. R. Nebreda, *Biochem. J.* **372** (Pt 1), 1 (2003).
6. K. Shah, Y. Liu, C. Deirmengian et al., *Proc. Natl. Acad. Sci. U S A* **94** (8), 3565 (1997).
7. L. A. Witucki, X. Huang, K. Shah et al., *Chem. Biol.* **9** (1), 25 (2002).
8. J. A. Ubersax, E. L. Woodbury, P. N. Quang et al., *Nature* **425** (6960), 859 (2003).
9. N. Dephoure, R. W. Howson, J. D. Blethrow et al., *Proc. Natl. Acad. Sci. U S A* **102** (50), 17940 (2005).
10. W. C. Lee and K. H. Lee, *Anal. Biochem.* **324** (1), 1 (2004).
11. S. T. Eblen, N. V. Kumar, K. Shah et al., *J. Biol. Chem.* **278** (17), 14926 (2003).
12. A. Jaeschke, M. Karasarides, J. J. Ventura et al., *Mol. Cell* **23** (6), 899 (2006).
13. H. Wang, E. Shimizu, Y. P. Tang et al., *Proc. Natl. Acad. Sci. U S A* **100** (7), 4287 (2003).
14. X. Chen, H. Ye, R. Kuruvilla et al., *Neuron* **46** (1), 13 (2005).
15. J. J. Allen, S. E. Lazerwith, and K. M. Shokat, *J. Am. Chem. Soc.* **127** (15), 5288 (2005).
16. D. Sondhi, W. Xu, Z. Songyang et al., *Biochemistry* **37** (1), 165 (1998).
17. J. V. Olsen, B. Blagoev, F. Gnad et al., *Cell* **127** (3), 635 (2006).

18. C. Hoffman, Genieser, H.G., Veron, M., and Jastorff, B., *Bioorganic & Medicinal Chemistry Letters* **6** (21), 2571 (1996).

19. R.S. Goody, Eckstein, F., *J. Am. Chem. Soc.* **93** (23), 6252 (1971).

20. U. Kikkawa, H. Matsuzaki, and T. Yamamoto, *J Biochem (Tokyo)* **132** (6), 831 (2002).

21. K. S. Lee, J. E. Park, S. Asano et al., *Oncogene* **24** (2), 217 (2005).

22. C. R. Weston and R. J. Davis, *Curr. Opin. Genet. Dev.* **12** (1), 14 (2002).

23. W.A. Gaarde, Hunter, T., Brady, H., Murray, B.W., and Goldman, M.E., *Journal of Biomolecular Screening* **2** (4), 213 (1997).

24. C. Zhang, D. M. Kenski, J. L. Paulson et al., *Nat. Methods* **2** (6), 435 (2005).

25. J. Rush, A. Moritz, K. A. Lee et al., *Nat. Biotechnol* **23** (1), 94 (2005).

26. H. Zhang, X. Zha, Y. Tan et al., *J. Biol. Chem.* **277** (42), 39379 (2002).

27. J. A. Prescher and C. R. Bertozzi, *Nat. Chem. Biol.* **1** (1), 13 (2005).

28. K. Kikugawa, K. Iizuka, and M. Ichino, *J. Med. Chem.* **16** (4), 358 (1973).

29. M. Holzenberger, C. Lenzner, P. Leneuve et al., *Nucleic Acids Res.* **28** (21), E92 (2000).

Supplementary Information

Supplementary Figure 1a. Western Blot Analysis of α-hapten-IgY Specificity. HeLa lysates were treated with ATPγS and PNBM as shown and probed with affinity purified α-hapten-IgY.

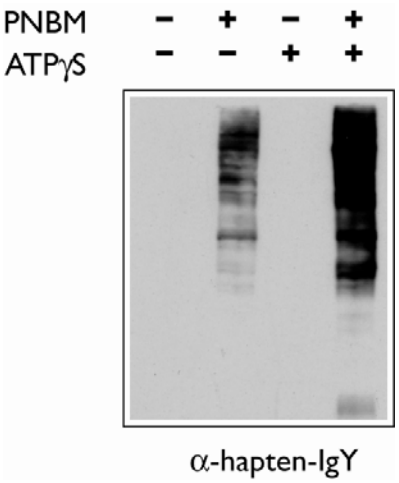

1b. Full Length Western Blots for Main Text **Figure 1c**

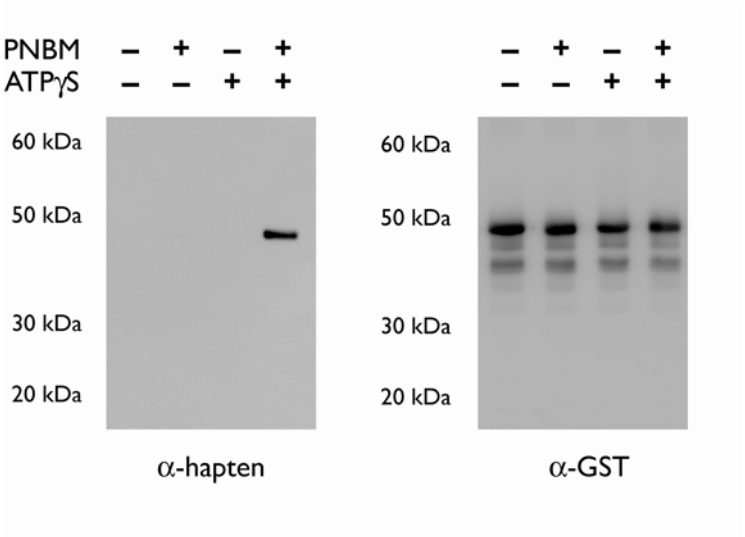

1c. Full Length Western Blots for Main Text **Figure 3**

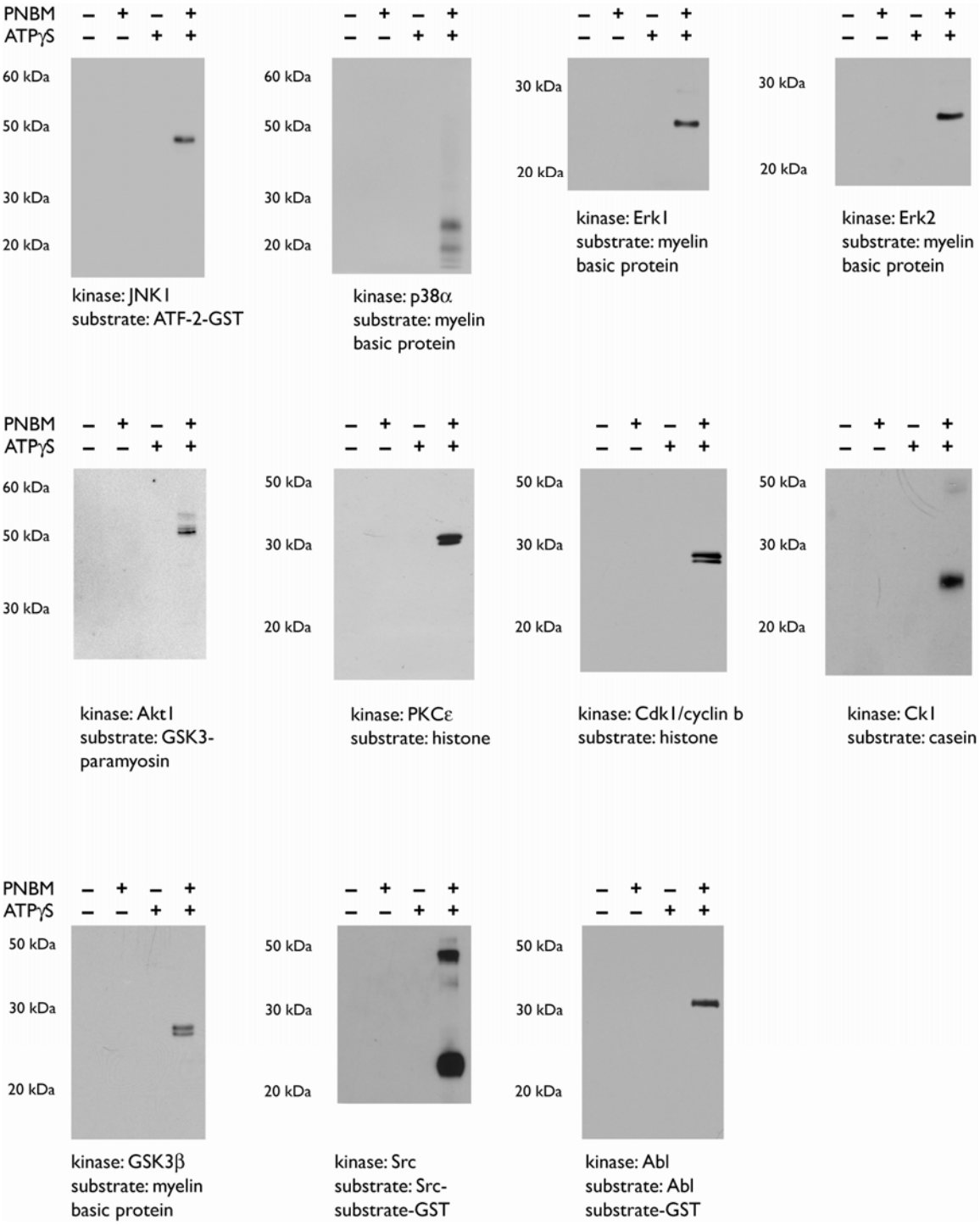

1d. Full Length Western Blots for Main Text **Figure 4**

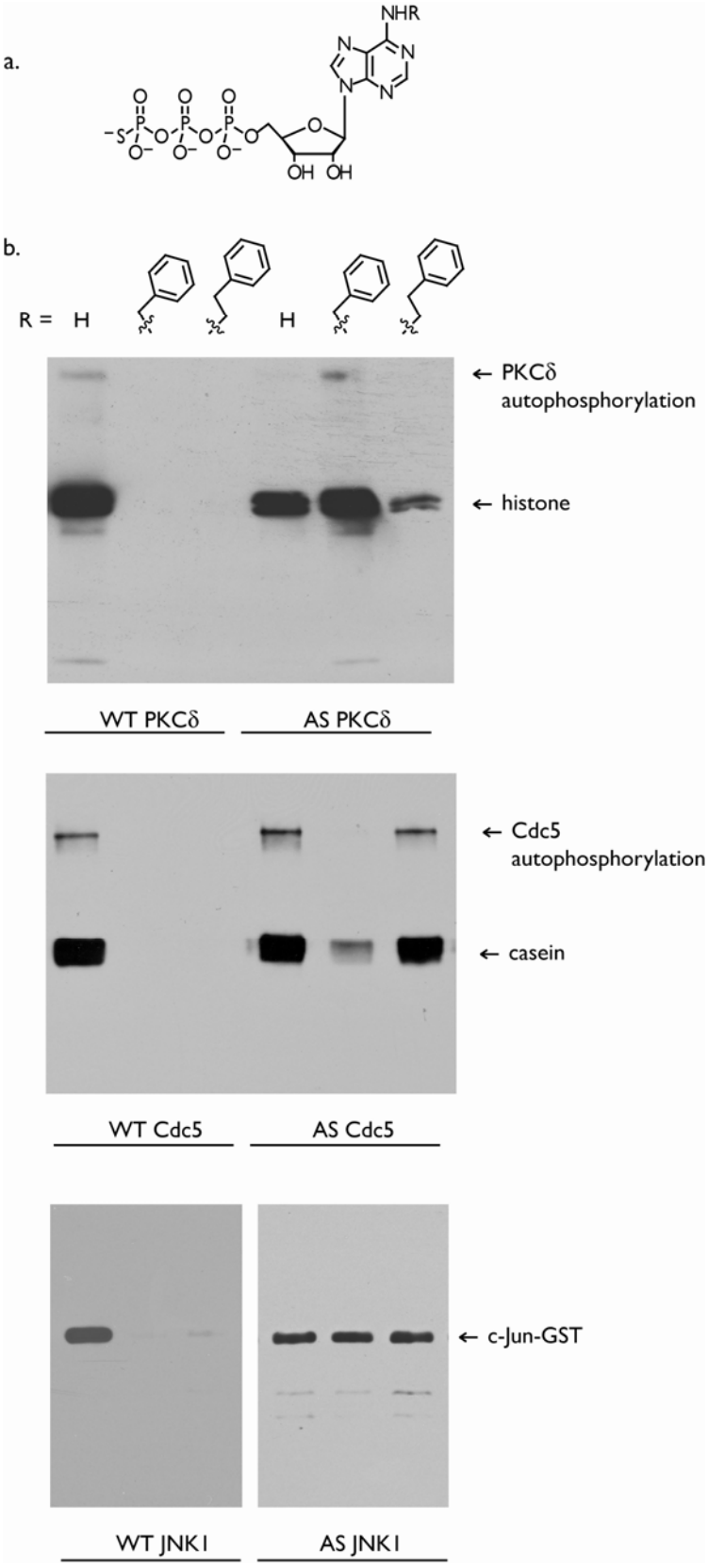

1e. Full Length Western Blots and Silver Stained Gel for Main Text **Figure 5**

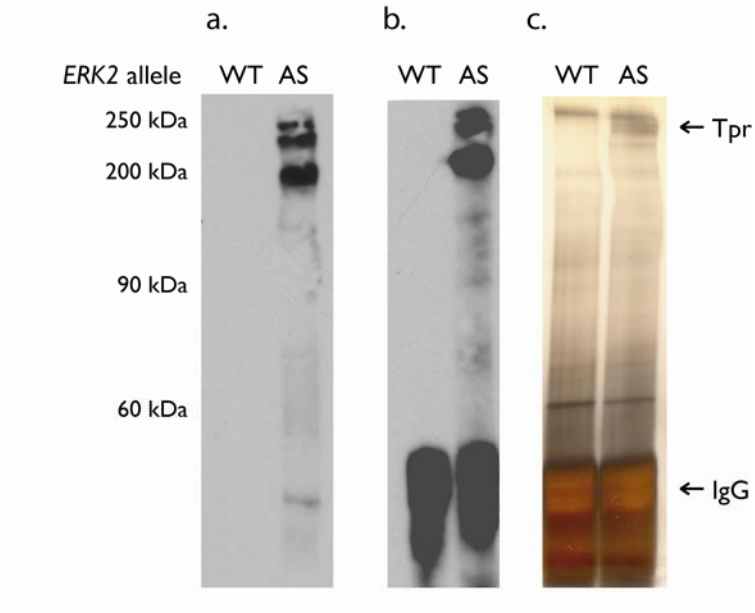

Supplementary Figure 2. Screen for Thiophosphate Ester Specific IgG

a.

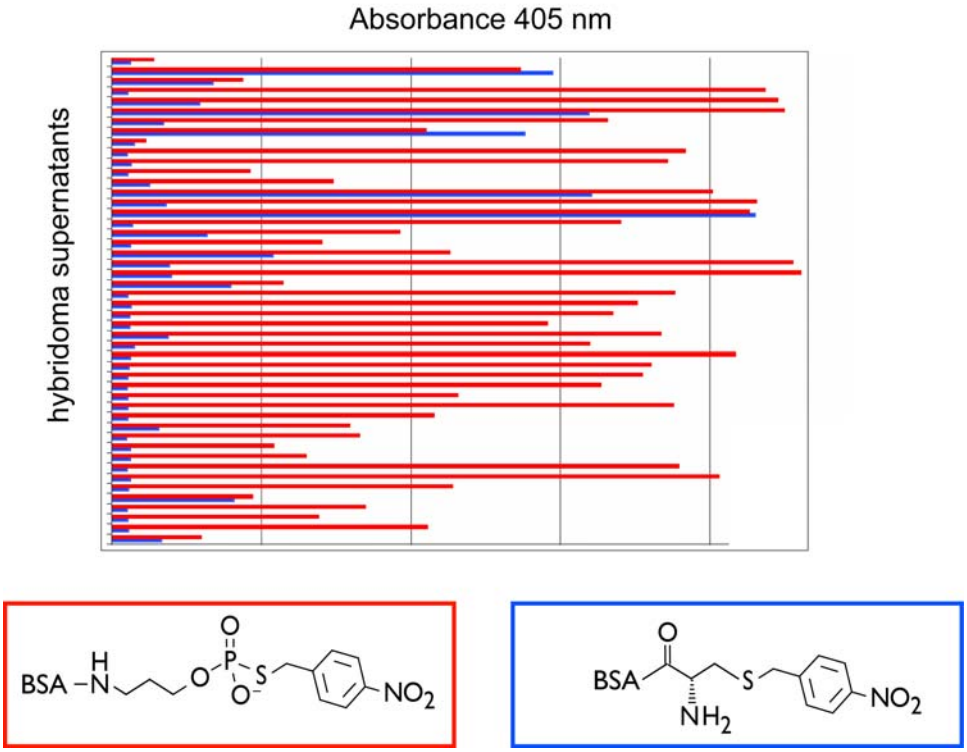

(a) ELISA of hybridoma supernatants. BSA-hapten (red bars) and BSA-thioether (blue bars) were coated and analyzed by indirect ELISA, each set of grouped bars represents one clone.

b.

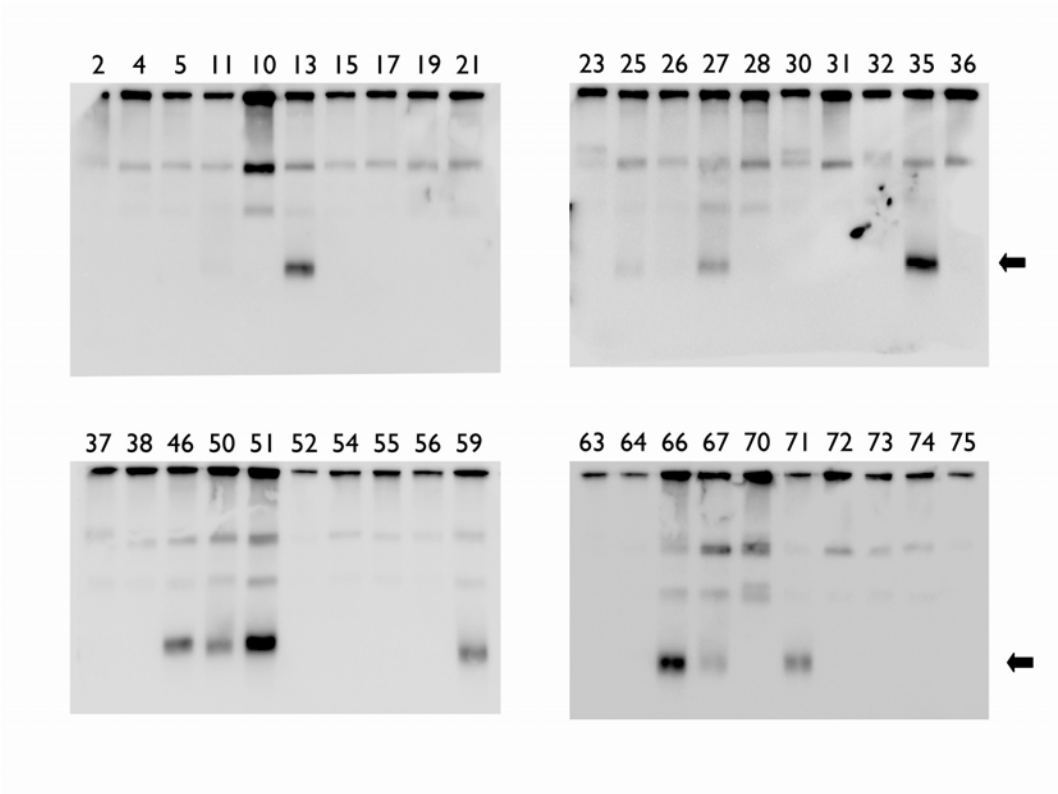

(b) Affinity tagged Histone H1 was immunoprecipitated with each hybridoma supernatant and analyzed by western blotting with polyclonal α-hapten-IgG. Antibody chains (upper bands) provide an estimation of the amount of antibody. The indicated band is immunoprecipitated Histone H1.

c.

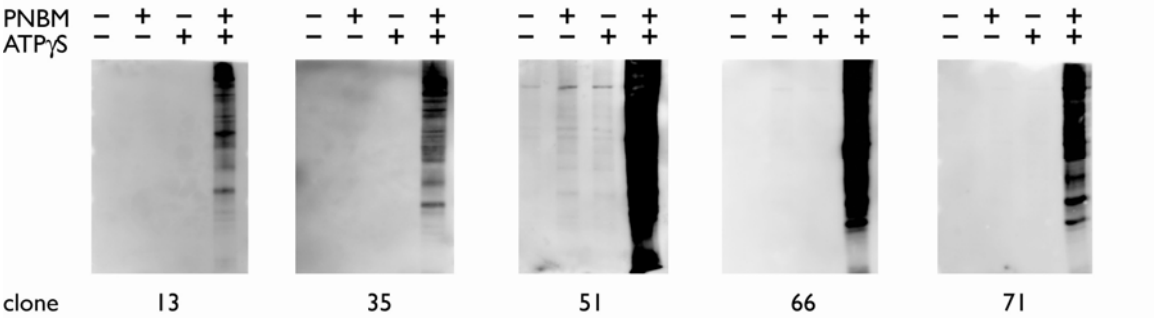

(c) HeLa lysate was treated as indicated and blotted with each hybridoma supernatant.

(d) Recognition of Labeled Kinase Substrates with RmAb 51-8 α-hapten-IgG

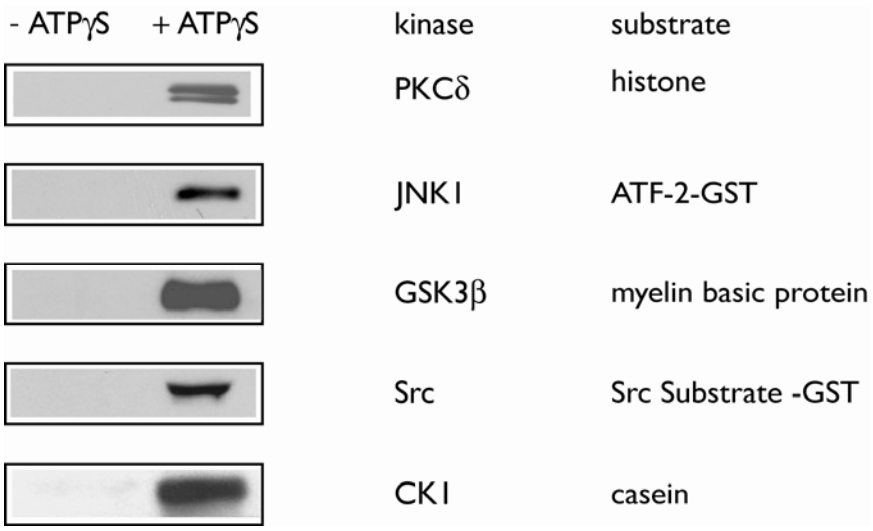

Supplementary Figure 3. Specificity and Yield of PNBM Alkylation

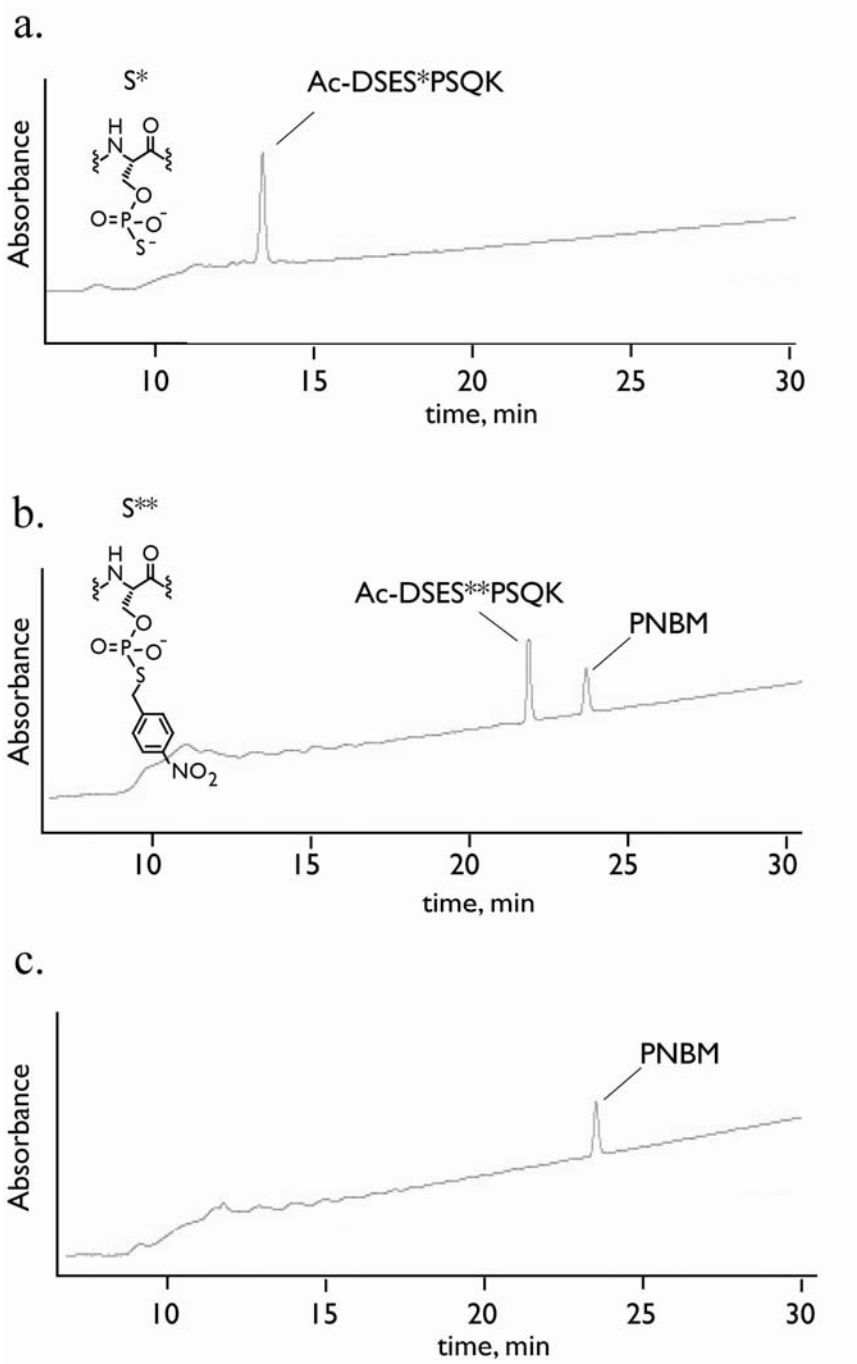

(a) HPLC elution profile of unmodified thiophosphopeptide. (**b)** Elution profile of the thiophosphate ester modified peptide. **(c)** PNBM only control. (Ac=acetyl, S*=thiophosphate modified serine, S**=thiophosphate ester modified serine)

d.

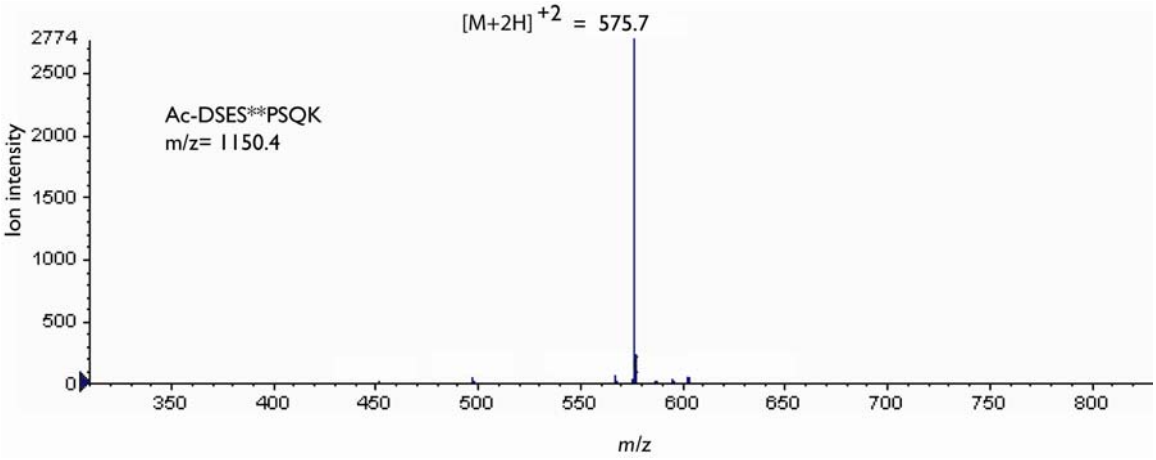

(d) Mass spectrometric analysis of the peptide that eluted at 22 minutes in **3b**. Note that the $[M+H]^+$ has a *m/z* of 1150.4.

Supplementary Figure 4. DELFIA for Thiophosphorylation Kinetics

(a) Time resolved fluorescence (TRF), in counts per second (cps), was measured as a function of the coating concentration of the PKCδ substrate, histone. 8 nM AS PKCδ, and 250 μM ATPγS were used in the thiophosphorylation reaction. (**b)** TRF was measured as a function of AS PKCδ concentration, ATPγS was used at 250 μM.

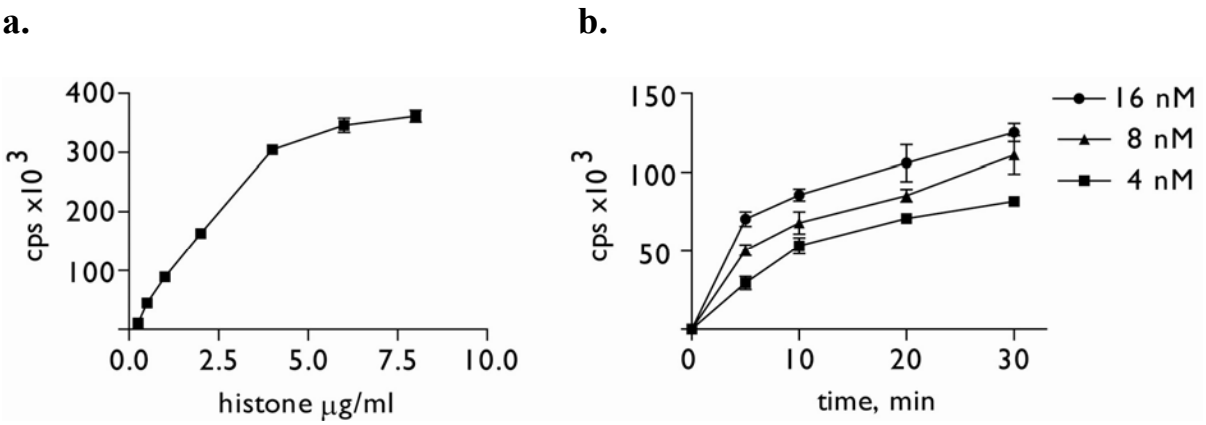

(**c)** Relative kinetic parameters for ATPγS and A*TPγS analogs. Error is represented as standard error about the mean. WT= wild-type, AS= analog specific

c.

	K_m (μM)	k_{cat} (cps/nM)	k_{cat}/K_m (cps · nM^2)
PKCδ WT: ATPγS	6.9 +/- 2.1	15,500 +/-1000	2.2 +/- 0.69
PKCδ AS: ATPγS	29 +/- 0.9	4,900 +/-900	0.17 +/- 0.06
PKCδ AS: N-6-benzyl-ATPγS	7.5 +/- 0.9	6,800 +/-670	0.91 +/- 0.22
Cdc5 WT: ATPγS	1.3 +/- 0.50	436,000 +/- 35,000	335 +/- 131
Cdc5 AS: ATPγS	1.7 +/- 0.75	90,700 +/-8,500	53 +/- 24
Cdc5 AS: N-6-phenethyl-ATPγS	1.2 +/- 0.52	156,000 +/- 13,000	130 +/- 58
JNK1 WT: ATPγS	0.78 +/-0.18	38,000 +/- 1,500	49 +/- 11
JNK1 AS: ATPγS	11 +/- 3.3	30,900 +/- 2,300	2.8 +/- 0.87
JNK1 AS: N-6-benzyl-ATPγS	3.6 +/- 1.2	15,100 +/- 1,100	4.2 +/- 1.4
JNK1 AS: N-6-phenethyl-ATPγS	4.5 +/- 1.3	22,800 +/- 1,400	5.0 +/- 1.5

Supplementary Figure 5. Synthesis of Hapten and Thioether Control

1a. Synthetic Scheme for Hapten (**4**) and Succinylated Hapten (**5**)

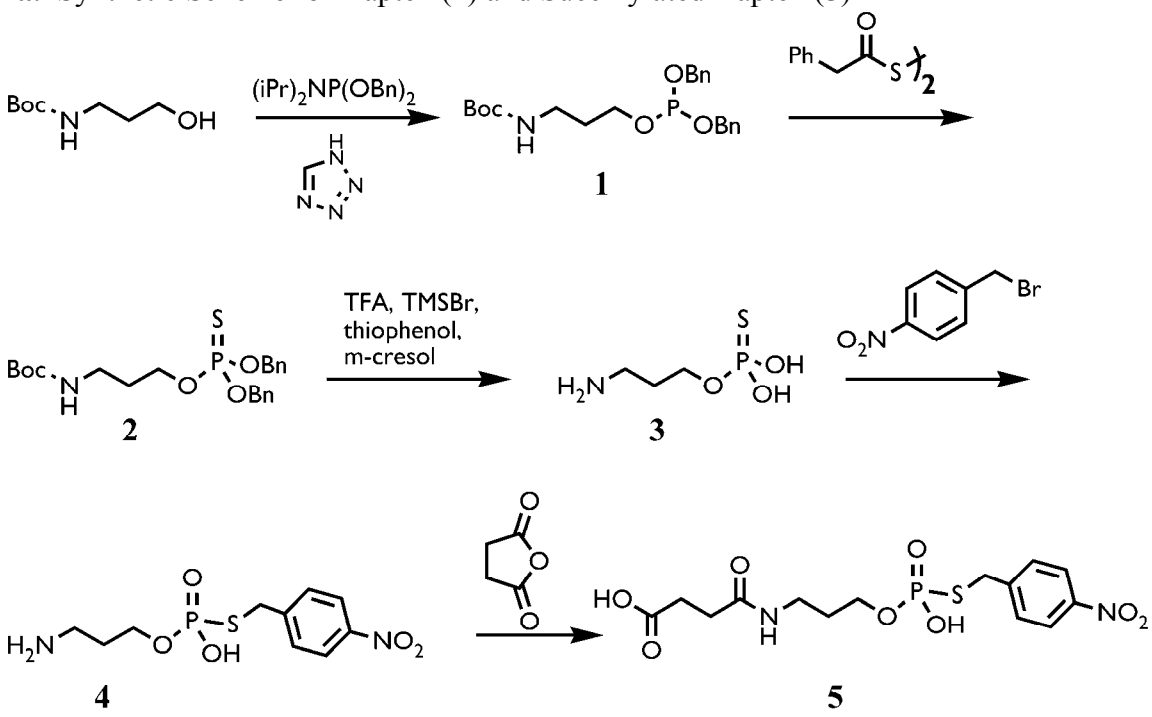

1b. Synthetic Scheme for Thioether Control (**9**)

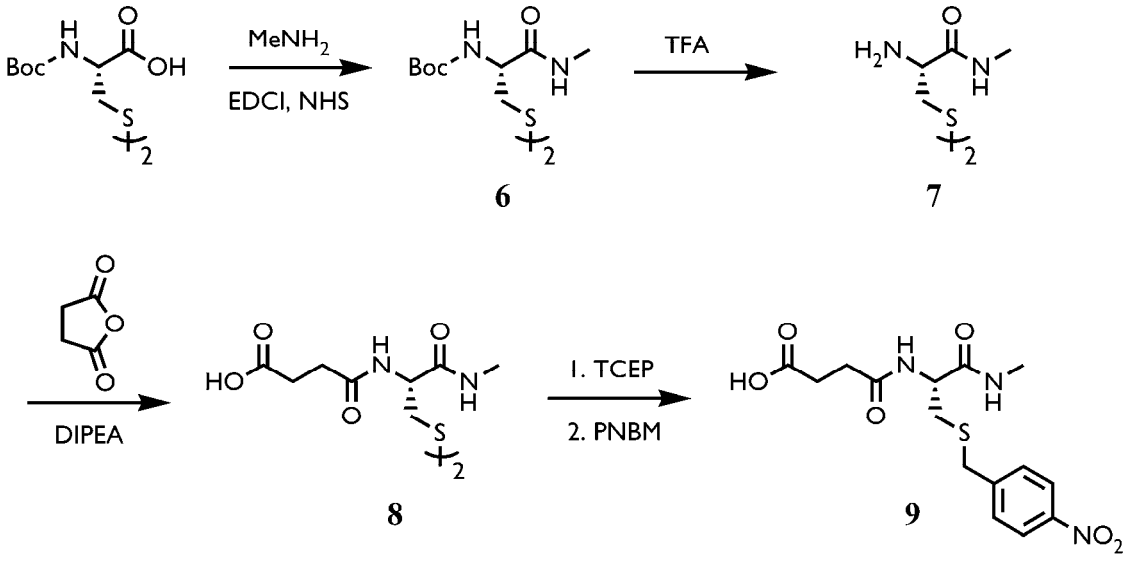

Supplementary Figure 6. Synthesis and Purification of A*TPγS Analogs

1a. A*TPγS Synthetic Scheme

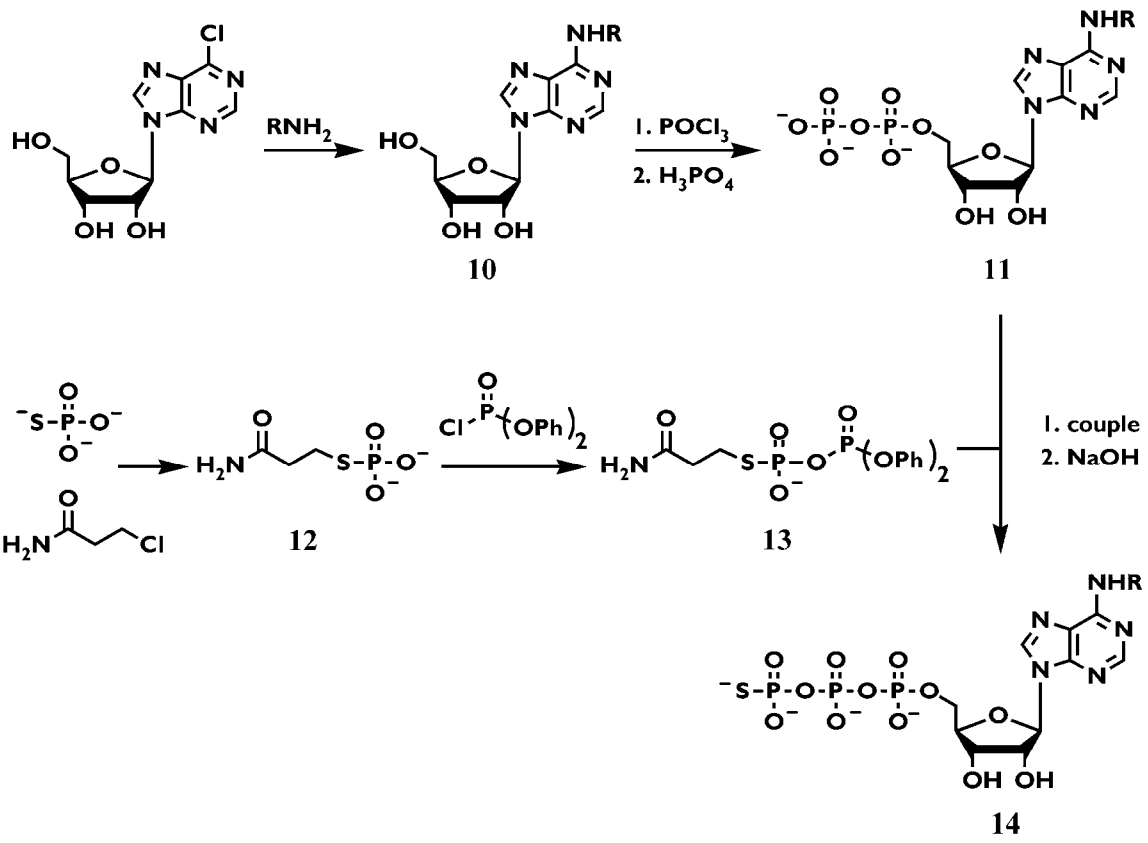

1b. FPLC Purification of N-6-benzyl ADP

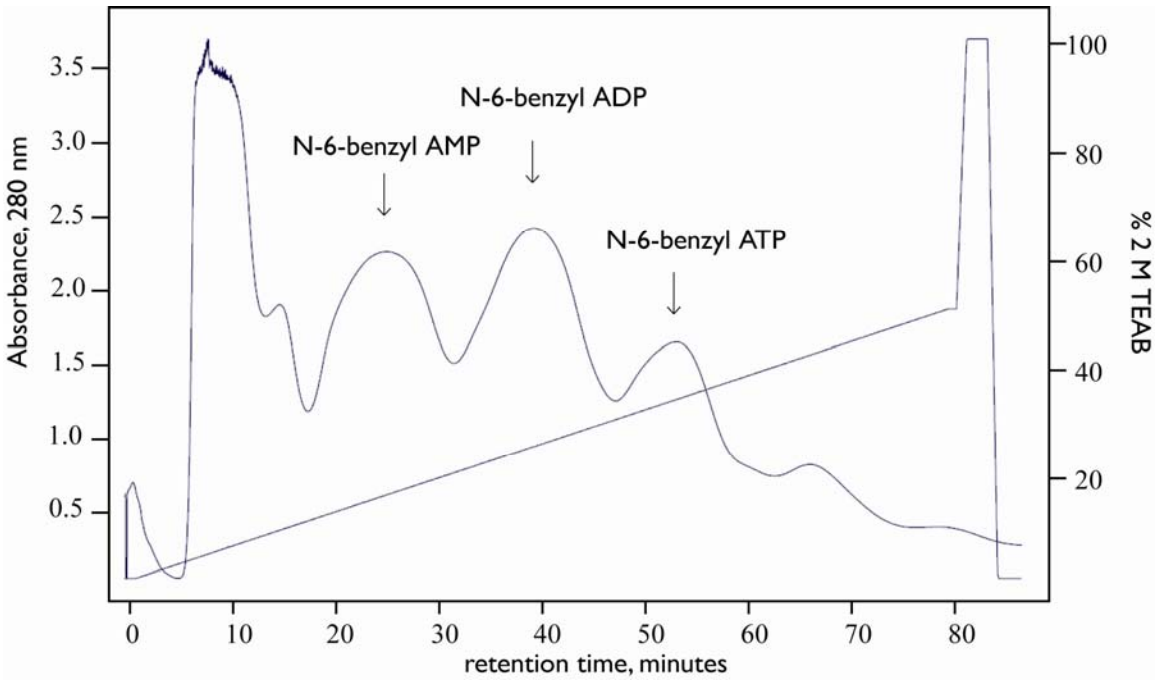

1c. FPLC Purification of N-6-benzyl ATPγS

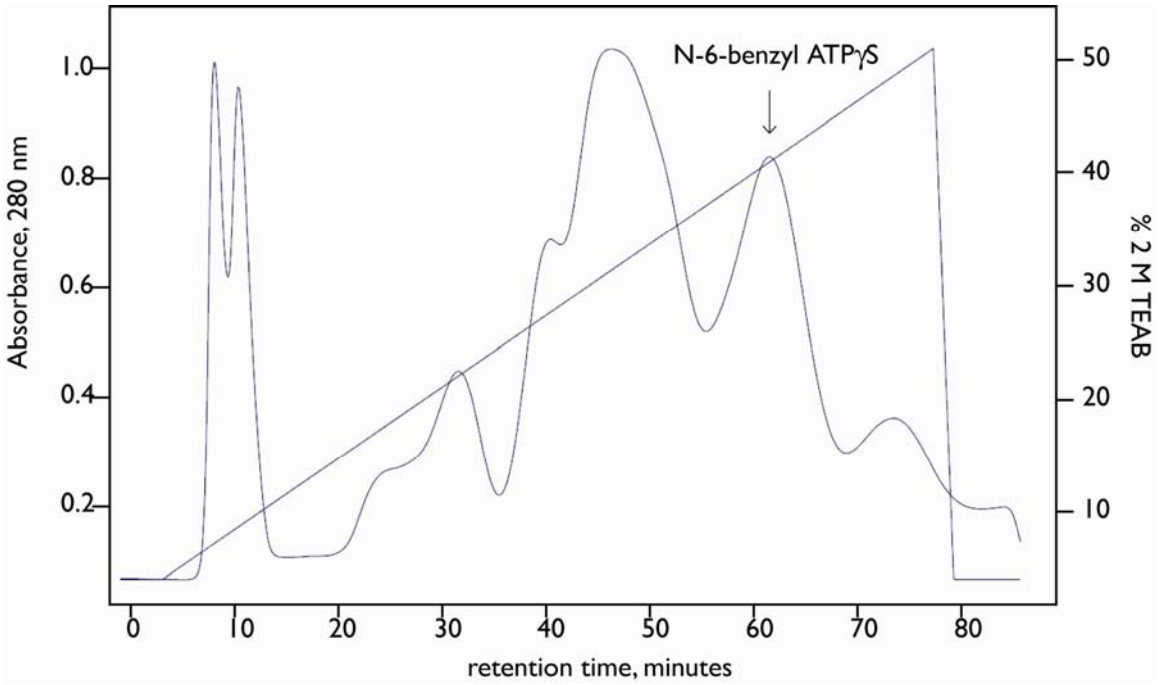

Supplementary Table 1. Kinases that have been studied using chemical genetics.

Mammalian	Yeast/Other
CAMIIKα[1]	Apg1[2]
Cdk7[3]	Cbk1[4]
Cdk1[5]	Cdc5[6]
Cdk2[5]	Cdc15[7]
ERK2[8]	Cdc28[9]
GRK2[10]	Elm1[11]
JNK1[12]	Ipl1[13]
JNK2[12]	Ime2[14]
p38 MAPK[15]	Ire1[16]
PKAα[17]	Kin28[18]
PKAβ[17]	Mek1[19]
Raf1[20]	Mps1[21]
BCR-Abl[22]	Pho85[23]
c-Src[24]	Prk1p[25]
v-erbB[26]	Pto[6]
Fyn[27]	Srb10[18]
Lck[28]	YpkA[29]
TrkA[30]	
TrkB[30]	
TrkC[30]	

REFERENCES (Supplementary Table 1)

1. Wang, H.; Shimizu, E.; Tang, Y. P.; Cho, M.; Kyin, M.; Zuo, W.; Robinson, D. A.; Alaimo, P. J.; Zhang, C.; Morimoto, H.; Zhuo, M.; Feng, R.; Shokat, K. M.; Tsien, J. Z., Inducible protein knockout reveals temporal requirement of CaMKII reactivation for memory consolidation in the brain. *Proc Natl Acad Sci U S A* **2003,** *100*, (7), 4287-92.

2. Abeliovich, H.; Zhang, C.; Dunn, W. A., Jr.; Shokat, K. M.; Klionsky, D. J., Chemical genetic analysis of Apg1 reveals a non-kinase role in the induction of autophagy. *Mol Biol Cell* **2003,** *14*, (2), 477-90.

3. Larochelle, S.; Batliner, J.; Gamble, M. J.; Barboza, N. M.; Kraybill, B. C.; Blethrow, J. D.; Shokat, K. M.; Fisher, R. P., Dichotomous but stringent substrate selection by the

dual-function Cdk7 complex revealed by chemical genetics. *Nat Struct Mol Biol* **2006,** *13*, (1), 55-62.

4. Weiss, E. L.; Kurischko, C.; Zhang, C.; Shokat, K.; Drubin, D. G.; Luca, F. C., The Saccharomyces cerevisiae Mob2p-Cbk1p kinase complex promotes polarized growth and acts with the mitotic exit network to facilitate daughter cell-specific localization of Ace2p transcription factor. *J Cell Biol* **2002,** *158*, (5), 885-900.

5. Polson, A. G.; Huang, L.; Lukac, D. M.; Blethrow, J. D.; Morgan, D. O.; Burlingame, A. L.; Ganem, D., Kaposi's sarcoma-associated herpesvirus K-bZIP protein is phosphorylated by cyclin-dependent kinases. *J Virol* **2001,** *75*, (7), 3175-84.

6. Zhang, C.; Kenski, D. M.; Paulson, J. L.; Bonshtien, A.; Sessa, G.; Cross, J. V.; Templeton, D. J.; Shokat, K. M., A second-site suppressor strategy for chemical genetic analysis of diverse protein kinases. *Nat Methods* **2005,** *2*, (6), 435-41.

7. D'Aquino, K. E.; Monje-Casas, F.; Paulson, J.; Reiser, V.; Charles, G. M.; Lai, L.; Shokat, K. M.; Amon, A., The protein kinase Kin4 inhibits exit from mitosis in response to spindle position defects. *Mol Cell* **2005,** *19*, (2), 223-34.

8. Eblen, S. T.; Kumar, N. V.; Shah, K.; Henderson, M. J.; Watts, C. K.; Shokat, K. M.; Weber, M. J., Identification of novel ERK2 substrates through use of an engineered kinase and ATP analogs. *J Biol Chem* **2003,** *278*, (17), 14926-35.

9. Ubersax, J. A.; Woodbury, E. L.; Quang, P. N.; Paraz, M.; Blethrow, J. D.; Shah, K.; Shokat, K. M.; Morgan, D. O., Targets of the cyclin-dependent kinase Cdk1. *Nature* **2003,** *425*, (6960), 859-64.

10. Kenski, D. M.; Zhang, C.; von Zastrow, M.; Shokat, K. M., Chemical genetic engineering of G protein-coupled receptor kinase 2. *J Biol Chem* **2005,** *280*, (41), 35051-61.

11. Sreenivasan, A.; Bishop, A. C.; Shokat, K. M.; Kellogg, D. R., Specific inhibition of Elm1 kinase activity reveals functions required for early G1 events. *Mol Cell Biol* **2003,** *23*, (17), 6327-37.

12. Ventura, J. J.; Hubner, A.; Zhang, C.; Flavell, R. A.; Shokat, K. M.; Davis, R. J., Chemical Genetic Analysis of the Time Course of Signal Transduction by JNK. *Mol Cell* **2006,** *21*, (5), 701-10.

13. Pinsky, B. A.; Kung, C.; Shokat, K. M.; Biggins, S., The Ipl1-Aurora protein kinase activates the spindle checkpoint by creating unattached kinetochores. *Nat Cell Biol* **2006,** *8*, (1), 78-83.

14. Benjamin, K. R.; Zhang, C.; Shokat, K. M.; Herskowitz, I., Control of landmark events in meiosis by the CDK Cdc28 and the meiosis-specific kinase Ime2. *Genes Dev* **2003,** *17*, (12), 1524-39.

15. Ulrich, S. M.; Sallee, N. A.; Shokat, K. M., Conformational restraint is a critical determinant of unnatural nucleotide recognition by protein kinases. *Bioorg Med Chem Lett* **2002,** *12*, (21), 3223-7.

16. Papa, F. R.; Zhang, C.; Shokat, K.; Walter, P., Bypassing a kinase activity with an ATP-competitive drug. *Science* **2003,** *302*, (5650), 1533-7.

17. Niswender, C. M.; Ishihara, R. W.; Judge, L. M.; Zhang, C.; Shokat, K. M.; McKnight, G. S., Protein engineering of protein kinase A catalytic subunits results in the acquisition of novel inhibitor sensitivity. *J Biol Chem* **2002,** *277*, (32), 28916-22.

18. Liu, Y.; Kung, C.; Fishburn, J.; Ansari, A. Z.; Shokat, K. M.; Hahn, S., Two cyclin-dependent kinases promote RNA polymerase II transcription and formation of the scaffold complex. *Mol Cell Biol* **2004,** *24*, (4), 1721-35.

19. Wan, L.; de los Santos, T.; Zhang, C.; Shokat, K.; Hollingsworth, N. M., Mek1 kinase activity functions downstream of RED1 in the regulation of meiotic double strand break repair in budding yeast. *Mol Biol Cell* **2004,** *15*, (1), 11-23.

20. Hindley, A. D.; Park, S.; Wang, L.; Shah, K.; Wang, Y.; Hu, X.; Shokat, K. M.; Kolch, W.; Sedivy, J. M.; Yeung, K. C., Engineering the serine/threonine protein kinase Raf-1 to utilise an orthogonal analogue of ATP substituted at the N6 position. *FEBS Lett* **2004,** *556*, (1-3), 26-34.

21. Jones, M. H.; Huneycutt, B. J.; Pearson, C. G.; Zhang, C.; Morgan, G.; Shokat, K.; Bloom, K.; Winey, M., Chemical genetics reveals a role for Mps1 kinase in kinetochore attachment during mitosis. *Curr Biol* **2005,** *15*, (2), 160-5.

22. Wong, S.; McLaughlin, J.; Cheng, D.; Zhang, C.; Shokat, K. M.; Witte, O. N., Sole BCR-ABL inhibition is insufficient to eliminate all myeloproliferative disorder cell populations. *Proc Natl Acad Sci U S A* **2004,** *101*, (50), 17456-61.

23. Dephoure, N.; Howson, R. W.; Blethrow, J. D.; Shokat, K. M.; O'Shea, E. K., Combining chemical genetics and proteomics to identify protein kinase substrates. *Proc Natl Acad Sci U S A* **2005,** *102*, (50), 17940-5.

24. Shah, K.; Liu, Y.; Deirmengian, C.; Shokat, K. M., Engineering unnatural nucleotide specificity for Rous sarcoma virus tyrosine kinase to uniquely label its direct substrates. *Proc Natl Acad Sci U S A* **1997,** *94*, (8), 3565-70.

25. Sekiya-Kawasaki, M.; Groen, A. C.; Cope, M. J.; Kaksonen, M.; Watson, H. A.; Zhang, C.; Shokat, K. M.; Wendland, B.; McDonald, K. L.; McCaffery, J. M.; Drubin, D. G., Dynamic phosphoregulation of the cortical actin cytoskeleton and endocytic machinery revealed by real-time chemical genetic analysis. *J Cell Biol* **2003,** *162*, (5), 765-72.

26. Fan, Q. W.; Specht, K. M.; Zhang, C.; Goldenberg, D. D.; Shokat, K. M.; Weiss, W. A., Combinatorial efficacy achieved through two-point blockade within a signaling pathway-a chemical genetic approach. *Cancer Res* **2003,** *63*, (24), 8930-8.

27. Ulrich, S. M.; Kenski, D. M.; Shokat, K. M., Engineering a "methionine clamp" into Src family kinases enhances specificity toward unnatural ATP analogues. *Biochemistry* **2003,** *42*, (26), 7915-21.

28. Denzel, A.; Hare, K. J.; Zhang, C.; Shokat, K.; Jenkinson, E. J.; Anderson, G.; Hayday, A., Cutting edge: a chemical genetic system for the analysis of kinases regulating T cell development. *J Immunol* **2003,** *171*, (2), 519-23.

29. Juris, S. J.; Shah, K.; Shokat, K.; Dixon, J. E.; Vacratsis, P. O., Identification of otubain 1 as a novel substrate for the Yersinia protein kinase using chemical genetics and mass spectrometry. *FEBS Lett* **2006,** *580*, (1), 179-83.

30. Chen, X.; Ye, H.; Kuruvilla, R.; Ramanan, N.; Scangos, K. W.; Zhang, C.; Johnson, N. M.; England, P. M.; Shokat, K. M.; Ginty, D. D., A chemical-genetic approach to studying neurotrophin signaling. *Neuron* **2005,** *46*, (1), 13-21.

Supplementary Methods

All chemicals and reagents were obtained from Sigma-Aldrich unless otherwise stated.

Synthesis of *p*-nitrobenzylmesylate (PNBM). *p*-nitrobenzyl alcohol (1.0 g, 6.5 mmol) in THF (10 mL) was treated with triethylamine (1.8 mL, 13 mmol), cooled to –10°C and treated dropwise with methanesulfonyl chloride (0.61 mL, 7.8 mmol). After stirring for 30 min (a precipitate formed during this time) 10% HCl (25 mL) was added. An additional 10 mL of water was added and the mixture was extracted twice with ethyl acetate. The combined organic layers were dried over Na_2SO_4 (anhyd), filtered and concentrated to afford an off-white solid in 93% yield. Analytical data was consistent with the literature[30]. ^{1}H NMR (400 MHz, DMSO-D6) δ 8.25 (d, 2H), 7.68 (d, 2H), 5.38 (s, 2H), 3.25 (s, 3H).

Hapten Synthesis (See **Supplementary Figure 5a**)

Dibenzyloxyphosphorothioate 2. 3-(Boc-amino)-1-propanol (203 mg, 1.2 mmol) was dissolved in 10.2 mL anhydrous dioxane and N,N-diisopropyl dibenzyl phosphoramidite (500 mg, 1.45 mmol) was added, followed by 1-H-tetrazole (122 mg, 1.7 mmol). After 1.5 hour phenylacetyl disulfide (807 mg, 2.9 mmol) was added and the mixture was stirred for 2 hours and then stored at –20°C overnight. The solvent was removed under reduced pressure and the residue was partitioned with ethyl acetate (50 mL) and water (50 mL). The organic layer was washed with brine, dried with Na_2SO_4, and concentrated to a light yellow oil. After flash chromatography (10-20% ethyl acetate, 90-80% hexanes) a clear viscous liquid was obtained (409 mg, 78% yield). ^{1}H NMR (400 MHz,

DMSO-D6) □.□□□.m, 10H), 5.02 (d, 4H), 3.96 (m, 2H), 2.91 (q, 2H), 1.65 (p, 2H), 1.32 (s, 9H). ESI-MS (*m/z*): $[M+H]^+$ calcd for $C_{22}H_{30}NO_5PS$, 452.16; found, 452.13.

Hapten 4. A mixture of dibenzyloxyphosphorothioate **2** (100 mg, 0.22 mmol), *m*-cresol (0.46 mL, 4.4 mmol), and thiophenol (0.45 mL, 4.4 mmol) was cooled to 0 □C and treated with trifluoroacetic acid (2.95 mL) and bromotrimethylsilane (0.57 mL, 4.4 mmol). The mixture was stirred at 0□C for 1.5 hour and then diluted with 2 mL toluene and concentrated under reduced pressure. An additional 2 mL of toluene was added and the mixture was concentrated again. The residue was partitioned between 5 mL H_2O and 5 mL pentane. The pentane was discarded and the aqueous layer washed with an additional 5 mL of pentane. *p*-nitrobenzyl bromide (95 mg, 0.442 mmol) was dissolved in 1 mL of ethanol and added to the aqueous layer containing **3**. The pH was adjusted to 8.5 with saturated Na_2CO_3, and allowed to stir at RT for 2 hours. After extraction with 5 mL pentane the aqueous layer was filtered and separated by high performance liquid chromatography (HPLC) (^{18}C prep column, 60 min gradient, H_2O-CH_3CN 95:5 to H_2O-CH_3CN 40:60, 250 nm). The fractions containing the hapten (25 min) were collected and lyophilized to afford a white powder (15 mg, 22% yield over two steps). ^{1}H NMR (400 MHz, DMSO-D6) □.□□.m, 2H), 7.57 (m, 2H), 3.86 (d, 2H), 3.62 (m, 2H), 2.76 (t, 2H), 1.65 (p, 2H). ESI-MS (*m/z*): $[M+H]^+$ calcd for $C_{10}H_{15}N_2O_5PS$, 307.04; found, 307.07.

Hapten-KLH. Hapten **4** (5 mg, 0.016 mmol) was added to 1 mL of a 5 mg/mL solution of succinylated keyhole limpet hemocyanin solution (KLH). *N*-Ethyl-*N*'-(3-dimethylaminopropyl)carbodiimide HCl (EDCI) (50 mg, 0.26 mmol) and N-

hydroxysulfosuccinimide (Sulfo-NHS) (Pierce) (57 mg, 0.261 mmol) were added. The pH was adjusted to 8 with 1 M NaOH and the coupling proceeded overnight at RT (RT). The mixture was purified on a PD-10 column (Amersham Biosciences), using PBS as the eluent. Protein concentration was determined by Bradford assay (1.3 mg/mL), and the number of hapten molecules/ KLH (260 hapten molecules/KLH molecule) was determined by standard curves of hapten and KLH absorbances at 280 nm. A Hapten-BSA conjugate was prepared using this same procedure (100 hapten molecules/KLH molecule).

Succinylated Hapten 5. Hapten **4** (9.2 mg, 0.03 mmol) was dissolved in 0.4 mL N,N-diethylformamide (DMF) then diisopropyl ethylamine (DIPEA) (10 μL, 0.06 mmol) and succinic anhydride (3.6 mg, 0.036 mmol) were added. The reaction proceeded for 16 hours at RT. The solvent was removed under reduced pressure and the resulting oil was dissolved in 2 mL 1:4, acetonitrile:H_20 and separated by HPLC (^{18}C prep column, 60 min gradient, H_2O-CH_3CN 95:5 to H_2O-CH_3CN 40:60, 250 nm), using the same solvent and gradient as described for hapten **4**; the fractions containing the product (30 min) were lyophilized to afford a clear oil (11 mg, 90% yield). ESI-MS (*m/z*): $[M+H]^+$ calcd for $C_{14}H_{19}N_2O_8PS$, 407.06; found, 407.09.

Affinity Column Containing Succinylated Hapten 5. An affinity purification column was prepared as follows: diaminodipropyl amine gel (2 mL, 16-20 μmol/mL, Pierce) was placed in a small fritted column. Buffer was allowed to drain off and the remaining solid was washed with PBS (6 mL). Succinylated hapten **5** (10 mg, 0.025 mmol) in

conjugation buffer (2 mL, 0.1 M MES, 0.9% NaCl, pH= 7.4) was added to the washed column, followed by EDCI (60 mg, 0.312 mmol) and Sulfo-NHS (60 mg, 0.274 mmol) in conjugation buffer (0.5 mL). The ends of the column were capped and the column was placed on a rotator overnight at RT. The column was drained, washed with 10 mL of 1 M NaCl, and stored at 4°C in PBS with 0.05% sodium azide until use.

Purification of Polyclonal IgG and IgY. The affinity column was washed with PBS (10 mL), and 5 mL of total immune IgY (Aves Labs) or total immune IgG (Epitomics) was added. The column was drained until the anti-sera had fully entered the beads. Unbound antibodies were washed from the column with 150 mL PBS and bound antibodies were eluted with acidic elution buffer (0.1 M glycine, pH=2.8), followed by basic elution buffer (0.1 M triethylamine pH 11). Individual fractions (1 mL) were immediately neutralized with 50 □l 1M TRIS, pH= 9.5 or 50 □l 1M TRIS, pH= 3.5. Fractions were pooled, concentrated, and exchanged into PBS with an Amicon centrifugal 10,000 MWCO filter as per the manufacturer's instructions. Absorbance at 280 nm was used to determine the concentration (1 Au ~ 0.75 mg/mL): α-hapten-IgY (3.7 mg/mL, 900 µL recovered) and α-hapten-IgG (5.1 mg/mL, 500 µL recovered).

Synthesis of Thioether Control (See **Supplementary Figure 5b**)

6. N, N'-bis-Boc-L-cysteine (Novabiochem) (750 mg, 1.7 mmol) was dissolved in 8.5 mL of dichloromethane. NHS (469 mg, 4.1 mmol), EDCI (782 mg, 4.1 mmol), and

methylamine (4.25 mL of 2M in MeOH, 8.5 mmol) were added and the mixture was stirred overnight at RT. 50 mL of ethyl acetate was added and the mixture was washed with 50 mL of saturated sodium carbonate, followed by 50 mL of 10% citric acid. The organic layer was dried with Na_2SO_4 and concentrated under reduced pressure to afford 630 mg of white powder. The major product was the bisamide **6**: ESI-MS (*m/z*): $[M+H]^+$ calcd for $C_{18}H_{34}N_4O_6S_2$, 467.19; found, 467.1. A small amount of the monoamide was also formed: ESI-MS (*m/z*): $[M+H]^+$ calcd for $C_{17}H_{31}N_3O_7S_2$, 454.16; found, 454.1. This mixture was deprotected without further purification.

7. Crude **6** was dissolved in 5 mL TFA, 4.8 mL dichloromethane, and 200 µL water. The mixture was stirred at RT, and appearance of the free amine was monitored by TLC and ninhydrin staining. After two hours 30 mL toluene was added and the mixture was concentrated under reduced pressure. 580 mg of crude product was obtained: ESI-MS (*m/z*): $[M+H]^+$ calcd for $C_8H_{18}N_4O_2S_2$, 267.09; found, 267.2.

8. Crude **7 (**290 mg, 0.58 mmol) was dissolved in 5.8 mL of dichloromethane and then DIPEA (300 µL, 2.3 mmol) was added. Another 1.5 mL of DMF was added to further solubilize **7**, followed by succinic anhydride (139 mg, 1.4 mmol). The reaction proceeded overnight at RT, disappearance of the amine was monitored by TLC and ninhydrin staining. Ethylene diamine (0.5 mL, 7.5 mmol) was added to quench excess succinic anhydride. After stirring for one hour, ethyl acetate (50 mL) and 1 M HCl (50 mL) were added. The aqueous layer was lyophilized and purified with HPLC (^{18}C prep

column, 60 min gradient, H_2O-CH_3CN 0.1% TFA 95:5 to H_2O-CH_3CN 0.1% TFA 40:60, 215 nm). ESI-MS (*m/z*): $[M+H]^+$ calcd for $C_{16}H_{26}N_4O_8S_2$, 467.12; found, 467.1.

9. **8** (27 mg, 0.058 mmol) was dissolved in 1.2 mL H_2O and the pH was adjusted to 7.5 with saturated Na_2CO_3. Tris(2-carboxyethyl)phosphine HCl (TCEP) (33 mg, 0.12 mmol) was added and reduction proceeded at RT for 2 hours. *p*-nitrobenzyl mesylate (PNBM) (37 mg, 0.16 mmol), dissolved in 1.0 mL DMF, was added and the reaction proceeded overnight at RT. The reaction mixture was washed with 5 mL of pentane and concentrated under reduced pressure. HPLC purification was performed as described for **8**. ESI-MS (*m/z*): $[M+H]^+$ calcd for $C_{15}H_{19}N_3O_6S$, 370.10; found, 370.1.

Thioether-BSA

9 was coupled to BSA as described for hapten-KLH. The coupling ratio was 10 molecules of **9**/BSA molecule).

ELISA

96 well plates (Nunc Immunosorb) were coated overnight at 4º C with 2.5 μg/mL of BSA, BSA-hapten, or BSA-thioether in 50 μL/well of PBS. The wells blocked with 200 μL of 1% BSA in PBST (PBS with 0.05% Tween 20) for 1 hour at RT and washed twice with 200 μL PBST. 50 μL of each hybridoma supernatant was added and allowed to bind overnight at 4º C. The wells were washed as above and 100 μL/well of goat α-rabbit-IgG –HRP (Promega), diluted 1:2,000 in 0.25% BSA PBST was added. After 45 minutes at RT the plates were developed as described.[15]

HeLa lysate labeling

HeLa-S3 cell pellets ($0.75x10^9$ cells) were obtained from the National Cell Culture Center (NCCC). After thawing, 10 mL of RIPA lysis buffer (50 mM Tris pH 8, 150 mM NaCl, 1.0% NP-40, 0.1% SDS, with protease inhibitors (Roche, complete)) was added and the cells were rotated at 4ºC for 15 minutes. After centrifugation at 20,000 g for 10 minutes the supernatant was decanted and used for kinase assays. Alternatively the lysate could be stored at -80ºC. For assays of wild type cellular kinases, HeLa lysate (15 mg/mL in RIPA lysis buffer) was diluted 1:1 with 10 mM HEPES pH 7.4, 150 mM NaCl, 10 mM $MgCl_2$ in the presence or absence of 1 mM ATPγS. After 30 minutes at RT PNMB in DMSO (final concentration was 2.5 mM PNBM, 5% DMSO) or DMSO was added. Alkylation proceeded for 2 hours at RT, and the lysates were analyzed by western blotting.

Immunoprecipitation of Histone H1 with Hybridoma Supernatants.

100-200 µL of each hybridoma cell culture supernatant (Epitomics) was bound to 50 µL of a 50% slurry of rProtG agarose (Invitrogen) in a total volume of 500 µL RIPA. Antibodies bound to the beads for 2 hours at 4°C. The supernatant was removed and 500 µL of RIPA containing 0.4 mg/mL BSA and 2 µg affinity tagged H1 (prepared as described[15]) was added. Immunoprecipitations proceeded overnight at 4°C. The beads were washed three times with 1.0 mL RIPA and eluted with SDS-PAGE sample buffer (DTT was omitted to keep antibody molecules intact). The immunoprecipitates were analyzed by polyclonal α-hapten-IgG western blotting.

Purification of Rabbit Monoclonal Antibody (RmAb 51-8)

Concentrated tissue culture supernatant (Epitomics) was purified with an Immunopure IgG Purification Kit (Pierce), according to the manufacturers' instructions. The eluted fractions were pooled, concentrated, and exchanged into PBS using a 10,000 MWCO centrifugal filter (Amicon), according to the manufacturer's instructions. Absorbance at 280 nm was used to determine the concentration (1 Au ~ 0.75 mg/mL): RmAb 51-8 α-hapten-IgG (5.0 mg/mL, 750 μL recovered).

Synthesis of Thiophosphorylated Peptide (Ac-DSES*PSQK)

FMOC-L-Lys(Boc)-Wang Resin (120 mg) (Novabiochem) was swollen with DMF (EM Science, peptide synthesis grade) in a 3 mL syringe vessel (Isolute®). Synthesis was performed using standard FMOC solid phase peptide synthesis, with diisopropylcarbodiimide (DIC)/1-hydroxybenzotriazole (HOBT) (Novabiochem) activation of amino acids. The amino acids were protected as follows FMOC-Asp(Boc)-OH, FMOC-Glu(Boc)-OH, FMOC-Ser(OtBu)-OH, FMOC-Gln(trt)-OH. The N-terminus was acetylated using the same coupling procedure, by substituting the amino acid with acetic acid. For example, 0.48 mmol of FMOC-Ser-OH and 74 mg HOBT were dissolved in 1.2 mL DMF and then activated with 70 μL DIC for 10 minutes. The mixture was added to the washed resin and reacted at room temperature for 3 hours and then washed with DMF. The FMOC protecting group was removed after each coupling by treatment with 20% piperidine in DMF for 20 minutes. As described[31], the serine to be thiophosphorylated was incorporated as the unprotected FMOC-Ser-OH. After the

solid phase synthesis was complete the resin was washed (three times with DMF, three times with dichloromethane, three times with methanol), dried overnight in a vacuum desiccator, and flushed with argon. A solution containing 1-H-tetrazole (1.4 mmol, 100 mg (obtained from concentration of a 3% solution in acetonitrile)), dibenzyl N,N-diisopropylphosphoramidite (0.47 mmol, 167 μL), and anhydrous DMF (1.6 mL) were added to the dried resin and allowed to react for 1.0 hour at RT with rotation. The resin was then washed (three times with DMF, three times with acetonitrile) and reacted with phenylacetyl disulfide (0.66 mmol, 204 mg) in acetonitrile (1.6 mL) for two hours at RT with rotation. The resin was washed (three times with DMF, three times with dichloromethane, three times with methanol, three times with dichloromethane) and treated with a cleavage cocktail (67% trifluoroacetic acid (TFA), 11.5% trimethylsilyl bromide, 10.4% thiophenol, and 10.4% m-cresol) for 2 hours at RT. After *in vacuo* concentration and filtration the peptide was HPLC purified (^{18}C prep column, 60 min gradient, H_2O-CH_3CN 98:2 to H_2O-CH_3CN 60:40, 215 nm) and lyophilized to afford a white powder. ESI-MS (*m/z*): $[M+H]^+$ calcd for $C_{36}H_{60}N_{10}O_{20}PS$, 1015.34; found, 1015.10.

Alkylation and Analytical HPLC of Thiophosphorylated Peptide (See **Supplementary Figure 3)**

Peptide (Ac-DSES*PSQK, 750 μM) in 10 mM HEPES pH 7.4, 150 mM NaCl, 10 mM $MgCl_2$ was treated with DMSO or PNMB in DMSO (final concentration 2.5 mM PNBM, 5% DMSO) for 1 hour at RT. The reaction was diluted and a portion was analyzed by HPLC (^{18}C analytical column, 60 min gradient, H_2O-CH_3CN 98:2 to H_2O-CH_3CN 70:30,

215 nm). Mass spectrometric analysis of the peak eluting at 22 minutes was performed on a QSTAR XL (Applied Biosystems) as described for c-Jun-GST.

Synthesis of A*TPγS (see **Supplementary Figure 6a**)

N-6-benzyladenosine (**10, R=benzyl**) is commercially available (Acros Organics).

N-6-phenethyladenosine (10, R=phenethyl)

6-chloropurine ribonucleoside (3.5 mmol) was refluxed overnight in ethanol (21 mL) containing phenethylamine (21 mmol) as described[28]. After evaporation *in vacuo*, 150 mL of ethanol was added and the mixture was crystallized at 4°C for 5 hours. The crystals were filtered, washed with ice cold ethanol, and obtained in 51% yield. Higher yields could be obtained by performing another round of crystallization on the remaining liquid. ESI-MS (*m/z*): $[M+H]^+$ calcd for $C_{18}H_{21}N_5O_4$, 372.16; found, 372.22.

N-6- benzyl-ADP (11, R=benzyl) and N-6-phenethyl-ADP (11, R=phenethyl)

Formation of the intermediate dichlorophosphate was performed essentially as described[32], with slight modifications. 2 mmol of **10** (R=phenethyl or R=benzyl) was dissolved in 5 mL of triethylphosphate (TEP) and cooled to 0°C. $POCl_3$ (4 mmol) was added dropwise and the mixture was stirred at 0°C for two hours. To form the diphosphates[18] a mixture of 10 mmol of H_3PO_4 (solid) and 10 mmol 1,8-diazabicyclo[5.4.0]undec-7-en (DBU) in 5 mL of TEP was added. Formation of a light yellow solid was instantaneous and after two minutes the reaction was quenched with 30 mL of 0.1M triethylammonium bicarbonate (TEAB). After stirring at for 30 minutes at RT the reaction was filtered with a PTFE syringe filter (0.45 μm, Acrodisk). Aliquots of

the reaction were purified by strong anion exchange chromatography on an Acta FPLC (Amersham Biosciences). Two HiPrep 16/10 QFF anion exchange columns (Amersham Biosciences) were set up in series and the products were separated using an 80 min gradient (100% 0.1 M TEAB to 50:50 0.1M TEAB: 2M TEAB, 280 nm (see **Supplementary Fig. 6b**)). TEAB was prepared by bubbling CO_2 into a 2 M solution of triethylamine. The fractions containing the diphosphate (33-43 min) were pooled and lyophilized*, yields for the ADP analogs ranged from 25-30%. For N-6-benzyl-ADP, ESI-MS (*m/z*): $[M-H]^-$ calcd for $C_{17}H_{21}N_5O_{10}P_2$, 516.08; found, 516.10. For N-6-phenethyl-ADP, ESI-MS (*m/z*): $[M-H]^-$ calcd for $C_{18}H_{23}N_5O_{10}P_2$, 530.08; found 530.10. Significant amounts of the AMP and ATP analogs are also obtained in this synthesis.

Disodium S-2-Carbamoylethyl Phosphorothioate (12).

This procedure is adapted from Cook[33], with the substitution of trisodium thiophosphate for trilithium thiophosphate. A solution of trisodium thiophosphate (18.6 mmol) in 28 mL of water was treated with a solution of 3-chloropropionamide (28 mmol) in 5.6 mL of DMF for 48 hours at RT. The reaction was then filtered and 100 mL of ethanol was added to the filtrate. Upon addition a white precipitate formed, to increase the size of the crystals an additional 100 ml of ethanol was added and the mixture was chilled at 4ºC overnight. The precipitate was then filtered, washed with ethanol, and dried *in vacuo* to afford disodium S-2-carbamoylethyl phosphorothioate (**12**) in 86% yield. ^{1}H NMR (400 MHz, MeOH-D4 with D_2O) □̣□̃□□̣m, 2H), 2.63 (t, 2H). ESI-MS (*m/z*): $[M-H]^-$ calcd for $C_4H_8NO_4PS$, 183.99; found, 184.00.

13.

This procedure is adapted from Goody et al[19]. Disodium S-2-carbamoylethyl phosphorothioate (**12**) (2.0 mmol) was dissolved in 10 mL of methanol:H_20 (1:1) and applied to a column containing DOWEX® 501-X8 ion exchange resin (5 mL, pyridinium form**). The pyridinium salt of **12** was eluted with another 10 mL of methanol:H_20 (1:1). Solvent was removed *in vacuo* and 20 mL of methanol was added to the residue, which was then converted to the mono(tri-*n*-octylammonium) salt by addition of tri-*n*-octylamine (2 mmol). Again the solvent was removed *in vacuo* and the residue was dried by repeated evaporation (twice) of 10 mL aliquots of dry DMF. The residue was dissolved in dioxane (14 mL) and diphenyl phosphorochloridate (0.6 mL) was added, followed by tri-*n*-butylamine (0.92 mL). The reaction proceeded at RT for 2 hours, with stirring. The solvent was removed under reduced pressure and ether (20 mL) was added. After the residue had dissolved warm petroleum ether (40 mL) was added and the mixture was chilled at 4°C for 30 minutes. An oily residue separated and the supernatant was decanted. The residue was then dissolved in 10 mL of dioxane and the solvent was removed under reduced pressure. At this point the reaction was split and put on a high vacuum line for one hour and then stored overnight at -20ºC. The reaction product was not characterized, and 100% yield was assumed.

N-6-benzyl-ATPγS (14, R=benzyl) and N-6-phenethyl-ATPγS (14, R=phenethyl)

Either N-6- benzyl-ADP (**11**, R=benzyl) (0.3 mmol) or N-6-phenethyl-ADP (**11**, R=phenethyl) (0.3 mmol) as the triethylammonium (TEA) salts, were dissolved in 5 mL methanol:H_20 (1:1). It was assumed that there were three TEA molecules per ADP analog. ADP analogs were converted to the pyridinium salts using the same procedure as described above for compound **12,** except that 5 mL of methanol:H_20, 1:1 was used as the eluent. After removal of solvent *in vacuo*, methanol (12 mL), tri-*n*-octylamine (0.3 mmol), and tri-*n*-butylamine (0.3 mmol) were added. After solution had occurred the solvent was removed and the residue dried by repeated (three times) evaporation of 5 mL aliquots of pyridine. The residue was then dissolved in 3.3 mL of pyridine and added to 0.6 mmol of **13**, the reaction was stirred at RT for 2 hours during which time a precipitate formed. Solvent was removed, 20 mL of 0.2 M NaOH was added, and the reaction was then heated to 100°C for 10 minutes. The pH was adjusted to pH 7 with DOWEX® 501-X8 ion exchange resin (pyridinium form) and 0.4 mL β-mercaptoethanol was added. The crude reaction could be stored at -20°C until purification. The reaction was then filtered and purified as described for the ADP analogs (see **Supplementary Figure 6c**). The fractions containing ATPγS analogs were pooled and lyophilized*. The compounds were obtained in 6-8% yield and were analyzed using mass spectrometry. For N-6-benzyl-ATPγS, ESI-MS (*m/z*): $[M-H]^-$ calcd for $C_{17}H_{22}N_5O_{12}P_3S$, 612.02; found 611.95. For N-6-phenethyl-ATPγS, ESI-MS (*m/z*): $[M-H]^-$ calcd for $C_{18}H_{24}N_5O_{10}P_2$, 626.02; found 625.90. Absorbance at 280 nm, as compared to the N-6-modified adenosines, was used to obtain accurate concentrations. Degradation was observed after freeze thaw cycles, so small aliquots were stored at -80°C.

*A second round of lyophilization was performed to obtain a white solid and to remove excess TEAB.

** DOWEX® 501-X8 ion exchange resin (approximately 20 mL of dry resin) was swollen with 20 mL of methanol:H_20:pyridine (50:45:5). Two fritted columns were loaded with 5 mL of the swollen resin and washed with 20 mL of methanol:H_20 (1:1), these columns were used to exchange the counter-ions on **11** and **12.** The additional resin was kept for neutralization of the thiophosphorylation reaction after deprotection.

Cell Culture and Plasmids

The WT and AS Erk2 mouse embryonic fibroblasts (MEFs) were prepared from 13.5-day old embryos of *Erk1*$^{-/-}$ *Erk2*$^{+/+}$ and *Erk1*$^{-/-}$ *Erk2*$^{AS/AS}$ mice respectively. The MEFs were grown in Dulbecco's modified Eagle medium (DMEM, high glucose with L-glutamine), supplemented with 10% fetal bovine serum, 0.292 mg/mL L-glutamine, 1 mM sodium pyruvate, 55 □M 2- mercaptoethanol, 1X MEM non-essential amino acids (Gibco), 100 μg/mL streptomycin, and 100 units/mL penicillin, at 37°C, 5% CO_2. Cells at or before pass 5 were used in the experiments. COS-7 cells were purchased from American Type Culture Collection (ATCC), and grown in Dulbecco's modified Eagle's medium (DMEM), supplemented with 10% fetal bovine serum, 2 mM glutamine, 0.1 mg/mL sodium pyruvate, 100 μg/mL streptomycin, and 100 units/mL penicillin. The cells were maintained at 37°C, 10% $C0_2$. pCDNA3-FLAG-*JNK1* M108G, L168A, (JNK1 AS kinase) has been described previously[34]. Rat PKCδ was aligned with other protein kinases and the gatekeeper amino acid was identified as methionine 425 in *PKCδ*. Flag-*PKCδ* was generated by performing PCR with the following 5' primer (5'-

CGCGGATCCATGGACTATAAGGACGATGATGACAA AGCACCGTTCCTGC GCATCTCCTTC-3') and 3' primer (5'-CCGGAATTCCTATTC CAGGAATTGCTCA TATTTGG -3') using pRSV-rat *PKCδ* as the template. The PCR product was digested with *Bam*HI and *Eco*RI, and ligated into pcDNA3 vector (Invitrogen). The *PKCδ* AS mutant (M425A) was generated with 5' primer (5'-GGACCACC TCTTCTTTGTGGCCGAGTTCCTCAATGGGGGCG-3') and 3' primer (5'-CGCCCCCATTGAGGAACTCGGCCACAAAGAAGAGGTGGTCC-3') using QuickChange site-directed mutagenesis kit (Stratagene). The coding sequence was sequenced to confirm error free PCR and the M425A mutation. Yeast *CDC5* (YMR001C) cloned into pFastBacHT-A (Invitrogen) (pFastBacHT A-*CDC5*) was a kind gift of David Morgan (University of California, San Francisco). pFastBacHT A-*CDC5* L158G, encoding the AS Cdc5 kinase[24], was constructed from pFastBacHT A-*CDC5* by QuikChange site-directed mutagenesis (Stratagene).

Kinase Expression and Purification

PKCδ wild type (WT) and analog specific (AS)

FLAG- *PKCδ* (WT or AS) plasmids (90 μg) were transfected into COS-7 cells (4x150 cm plates per plasmid) using Superfect (Quiagen) according to the manufacturer's instructions. After 72 hours the cells were washed 1X with PBS and then FLAG lysis buffer (50 mM Tris-HCl pH 7.4, 150 mM NaCl, 1mM EDTA, 1% Triton X-100, phosphatase inhibitor cocktail 1, and complete protease inhibitor cocktail (Roche)) was added. After 20 minutes of incubation on a rocker at 4°C the cells were collected and centrifuged at 12,000g for 10 min. The supernatants were added to anti-FLAG M2-

agarose gel and incubated at 4°C for three hours. The beads were transferred to a small column and washed extensively with ice cold lysis buffer, followed by wash buffer (50 mM Tris-HCl pH 7.4, 150 mM NaCl, phosphatase inhibitor cocktail 1, and complete protease inhibitor cocktail (Roche)). The immunoprecipitated PKCδ was eluted into storage buffer containing FLAG peptide (20 mM HEPES pH 7.4, 0.1 mM EGTA, 25% glycerol, 0.03% Triton X-100, 150 ng/μL FLAG peptide). Concentrations of WT and AS PKCδ were determined by comparison with pure PKCδ ((Panvera) using Sypro Ruby (Molecular Probes). Approximately 150 μL of purified kinase was obtained: WT = 94 ng/μL, AS = 25 ng/ μL. The kinases were aliquoted and stored at -80°C until further use.

JNK1 (WT and AS)

FLAG-*JNK1* WT plasmid (70 μg) was transfected into COS-7 cells (3x150 mm plates) using Superfect (Qiagen) according to the manufacturer's instructions. FLAG-*JNK1* AS plasmid (225 μg) was transfected into COS-7 cells (7x150 mm plates) using Superfect (Qiagen) according to the manufacturer's instructions. After 48 hours the medium was removed and the cells were exposed to 60 J/m^2 ultraviolet light (using the tissue culture hood UV lamp) for 45 seconds to activate JNK1. The medium was replaced and the cells were incubated at 37ºC, 5% CO_2 for another 30 minutes. After washing 1X with PBS, FLAG lysis buffer (50 mM Tris-HCl pH 7.4, 150 mM NaCl, 1mM EDTA, 1% Triton X-100, phosphatase inhibitor cocktail 1, phosphatase inhibitor cocktail 2, and complete protease inhibitor cocktail (Roche)) was added. Cells were incubated for 20 on a rocker at 4°C and then collected and centrifuged at 12,000 g for 10 min. Supernatants were added to anti-FLAG M2-Agarose gel and incubated for three hours at 4°C. The beads

were transferred to a small column and washed extensively with ice cold lysis buffer. Immunoprecipitated JNK1 was eluted into storage buffer containing FLAG peptide (20 mM HEPES pH 7.4, 0.1 mM EGTA, 25% glycerol, 0.03% Triton X-100, phosphatase inhibitor cocktail 1, phosphatase inhibitor cocktail 2, complete protease inhibitor cocktail (Roche), and 150 ng/μL FLAG peptide). Western blotting against dually phosphorylated JNK1 (α–pT183, α–pY185 IgG, Cell Signaling), was used to quantitate the amount of activated kinase, as compared to a JNK1 standard (Upstate). Yield: 100 μL of wild-type JNK1 (5 ng/μL) and 200 μL of AS JNK1 (5 ng/μL). The kinases were aliquoted and stored at -80°C until further use.

Cdc5 (WT and AS)

Purified wild type 6xHis-Cdc5 was a kind gift of D. Randle and David Morgan (University of California, San Francisco). Purified analog specific 6xHis-Cdc5 was prepared as follows. Bacmid was produced from pFastBacHT A-*CDC5* L158G and transfected into Sf9 insect cells with Cellfectin using the Bac-to-Bac Baculovirus expression system (Invitrogen) according to the manufacturer's instructions. For AS Cdc5 expression, 1 L of Sf9 cells at $2x10^6$ cells/mL was infected with 30 mL of pass 3 baculovirus. Cells were harvested after 2 days at 27°C, and lysate was prepared by douncing in Cdc5 lysis buffer (CLB: 25mM HEPES pH 7.4, 300 mM NaCl, 10% glycerol, 5 mM NaF, 5 mM beta-glycerophosphate) with protease inhibitors (1 mM PMSF, 1 μg/mL leupeptin, 1 μg/mL aprotinin, 1 μg/mL pepstatin). The lysate was cleared by centrifugation at 7,649 x g for 15 min, followed by ultracentrifugation at 227,220 x g for 1 hr. The filtered supernatant was applied at 0.5 mL/min to a 1 mL

HiTrap Chelating HP column (Amersham) chelated with $CoCl_2$. The column was washed with CLB, followed by CLB with 2 mM imidazole. 6xHis-Cdc5 L158G was eluted with CLB containing a gradient of imidazole from 100 mM to 200 mM. Peak 6xHis-Cdc5 L158G containing fractions were pooled, aliquoted and stored at -80°C until further use. The concentration of AS Cdc5 (150 ng/μL) was calculated from a Sypro Ruby (Molecular Probes) stained gel that contained known amounts of BSA.

***in vitro* Kinase Assays followed by PNBM alkylation**

PKCδ (WT and AS)

For Western Blot Analysis:

100 ng of kinase was added to a 30 μL reaction containing PKC kinase buffer (20 mM HEPES pH 7.4, 1 mM EGTA, 10 mM $MgCl_2$, 0.3% Triton X-100, 1 μM PMA, 500 μg/mL phosphatidyl serine (diluted 10X from a fresh 5 mg/mL aqueous stock), 2 μg Histone (Sigma, suitable for PKC assay), and 1 mM nucleotide (ATPγS, N-6-benzyl ATPγS, or N-6-phenethyl ATPγS)). The kinase reaction proceeded for 30 minutes at RT then 1.5 μL of 50 mM PNBM in DMSO was added (to afford a final concentration of 2.5 mM PNBM, 5% DMSO). After two hours at RT the samples were analyzed by western blotting.

For DELFIA Based Kinetic Measurements:

30 μL kinase reactions, in 96 well PCR plates, were carried out as above with the following exceptions: 10 μg of Histone was used in each reaction and PKCδ wild type and analog sensitive kinases were used at 4 nM and 8 nM respectively. The reactions were initiated by addition of various concentrations of nucleotide (ATPγS or N-6-benzyl-

ATPγS) and terminated after 30 minutes by addition of EDTA to a final concentration of 20 mM. Alkylation (2.5 mM PNBM, 5% DMSO) proceeded for 2 hours and the reactions were analyzed by DELFIA.

JNK1 (WT and AS)

For Western Blot Analysis:

10 ng of kinase was added to a 30 μL reaction containing 10 mM HEPES pH 7.4, 150 mM NaCl, 10 mM $MgCl_2$, 2 μg GST-c-Jun or 2 μg GST-ATF-2 (Cell Signaling Technology) and 1 mM nucleotide (ATPγS, N-6-benzyl ATPγS, or N-6-phenethyl ATPγS). The kinase reaction proceeded for 30 minutes at RT then 1.5 μL of 50 mM PNBM in DMSO was added (to afford a final concentration of 2.5 mM PNBM, 5% DMSO). After two hours at RT the samples were analyzed by western blotting.

For DELFIA based Kinetic Measurements:

15 μL kinase reactions, in 96 well PCR plates, were performed as above with the following exceptions: 2.5 μg of GST-c-Jun was used in each reaction, JNK1 wild type and analog sensitive kinases were used at 5 nM. The reactions were initiated by addition of various concentrations of nucleotide (ATPγS or N-6-benzyl-ATPγS), and terminated after 30 minutes by addition of EDTA to a final concentration of 20 mM. Alkylation (2.5 mM PNBM, 5% DMSO) proceeded for 2 hours and the reactions were analyzed by DELFIA.

Preparation of c-Jun-GST for Mass Spectrometry

200 ng of JNK1 (Upstate) was added to 30 μL reactions containing 10 mM HEPES pH 7.4, 150 mM NaCl, 10 mM $MgCl_2$, and 2 μg c-Jun-GST (Cell Signaling Technology) in

the presence or absence of 1 mM ATPγS. After 30 minutes PNBM was added to a final concentration of 2.5 mM PNBM, 5% DMSO. Alkylation proceeded for 2 hours at RT. Following SDS-PAGE and coomassie staining the c-Jun-GST bands were excised.

Cdc5 (WT and AS)

For Western Blot Analysis:

Cdc5 (6 ng of WT or 30 ng of AS) was added to a 30 μL reaction containing 25 mM HEPES pH 7.4, 50 mM NaCl, 15 mM $MnCl_2$, 10 μg α-casein (Sigma, dephosphorylated), 10 μg/mL BSA, 1mM 1,4-dithiothreitol (DTT), and 1 mM nucleotide (ATPγS, N-6-benzyl ATPγS, or N-6-phenethyl ATPγS). The kinase reaction proceeded for 30 minutes at RT and then 1.5 μL of 100 mM PNBM in DMSO was added, to afford a final concentration of 5 mM PNBM. Note the concentration of PNBM was increased to account for the fraction that could be consumed by DTT. After two hours at RT the samples were analyzed by western blotting.

For DELFIA based Kinetic Measurements:

30 μL kinase reactions, in 96 well PCR plates, were performed as above with the following exception: Cdc5 wild type and analog sensitive kinases were used at 0.3 nM and 1.5 nM respectively. Reactions were initiated by addition of various concentrations of nucleotide (ATPγS or N-6-phenethyl-ATPγS) and terminated after 20 minutes by addition of EDTA to a final concentration 30 mM. PNBM alkylation proceeded for 2 hours as described above for western blot analysis, and the reactions were analyzed by DELFIA.

***in vitro* Kinase Assay of Erk2 (WT and AS)**

1.5 x10^6 WT or AS Erk2 MEFs cells were trypsinized, pelleted, and resuspended with DMEM to afford 10x10^6 cells/mL. To activate Erk2 the cells were stimulated with 20 ng/mL of phorbol 12-myristate 13-acetate (PMA) and 1 μM ionomycin for 5 minutes at 37°C. Activated cells were lysed in 250 □l cell lysis buffer (1% NP-40, 5 mM EDTA, 25 mM HEPES, 150 mM NaCl supplemented with complete mini protease inhibitor cocktail (Roche) and phosphatase inhibitor cocktail sets I & II (Calbiochem)). Lysates were cleared by centrifugation at 14,000 g, 4°C for 10 minutes, then incubated with 15 □l immobilized anti-phospho-ERK1/2 mouse monoclonal antibody (Cell Signaling) per reaction at 4°C overnight. Immunoprecipitates were washed twice with 400 □l cell lysis buffer and once with 400 □l kinase buffer (Cell Signaling, 25 mM Tris-HCl (pH 7.5), 5 mM beta-glycerophosphate, 2 mM dithiothreitol (DTT), 0.1 mM Na_3VO_4, 10 mM $MgCl_2$) pre-chilled on ice. Immunoprecipitates were then incubated with 2 □g Elk-1 fusion protein (Cell Signaling) and 1 mM nucleotide (ATPγS, N-6-benzyl ATPγS or N-6-phenethyl ATPγS) in 30 □l of kinase buffer. The kinase reaction proceeded at 30 °C for 30 minutes with gentle rocking and then alkylated with 15 mM PNBM, 5 % DMSO for two hours at RT. The samples were resolved by 10% SDS-PAGE, transferred to PVDF membrane, and blotted with α-hapten-IgG.

For the following list of kinases the reaction conditions are described. Each reaction proceeded at RT for 30 minutes, and then 1.5 μL of 50 mM PNBM in DMSO was added (to afford a final concentration of 2.5 mM PNBM, 5% DMSO). Alkylation proceeded for two hours at RT and samples were analyzed by western blotting.

p38α

Kinase (10 ng) was added to a 30 μL reaction containing 10 mM HEPES pH 7.4, 150 mM NaCl, 10 mM $MgCl_2$, and 2 μg myelin basic protein in the presence or absence of 1 mM ATPγS.

ERK1 and ERK2

Kinase (25 ng; Upstate) was added to a 30 μL reaction containing 10 mM HEPES pH 7.4, 150 mM NaCl, 10 mM $MgCl_2$, and 2 μg myelin basic protein in the presence or absence of 1 mM ATPγS.

Akt1

Kinase (50 ng; Calbiochem) was added to a 30 μL reaction containing 10 mM HEPES pH 7.4, 150 mM NaCl, 10 mM $MgCl_2$, and 2 μg GSK3β-paramyosin fusion (Cell Signaling) in the presence or absence of 1 mM ATPγS.

Abl

Kinase[35] (500 ng) was added to a 30 μL reaction containing 25 mM HEPES pH 7.4, 5 mM $MgCl_2$, 5 mM $MnCl_2$, 2 μg GST-Abl substrate (Stratagene), and 0.5 mg/mL BSA in the presence or absence of 1 mM ATPγS.

Src

Kinase[35] (500 ng) was added to a 30 μL reaction containing 25 mM HEPES pH 7.4, 5 mM $MgCl_2$, 5 mM $MnCl_2$, 2 μg GST-Src substrate (Stratagene), and 0.5 mg/mL BSA in the presence or absence of 1 mM ATPγS.

CK1

Kinase (1000 units; New England Biolabs) was added to a 30 μL reaction containing 25 mM HEPES pH 7.4, 10 mM $MgCl_2$, 1 mM DTT, 2 μg casein (α- dephosphorylated), and 0.5 mg/mL BSA in the presence or absence of 1 mM ATPγS.

GSK3β

Kinase (1000 units; New England Biolabs) was added to a 30 μL reaction containing 25 mM HEPES pH 7.4, 10 mM $MgCl_2$, 2 μg myelin basic protein, and 0.5 mg/mL BSA in the presence or absence of 1 mM ATPγS

PKCε

Kinase (100 ng; Invitrogen) was added to a 30 μL reaction containing 20 mM HEPES pH 7.4, 1 mM EGTA, 10 mM $MgCl_2$, 0.3% Triton X-100, 1 μM PMA, 500 μg/mL phosphatidyl serine (diluted 10X from a fresh 5 mg/mL aqueous stock), and 2 μg histone (suitable for PKC assay) in the presence or absence of 1 mM ATPγS.

Western Blotting

Ten microliters of the SDS-PAGE sample buffer quenched kinase reactions were electrophoresed and transferred to nitrocellulose. The blots were blocked with 4% milk in TBST (20 mM Tris, 137 mM NaCl, 0.05% Tween 20) and then incubated overnight at 4º C with α-hapten-IgG (1:20,000 in 4% milk, TBST), α-hapten-IgY (1:15,000 in 5% BSA, TBST), or RmAb 51-8 (1:20,000 in 4% milk, TBST). For monoclonal screening experiments the hybridoma supernatants were diluted 1:100 in 5% BSA PBST and incubated overnight at 4º C. After washing with TBST the blot was incubated with secondary antibody (goat α-rabbit-IgG, Promega (1:15,000 in 5 % milk TBST)) for one hour at RT. The blots were imaged with film (Pierce) using chemiluminescence (West Pico, Pierce) or by camera (Alpha Innotech).

DELFIA

After PNBM alkylation the kinase reactions were diluted in coating buffer (35 mM $NaHCO_3$, 15 mM Na_2CO_3, pH 9.5) to concentrations that fell within the linear range of detection (as determined by coating concentration experiments, see **Supplementary Fig. 4a**). Ninety Six well plates (MaxiSorp, NUNC) were coated overnight (50 µL/well) with the following concentrations of each kinase substrate: 2.5 µg/mL of histone (PKCδ substrate), 2 µg/mL of c-Jun- GST (JNK1 substrate), and 2.5 µg/mL of α-casein (Cdc5 substrate). Each sample was coated in triplicate and each experiment was repeated at least three times. After removal of the coating buffer the plates were blocked (1% BSA in TBST, 200 µL/well) for 1-2 hours at RT. Blocking buffer was removed, the wells

were washed twice with 200 µL/well TBST wash buffer, and Eu^{3+} labeled polyclonal α-hapten-IgG[§] (1:400 in DELFIA assay buffer (Perkin Elmer)) was added. Binding proceeded overnight at 4ºC. The plates were washed 4X with 200 µL/well TBST followed by DELFIA enhancement solution (75 µL/well). After shaking for five minutes, time resolved fluorescence was measured with an Analyst HT plate reader (LJL Biosystems).

§ Eu^{3+} labeled α–hapten–IgG was prepared and quantified with a DELFIA Eu^{3+} labeling kit (Perkin Elmer). 100 µL of polyclonal α–hapten–IgG (10 mg/mL in PBS) was diluted to 4 mg/mL by adding 150 µL of 100 mM Na_2CO_3 pH 11. This solution was added to 0.2 mg of Perkin Elmer Eu^{3+} reagent, and incubated overnight at 4ºC. The antibody was purified with size exclusion chromatography, using PD-10 column matrix in a 1 mL column. Eu^{3+} labeled α–hapten–IgG was obtained at 0.95 mg/mL with 0.75 Eu^{3+} molecules/ IgG molecule.

Substrate Labeling in Digitonin Permeabilized MEFs

15 x10^6 *Erk1*$^{-/-}$ *Erk2*$^{+/+}$ or *Erk1*$^{-/-}$ *Erk2*$^{AS/AS}$ MEFs cells were trypsinized, pelleted, and resuspended in DMEM to afford 5x10^6 cells/mL. To activate Erk2 the cells were stimulated with 20 ng/mL of PMA and 1 µm ionomycin for 5 minutes at 37°C. Cells were transferred on ice and pelleted at 4°C. Permeabilization proceeded on ice for 5 min in a buffer containing 1X Dulbecco's phosphate buffered saline (DPBS), 1X kinase buffer (Cell Signaling), complete mini protease inhibitor cocktail (Roche), phosphatase inhibitor cocktails I and II (Calbiochem), and 50 µg/mL digitonin (Sigma). Cells were then pelleted at 4°C (200 xG) for 5 min and resuspended in the same buffer with the

following exceptions: 100 μM N-6-phenethyl ATPγS and 1 mM GTP were included, and digitonin was omitted. The kinase reaction proceeded at 30 °C for 30 minutes with gentle rocking. Cells were then pelleted as above and lysed on ice for 15 min in 0.5 mL RIPA buffer containing 25 μM EDTA. Lysates were cleared by centrifugation at 14,000 g, 10 minutes 4°C. Proteins were alkylated with PNBM (8 mM PNBM, 2.5 % DMSO) for two hours at RT and frozen at -75°C. Ten μL of each sample was analyzed by western blot and the remainder was immunoprecipitated with α-hapten-IgG RmAb 51-8.

Immunoprecipitation with α-hapten-IgG (51-8 RmAb)

Samples labeled as above were thawed on ice and PNBM was removed as below. Note: PNBM is a potent inhibitor of immunoprecipitation and its' removal is absolutely necessary. Size exclusion chromatography has been the most effective method we have found to date. PD-10 columns (Amersham Biosciences) were equilibrated with RIPA containing protease inhibitors (Complete Protease Inbibitor Cocktail, Roche), 0.5 mL of alkylated proteins were applied to the column and eluted with RIPA containing protease inhibitors. Fractions (0.5 mL) were collected and the protein containing fractions (7-9), as determined by Bradford Assay (Promega), were pooled and pre-cleared with 100 μL of 50% rProtG agarose (Invitrogen) for 5 hours at 4 °C. Meanwhile 20 μg of 51-8 RmAb was bound to 100 μL of 50% rProtG agarose in 1.0 mL RIPA containing 0.5 mg/mL BSA for 5 hours at 4 °C. The beads were then removed from the lysates and the antibody coupled beads (washed 1X with 1.0 mL RIPA) were added to the precleared lysates (10 μg of antibody and 50 μL of 50 % beads per immunoprecipitation reaction). Immunoprecipitation proceeded overnight at 4°C. The samples were then washed 4X

with 1.0 mL RIPA and eluted by boiling in 30 µL SDS-PAGE sample buffer. Five µL of the immunoprecipitates were analyzed by western blot and the remaining 25 µL was analyzed by silver staining. The region of the gel from 200-60 KDa was cut into 1 mm slices (for both WT and AS immunoprecipitation reactions).

In Gel Digestion and Mass Spectrometry

All gel handling steps were performed in a laminar flow hood to minimize contamination. Methanol washed siliconized tubes (PGC Scientifics) and HPLC quality solvents were used. Gel slices were chopped into 1 mm cubes and washed twice with 200 µL aliquots of 25 mM ammonium bicarbonate, 50% acetonitrile. After desiccation (using vacuum centrifugation) the gel pieces were rehydrated with 20 µL of 5 ng/µL TPCK modified sequencing grade trypsin (Promega) and incubated at 37°C overnight. Peptides were extracted by addition of 30 µL of 5% formic acid in 50% acetonitrile. The samples were concentrated using vacuum centrifugation and analyzed by nano-liquid chromatography-electrospray ionization-quadrupole time of flight tandem mass spectrometry analysis as follows. Peptides were separated using a 75 µm × 15 cm reverse phase C-18 column (LC Packings) at a flow rate of 350 nL/min, running a 3–32% acetonitrile gradient in 0.1% formic acid on an Eksigent nano 1D HPLC (Eksigent) equipped with an auto sampler (Agilent Technologies). The liquid chromatography (LC) eluent was coupled to a microionspray source attached to a QSTAR XL mass spectrometer (MDS Sciex). Peptides were analyzed in positive ion mode. MS spectra were acquired for 1 s. For each MS spectrum, the most intense multiple charged peak was selected for generation of subsequent collision-induced dissociation (CID) mass spectra for 5 s. A dynamic

exclusion window was applied which prevented the same m/z from being selected for 1 min after its acquisition. For sequencing of unmodified or PNBM modified cysteine containing peptides the CID collision energy was automatically adjusted based upon peptide charge and mass to charge (*m/z*) ratio. To attain quality CID spectra of thiophosphate ester containing peptides the CID collision energy was set to a value of 30 eV.

Equipment and Settings

Figure 1a and **1b** were created using Adobe Illustrator and ChemDraw Ultra.

Figure 1c was acquired on an Alpha Innotech (30 s exposure) and processed using Adobe Photoshop and Adobe Illustrator.

Figure 2a was created in Microsoft Word and Adobe Illustrator.

Figure 2b and **2c** data was acquired as described under the '**In Gel Digestion and Mass Spectrometry'** in this **Supplementary Methods** file. Spectra were exported from Analyst Software (MDS Sciex) into Adobe Illustrator.

Figure 3 western blot analysis was recorded on film and then scanned into Adobe Photoshop, labels were added in Adobe Illustrator.

Figure 4 western blot analysis was recorded on film and then scanned into Adobe Photoshop, labels were added in Adobe Illustrator. Chemical structures were exported from ChemDraw Ultra into Adobe Illustrator.

Figure 5a-c western blot analysis (film) and the silver stained gel were scanned into Adobe Photoshop, labels were added in Adobe Illustrator.

Figure 5d data was acquired as described under the '**In Gel Digestion and Mass Spectrometry'** in this **Supplementary Methods** file. Spectra were exported from Analyst Software (MDS Sciex) into Adobe Illustrator.

Suppementary References

1. P. Dietze and W. P. Jencks, *J. Am. Chem. Soc.* **111** (15), 5880 (1989).
2. D.B.A. de Bont, Moree, W.J., van Boom, J.H., and Liskamp, R.M.J., *Journal of Organic Chemistry* **58**, 1309 (1993).
3. K. Kikugawa, K. Iizuka, and M. Ichino, *J. Med. Chem.* **16** (4), 358 (1973).
4. M. Yoshikawa, T. Kato, and T. Takenishi, *Tetrahedron Lett.* **50**, 5065 (1967).
5. C. Hoffman, Genieser, H.G., Veron, M., and Jastorff, B., *Bioorganic & Medicinal Chemistry Letters* **6** (21), 2571 (1996).
6. A.F. Cook, *J. Am. Chem. Soc.* **92** (1), 190 (1970).
7. R.S. Goody, Eckstein, F., *J. Am. Chem. Soc.* **93** (23), 6252 (1971).
8. J. J. Allen, S. E. Lazerwith, and K. M. Shokat, *J. Am. Chem. Soc.* **127** (15), 5288 (2005).
9. J. J. Ventura, A. Hubner, C. Zhang et al., *Mol. Cell.* **21** (5), 701 (2006).
10. C. Zhang, D. M. Kenski, J. L. Paulson et al., *Nat. Methods* **2** (6), 435 (2005).
11. M. A. Seeliger, M. Young, M. N. Henderson et al., *Protein Sci.* **14** (12), 3135 (2005).

Chapter 4

Purification, Quantitation, and Mass Spectral Fragmentation of Esterified Thiophosphopeptides

Purification, Quantitation, and Mass Spectral Fragmentation of Esterified Thiophosphopeptides

Running Title: MSMS Behavior of Esterified Thiophosphopeptides

Jasmina J. Allen[*], Shenheng Guan[†], Kevan M. Shokat[‡], and Alma Burlingame[†**]

[*]Graduate Program in Chemistry and Chemical Biology, University of California, San Francisco

[†]Department of Pharmaceutical Chemistry, University of California, San Francisco

[‡]Departments of Cellular and Molecular Pharmacology and Howard Hughes Medical Institute, University of California, San Francisco

Abstract

Kinase-substrate interactions represent key nodes in signaling networks, and only a small fraction of these connections have been identified. Previously we described a strategy, based on selective thiophosphorylation and alkylation, to immunopurify and identify individual kinase substrates at the protein level. Here we extended this technology to isotopically label and immunopurify modified peptides directly. Electrospray collision induced dissociation (CID) spectra revealed several modes of modification specific neutral losses in addition to sequence ions. Electrospray electron transfer dissociation (ETD) spectra cleaved P-S and S-C bonds exclusively. This study demonstrates the feasibility of immunoprecipitating and quantifying esterified thiophosphopeptides and details their modes of CID and ETD fragmentation.

Introduction

Kinases transduce cellular signals by phosphorylating their protein substrates. To map these regulatory events, we developed technology to tag and purify substrates of individual kinases [1,2]. Engineered kinases, which utilize N^6 alkylated ATPγS nucleotides, enable chemical differentiation of substrates of a single kinase from *all other* cellular phosphoproteins. Thiophosphorylated substrates can be alkylated, with *p*-nitrobenzylmesylate (PNBM), and immunoprecipitated with a modification-specific primary sequence context independent antibody[1] (Supplemental Scheme 1, which can be found in the electronic version of this article). Previously, substrates were identified based on sequencing unmodified peptides[1] or through chemical conversion of thiophosphophopeptides to phosphopeptides[2].

Incorporation of stable isotopes into peptides or proteins enables quantification of dynamic biological events, such as phosphorylation[3,4]. To isotopically encode peptides at the step of thiophosphate derivatization, we alkylated substrates with ^{13}C PNBM and ^{12}C PNBM, which created modified peptide isotope pairs. This mass signature aided in locating and identifying modified peptides in MS and MS/MS spectra, and guided an alogarithm we developed to localize these pairs in MS survey scans.

Previously we analyzed the CID behavior of a modified thiophosphopeptide and observed nitrobenzyl thiol loss, which gave rise to an alternative sequence ion series[1]. While the CID process deposits internal energy into ions, which can induce preferential loss of labile side chain modifications[5], ETD typically preserves such modifications[6,7]. In this study we prepared and analyzed several kinase substrates and observed additional modes of modification group specific neutral losses in CID, which precluded sequence

identification and modification site localization in most cases. Thus we investigated the possibility of using ETD to sequence esterified thiophosphopeptides; however, in the ETD spectra obtained, we observed cleavages exclusively at P-S and S-C bonds. Our results highlight the difficulty in sequencing esterified thiophosphopeptides by tandem mass spectrometry and provide insight into their vibronic and electron mediated fragmentation processes.

Experimental (detailed methods are provided in electronic version of this article)

Synthesis, Sample Preparation, and Peptide Immunoprecipitation

^{13}C PNBM was synthesized by reducing *p*-nitro benzoic acid, isotopically labeled (7X ^{13}C) to the benzyl alcohol as described[8], followed by conversion to the mesylate[1]. Thiophosphorylated HeLa lysate was alkylated with ^{13}C PNBM and a ½ thiophosphorylated lysate was alkylated with ^{12}C PNBM, both samples had equal total protein content. Following alkylation the reactions were mixed, purified on a PD-10 column, digested with trypsin, lyophilized, and immunoprecipitated with a thiophosphate ester specific antibody. Myelin basic protein (MBP) was thiophosphorylated with either Akt1 or ERK2. Fully thiophosphorylated reactions were alkylated with ^{12}C PNBM and ½ thiophosphorylated reactions were alkylated with ^{13}C PNBM. Following alkylation samples were mixed, resolved by SDS-PAGE and digested in-gel with trypsin or lysC.

Mass Spectrometry and Modification Site Assignment

LCMSMS was performed on QSTAR Pulsar, LTQFT, LTQ Orbitrap XL, and LTQ/ETD mass spectrometers. Samples were analyzed by LCMS, with a typical gradient of 3%-40% acetonitrile in 0.1% formic acid/water over 35 min, with a 350 nL/min flow rate.

On the QSTAR instrument, two CID scans were performed on the two most intense ions in the survey scan. On both LTQFT and Orbitrap instruments, survey scans were conducted in FTMS mode. Three CID scans in LTQ and three CID/ETD scans in the LTQ/ETD, analyzed the three most intense ions in the proceeding survey scan. MS/MS spectra were searched using Protein Prospector and MASCOT, with customized modifications for isotopically labeled thiophosphate groups. Matlab software was developed in-house to search for labeled peptides in high resolution survey scans. Centroid peak lists were deisotoped [9] and matched to theoretical isotope patterns.

Results and Discussion

As a first step toward quantifying kinase specific phosphorylation events, we synthesized an isotopically labeled alkylating reagent, ^{13}C PNBM, in 25% overall yield. A proteolyzed whole cell lysate, containing a 1:2 ratio of ^{12}C:^{13}C PNBM alkylated thiophosphopeptides, was prepared to determine if immunoprecipitation successfully enriched thiophosphorylated peptides in the expected ratios. In MS mode several peptide pairs, separated by 7 Da in the expected 1:2 ratio, were observed (Figure 1a), validating our purification and quantification strategy. In-gel digestion also maintained isotopic ratios; unmodified peptides were singlets, cysteine modified peptides were at a 1:1 ratio, and thiophosphorylated peptides were observed at the expected ratios, Supplementary Figure 1 and data not shown. CID of the precursor ions in Figure 1a, yielded spectra dominated by neutral losses of the thiophosphate moiety, Figure 1b. Although purification and recognition of modified precursor ions was successful, we were unable to obtain peptide identifications or modification site assignments from these samples.

Figure 1. (**a**) MS of peptides immunoprecipitated from a lysate with a thiophosphate ratio of 1:2 and alkylated with ^{12}C PNBM and ^{13}C PNBM, respectively. Insert, structure of a modified serine, with the seven ^{13}C labeled positions indicated by black circles. (**b**) CID of the 477.21 peak in panel a. Structures are given for the inferred fragments, assuming the modification is on a serine residue. β, n, p, and * denote beta-elimination, neutral loss, phosphenate residues and un-interpreted masses, respectively.

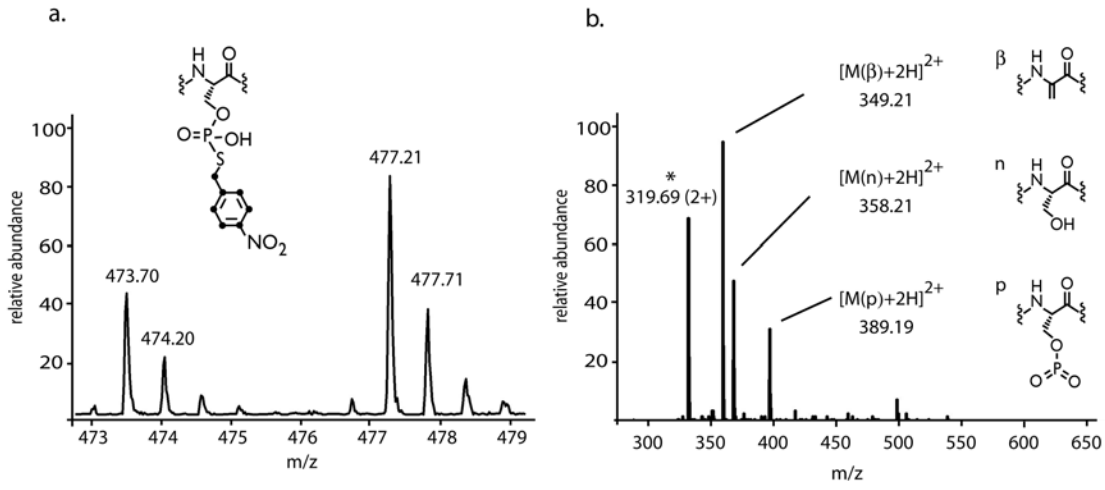

Previously, we obtained spectra of modified c-Jun, thiophosphorylated by the proline directed kinase JNK1[1], and the modification remained largely intact during the CID process with only minor phosphenate formation. We speculated that the proline +1 of the modification may partially shield the moiety from fragmenting during the CID process, by virtue of steric or bond angle strain, as observed with base catalyzed β-elimination of labile groups[10]. Indeed, MBP modified by the proline directed kinase ERK2 yielded the CID spectra (Figure 2a) in which the modification remains completely intact. However, MBP modified by Akt1, a non-proline directed kinase, yielded the CID spectra in Figure 2b, which contains multiple sequence ions. Using the CID spectra, both modified peptides could be identified by database searching. We utilized the MS isotope signature to interrogate MS scans for ions pairs separated by 7 Da, which enabled us to localize additional modified peptide pairs that were not identified by their MS/MS spectra. CID spectra of these ion pairs yielded spectra dominated by neutral losses, even in the case of ERK2 modified MBP, Supplementary Figure 1, indicating sequence specific elements in addition to proline influence the nature of these CID fragmentation patterns.

ETD, believed to be a nonergodic process in which electron transfer and C-N peptide bond dissociation is faster than internal energy redistribution processes, typically preserves labile peptide modifications, producing a more uniformed distribution of sequence specific ions[6]. Therefore, we explored the possibility that ETD could reliably provide sequence ion rich MS/MS spectra of esterified thiophosphopeptides. Figure 2c and 2d are ETD spectra of the ions selected for CID in Figure 2a and 2b, respectively. Strikingly, ETD spectra only produced fragment ions resulting from S-C and S-P bond

Figure 2. (a, b) CID spectra of the indicated peptide sequences, lowercase letters represent modified residues, (c, d) are the corresponding ETD spectra, respectively. β, n, p,*, and P^S denote beta-elimination, neutral loss, phosphenate residues (or the mass equivalent), un-interpreted masses and thiophosphate, respectively.

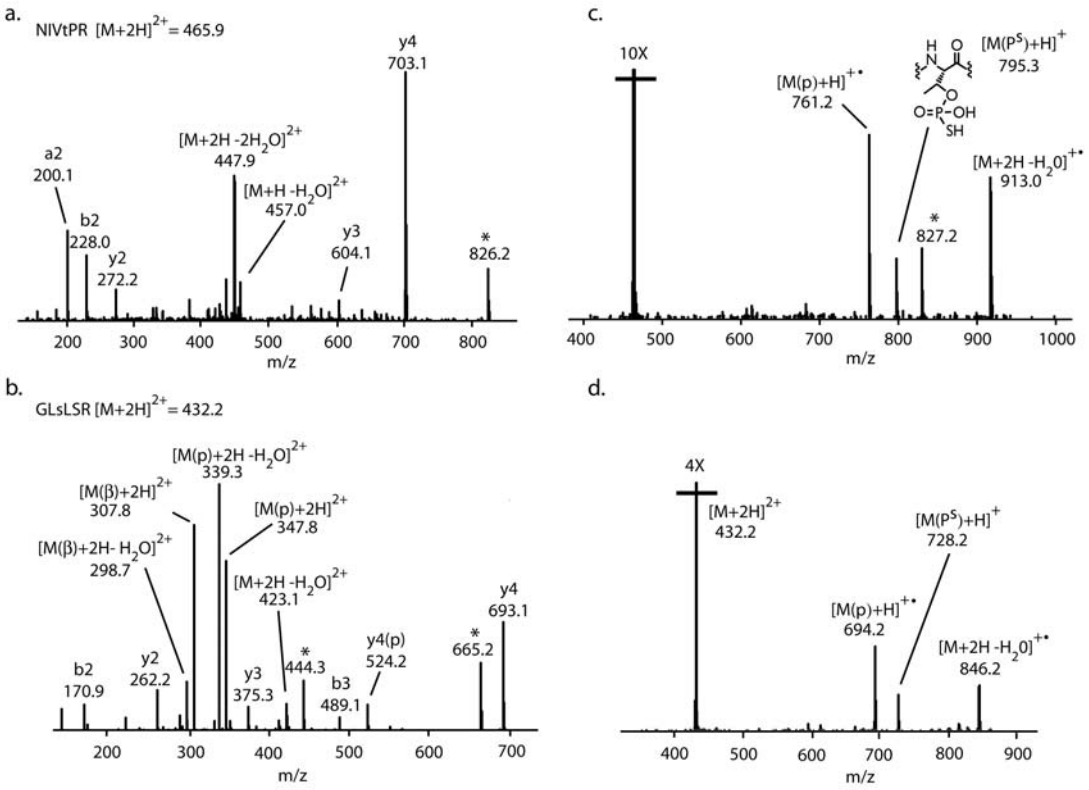

cleavages. We hypothesize these fragments are produced through the radical mediated mechanisms illustrated in Scheme 1. The absence of sequence ions in ETD spectra, suggests the affinity of thiophosphate esters for radicals precludes transfers that would lead to C-N bond cleavages. Disulfide linkages[11], sulfation[12], and alkylated cysteines[13], are also preferentially targeted in electron mediated fragmentation processes, illustrating a general trend for cleavages to occur in sulfur containing side chain modifications.

Conclusions

We have established that esterified thiophosphopeptides can be immunoprecipitated and analyzed by electrospray mass spectrometry, a technique previously only reported for phosphotyrosine containing peptides[14]. Installing an isotope label directly at the site of modification enabled localization of modified peptides, and unique side chain losses in MS/MS spectra further indicate modified peptides. In some cases, particularly when the modification was located -1 residue of proline, we collected CID spectra that enabled peptide sequencing and site assignment. Sodiated adducts of thiophosphate may produce more informative ETD spectra, as has been reported for sulfopeptides[12]. Alternatively, capturing and converting thiophosphopeptides to phosphopeptides[2], may provide a more general strategy for identifying kinase specific phosphorylation sites.

Scheme 1. Proposed mechanisms for modification specific losses by ETD, H˙ represents the radical donor. (a) S-C bond cleavage liberates a nitrobenzyl radical. (b) S-P bond cleavage liberates nitrobenzyl thiol.

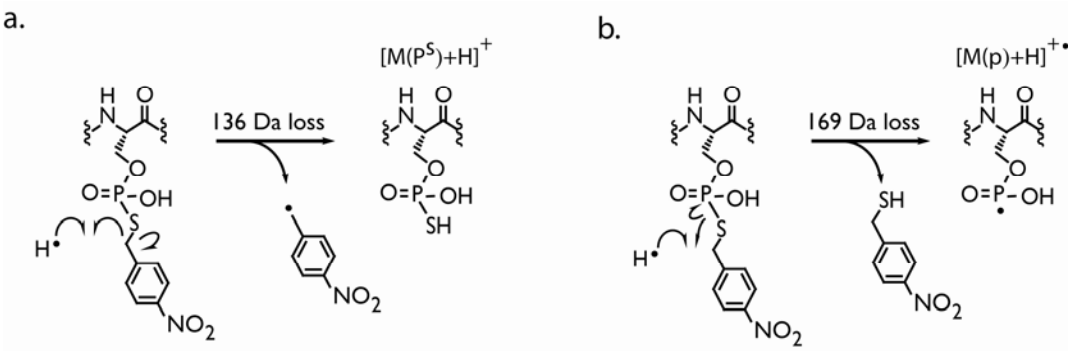

Acknowledgements

The authors are grateful to Robert Chalkley and Katlin Medzihradszky for helpful discussions, David Maltby for excellent technical assistance, and Aenoch Lynn for database assistance. Financial support was provided by NIH NCRR Grants RR 01614, to ALB, and RO1 EB0001987 to KMS.

References

1. J. J. Allen, M. Li, C. S. Brinkworth et al., *Nat Methods* **4** (6), 511 (2007).
2. J. D. Blethrow, J. S. Glavy, D. O. Morgan et al., *Proc Natl Acad Sci U S A* **105** (5), 1442 (2008).
3. F. M. White, *Curr Opin Biotechnol* (2008), *in press.*
4. J. C. Trinidad, A. Thalhammer, C. G. Specht et al., *Mol Cell Proteomics* **7** (4), 684 (2008).
5. H. Molina, R. Matthiesen, K. Kandasamy et al., *Anal Chem* **80** (13), 4825 (2008).
6. R.A. Zubarev, Haselmann, K.F., Budnik, B., Kjeldsen, F., Jensen, F., *Eur. J. Mass Spectrom.* **8**, 337 (2002).
7. K. Vosseller, Trinidad, J.C., Chalkley, R.J., Specht, C.G., Thalhammer, A., Lynn, A.J., Snedecor, J.O., Guan, S, Medzihradszky, K.F., Maltby, D.A., Schoepfer, R., Burlingame, A.L., *Mol Cell Proteomics* **5** (5), 923 (2006).
8. S. Cho, Y. Park, J. Kim et al., *Bull Korean Chem Soc* **25** (3), 407 (2004).
9. M. Wehofsky and R. Hoffmann, *J Mass Spectrom* **37** (2), 223 (2002).
10. E. Tarelli, *Carbohydr Res* **342** (15), 2322 (2007).
11. R. A. Zubarev, Kruger, N.A., Fridriksson, E.K., Lewis, M.A., Horn, D.M., Carpenter, B.K., McLafferty, F.W., *J Am Chem Soc* **121**, 2857 (1999).
12. K. F. Medzihradszky, S. Guan, D. A. Maltby et al., *J Am Soc Mass Spectrom* **18** (9), 1617 (2007).

13. R. J. Chalkley, C. S. Brinkworth, and A. L. Burlingame, *J Am Soc Mass Spectrom* **17** (9), 1271 (2006).

14. J. Rush, A. Moritz, K. A. Lee et al., *Nat Biotechnol* **23** (1), 94 (2005).

Supporting Information

Supplementary Scheme 1. Strategy for Labeling Kinase Substrates. Kinase substrates (**1**) are thiophosphorylated by their cognate kinase, which installs a chemically reactive thiophosphate. Second, alkylation with ^{13}C labeled PNBM (**3**) or ^{12}C PNBM (**4**) forms the semi-synthetic epitope (**5**) which is recognized by a modification specific monoclonal antibody. Note, cysteine residues are also alkylated by PNBM to form thioethers which are stable in CID MSMS.

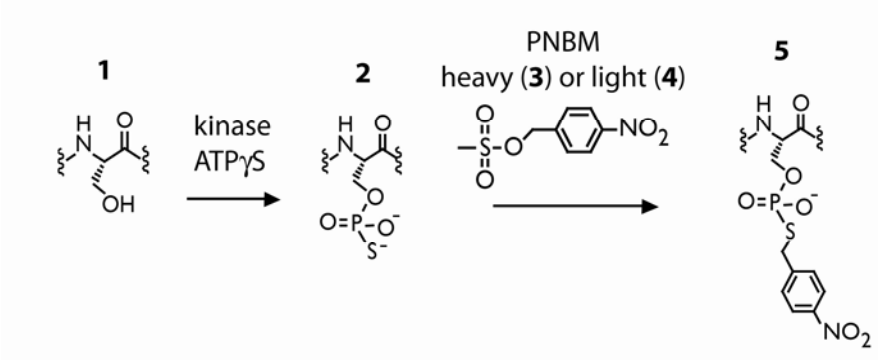

Supplementary Figure 1. MS isotope pairs as a guide to locating modified peptides. (**a**) MS spectra of an ion pair located using the described logarithm. (**b**) MSMS of the 861.9 ion. (**c**) MSMS of the 865.4 ion. β, n, and p denote beta-elimination, neutral loss, and phosphenate residues respectively.

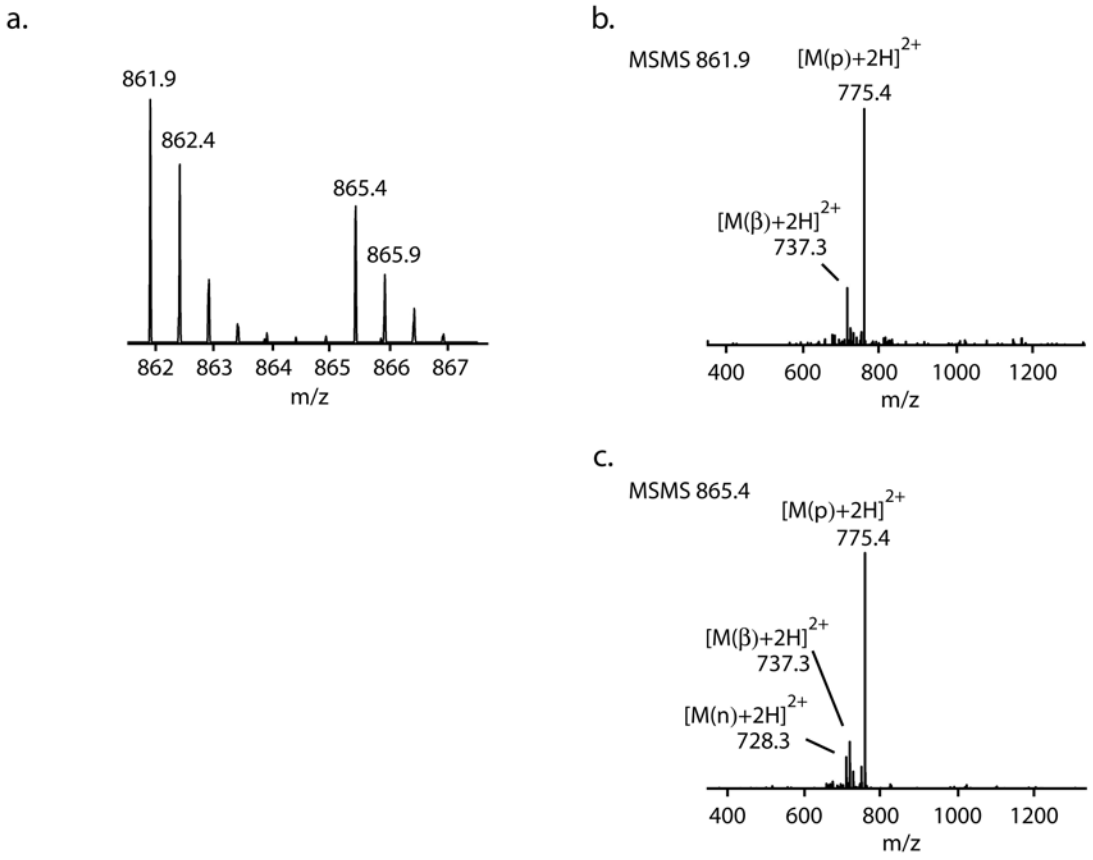

Supporting Methods

p-nitrobenzyl alcohol (7X 13C)

p-nitro benzoic acid, isotopically labeled with 13C at all seven carbons (95% purity, >99% isotopically enriched, (Cambridge isotopes) was reduced, as described for the unlabelled compound[1], as follows. *p*-nitro benzoic acid (350 mg, 2.1 mmol) and $NaBH_4$ (117 mg, 3.1 mmol) were placed in a 50 ml flask and dissolved in 15 ml of tetrahydrofuran (THF) and connected to a reflux condenser. In a separate flask, BF_3•Et_2O (168 µL, 1.3 mmol) was dissolved in 10 ml THF, and slowly added to the flask containing the other reactants. The reaction was refluxed at 80ºC for 5.5 hours, and the reaction monitored by TLC using 50:50 Ethyl acetate:hexanes containing 0.1% acetic acid as the solvent. After cooling, 15 ml H_20 was added and the reaction was concentrated under reduced pressure to remove the THF. The remaining aqueous solution was extracted twice with 30 ml of methylene chloride, washed with brine, dried with anhydrous $MgSO_4$, and concentrated under reduced pressure, to afford a yellow solid. The product was purified on an Analogics automated silica chromatography system by running a gradient of 20:80 (ethyl acetate:hexanes) to 60:40 (ethyl acetate:hexanes) over 30 minutes with a flow rate of 25 ml/min. The product eluted between 5 and 10 minutes and was obtained as a yellow solid in 44% yield after lyophilization. ^{1}H NMR, D6 DMSO, 400 MHz δ 4.6 (d, 2H, $J_{H\text{-}C}^{13}$, 140 Hz), 5.4 (s, 1H), 7.5 (d, 2H, $J_{H\text{-}C}^{13}$, 160 Hz), 8.3 (d, 2H, $J_{H\text{-}C}^{13}$, 160 Hz).

Compound 3

***p*-nitrobenzyl mesylate (7X 13C PNBM)**

p-nitro benzyl alcohol (7X 13C) was converted to the mesylate as described for the unlabelled compound[2, 3]. The product was further purified by dissolving it in 50% acetonitrile and separating it with reverse phase (C18) HPLC using a gradient from 0-50% acetonitrile (TFA was omitted). A white solid was obtained in 51% yield. 1H NMR, D6 DMSO, 400 MHz δ 3.3 (s, 3H), 5.4 (d, 2H, J_{H-C}^{13}, 140 Hz), 7.5 (d, 2H, J_{H-C}^{13}, 160 Hz), 8.3 (d, 2H, J_{H-C}^{13}, 160 Hz).

HeLa lysate labeling

HeLa-S3 cell pellets ($0.75x10^9$ cells) were obtained from the National Cell Culture Center (NCCC). After thawing, 10 mL of RIPA lysis buffer (50 mM Tris pH 8, 150 mM NaCl, 1.0% NP-40, 0.1% SDS, with protease inhibitors (Roche, complete)) was added and the cells were rotated at 4ºC for 15 minutes. After centrifugation at 20,000Xg for 10 minutes the supernatant was decanted and used for kinase assays. Alternatively the lysate was stored at -80ºC for later use. For labeling of cellular kinase substrates, HeLa lysate (15 mg/mL in RIPA lysis buffer) was diluted 1:1 with 10 mM HEPES pH 7.4, 150 mM NaCl, 10 mM $MgCl_2$ in the presence or absence of 1 mM ATPγS. After 2 hours the reaction was quenched by adding EDTA to 20 mM.

Peptide Immunoprecipitation

HeLa lysates were labeled as described above. A lysate containing a 1:2 ^{12}C:^{13}C PNBM alkylated thiophosphopeptide ratio was prepared by performing the kinase reaction in 3.75 mL and then adding 1.25 ml of the thiophosphorylated lysate to 1.25 ml of non-thiophosphorylated lysate. Alkylation was performed by adding 50 mM PNBM in

DMSO to afford a final concentration of 2.5 mM PNBM and 5% DMSO and allowing the lysates to react for 2 hours at room temperature. The reactions were then mixed and centrifuged at 14,000Xg for ten minutes to remove any insoluble material. Two PD-10 columns were ran, as each column has a maximum of 2 mL loading volume, using 8 M urea containing 20 mM HEPES pH 8.0 as the eluent. Peak protein containing fractions, as determined by Bradford assay, were pooled and diluted with 25 mM NH_4HCO_3 to afford 2 M Urea, a concentration suitable for tryptic digestion. This procedure served the purposes of removing the PNBM, which interferes with immunoprecipitation using the thiophosphate ester specific antibody, and denaturing the proteins prior to proteolysis. Modified sequencing grade trypsin (Promega), 120 µg, was added to the lysate and digestion proceeded overnight at 37ºC. Digestion was complete, as determined by Coomassie staining of digested and undigested lysates. Peptides were purified by reverse phase chromatography as described[4], helpful tips for this procedure were obtained in the product literature accompanying the Cell Signaling phosphotyrosine peptide immunoprecipitation kit (Catalog # 7900). Briefly, the digest was acidified to 1% TFA by adding 20% TFA to the digest, and centrifuged at 2000Xg for five minutes. The supernatant was loaded from a syringe into the short end of a Sep-Pak Column (Waters Cat# WAT051910), which had been pre-wetted with 5 mL of 40% acetonitrile, followed by 7 mL of 0.1% TFA. After washing the column with 6 mL of 0.1% TFA. The peptides were eluted stepwise with 1.4 mL of 5%, 10%, 15%, 20%, 25%, 30%, 35%, 40% acetonitrile containing 0.1% TFA. After lyophilization, for a minimum of 48 hours, the peptides were stored at -20 until further use. We noticed lyophilization and storage may cause oxidation of cysteine alkylation products, data not shown. 120 µg of α-KS mAb (5

mg/mL in PBS) was bound to 50 μL of 50% slurry of rProtG agarose in 1 mL of binding buffer (10 mM sodium phosphate pH 7.0, 150 mM NaCl) for five hours at 4ºC. After washing 1X with binding buffer the antibody bound beads were added to the lyophilized peptides, which had been resuspended in 1.4 mL of IP buffer (50 mM Tris pH 7.2, 10 mM sodium phosphate, 50 mM NaCl), rotated at room temperature for 30 minutes, sonicated, chilled on ice, checked for neutral pH, and then spun for 5 minutes at 2000 g. Immunoprecipitation proceeded overnight at 4ºC. The beads were washed 3X with 1.0 mL IP buffer, followed by 2X with 1.0 mL H_2O. The last bit of wash buffer was removed with a gel loading pipette tip and the proteins were eluted sequentially with 55 μL of 0.15% TFA for 10 minutes and then 45 μL of 0.15% TFA. To remove antibody from these samples, they were further purified with an OMIX 100 μL C18 pipette tip (Varian Cat# A57003100) according to the manufacturers' instructions. Peptides were eluted with 33 μL 50% acetonitrile containing 0.1% formic acid, concentrated under reduced pressure and analyzed on a QSTAR and LTQFT as described below.

Preparation of modified kinase substrates

Thiophosphorylated proteins were prepared as follows: dephosphorylated α-casein (Sigma) was incubated with CK2 (Calbiochem) in kinase buffer (1 mM ATPγS, 10 mM HEPES pH 7.4, 150 mM NaCl, 10 mM $MgCl_2$). Myelin Basic Protein (Upstate) was thiophosphorylated with either Akt1 (Invitrogen) or ERK2 (Upstate) in kinase buffer. After 6 hours, kinase reactions were quenched by adding EDTA to 20 mM. Samples were prepared to contain a 2:1 ^{12}C:^{13}C PNBM alkylated thiophosphopeptide ratio. Alkylation was performed by adding 50 mM PNBM in DMSO to afford a final concentration of 2.5 mM PNBM and 5% DMSO and allowing the lysates to react for 1-2

hours at room temperature. Following alkylation the reactions were mixed to achieve a 2:1 thiophosphorylation ratio. Proteins were resolved by SDS-PAGE and in-gel digested with modified Trypsin (Promega) or LysC (Roche). Peptides were analyzed on LTQorbitrap XL and LTQ/ETD instruments as described below.

Mass Spectrometry

Instrument Analysis

Peptides were subjected to LCMS/MS analysis on four different instruments, a QSTAR Pulsar mass spectrometer (Applied Biosystems, Foster City, CA, USA), a hybrid linear quadruple ion trap/FTICRMS (LTQFT, ThermoFisher, Bremen, Germany), a hybrid linear quadruple ion trap/orbitrap (LTQoribitrap XL, ThermoFisher, Bremen, Germany), and a LTQ/ETD instrument (ThermoFisher, San Jose, CA). These mass spectrometers were interfaced with different LC systems two microliters of samples were introduced to the LC systems through autosamplers. Typically a 3% to 40% of 0.1% formic acid in water 0.1% formic acid in acetonitrile gradient was developed in 35mins, allowing one hour of total LC analysis. The LC eluent of 350nL/mins flow was coupled to mass spectrometer with a nanospray source. On QSTAR instrument, survey scan MS took one minute followed by two MS/MS scans on the two most intense ions in the survey scan. The precursor ions were isolated in the first quadrupole with a selectivity of two m/z unit and collision-induced dissociation energy was adjusted based on the neutral loss (from the thiophosphate groups) behavior of modified peptides. Previously analyzed precursor ions were dynamically excluded from additional MS/MS scans for three minutes. On both LTQFT and orbitrap instruments, survey scans were conducted with a resolution of 50,000 in FTMS mode. Three collision-induced dissociation based MS/MS scans in LTQ

analyze the three most intense ions in the proceeding survey scan. A three-minute dynamic exclusion period was used. On LTQ/ETD, a survey scan with normal scan rate was followed by three pairs of CID/ETD analysis of the three most intense ions in the survey.

Peptide Identification and Modification Site Assignment

The raw MS/MS data were converted to peak list files in text mode and were searched against SWISS-Prot database with Protein Prospector (in house search engine) and MASCOT (Matrix Science, Boston, MA), with customized modifications for isotopically labeled thiophosphate group. In-house software (with Matlab software, MathWorks, Natick, MA) was developed to search for isotopically labeled-thiophosphorylated peptides in the high resolution survey scans of ThermoFisher instruments, such as LTQFT and LTQorbitrap. The survey scans extracted from the raw data files in profile mode were first converted to centroid mode. The centroided peak lists were deisotoped with a modified deisotoping algorithm[5]. The deisotoping procedure processed a peak list from the lightest peak and attempted to match theoretical isotope patterns with various charge states. After a match, the peak and associated isotope peaks were eliminated from further consideration. The process produced monoisotopic masses and the associated charge state and the intensity of the isotope cluster. The deisotoped peak lists were searched against any pair of ions with mass (not m/z) distance corresponding to pairs of peptides containing one or two thiophosphate modifications. The intensity ratio of the pairs can be used to distinguish alkylated cysteine or alkylated thiophosphate.

Supplemental References

1. Cho, S., Park, Y., Kim, J., Falck, J. & Yoon, Y. Facile Reduction of Carboxylic Acids, Esters, Acid Chlorides, Amides and Nitriles to Alcohols or Amines Using NaBH4/BF3 Et2O. *Bull Korean Chem Soc* 25, 407-409 (2004).
2. Dietze, P. & Jencks, W.P. Changes of Selectivity in the Reactions of Substituted 4-Nitrobenzyl Sulfonates with Nucleophilic-Reagents. *J Am Chem Soc* 111, 5880-5886 (1989).
3. Allen, J.J. et al. A semisynthetic epitope for kinase substrates. *Nat Methods* 4, 511-516 (2007).
4. Rush, J. et al. Immunoaffinity profiling of tyrosine phosphorylation in cancer cells. *Nat Biotechnol* 23, 94-101 (2005).
5. Wehofsky, M. & Hoffmann, R. Automated deconvolution and deisotoping of electrospray mass spectra. *J Mass Spectrom* 37, 223-229 (2002).

Chapter 5

Casein Kinase 2 Recognizes Plant Hormone Derived Nucleotide Triphosphates

Abstract

We interrogated the human proteome for new kinase-ATP reactions and discovered Casein Kinase 2 (CK2) accepts plant hormone-derived ATP analogs. Mutagenesis and molecular modeling and studies revealed features which distinguish CK2 from the rest of the kinome and control its affinity for ATP analogs.

Main Text

ATP (**1**) is thought to be the universal phosphodonor co-substrate for protein kinases. The conservation of the kinase-ATP reaction implies that protein kinases are not regulated through alternative nucleotides, and this commonality has created an opportunity to chemically re-code protein kinases, through a single point mutation. A single point mutation in the ATP binding produces a kinase with the ability to recognize N6 alkylated ATP analogs that are not efficient substrates of the corresponding wild-type protein kinases. Given the simplicity of engineering kinases to utilize N^6 alkylated ATP analogs (A*TPs), we considered if any kinases might naturally exhibit expanded nucleotide specificity, as a potentially unexplored form of kinase regulation. Another reason to propose ATP analogs might serve as natural ligands is that A*TPs are naturally produced metabolites of plant derived hormones, cytokinins[1], which induce diverse phenotypic effects in mammalian cells, targets are known[2]. Therefore, identification of proteins which recognize A*TPs may provide insights into the molecular mechanisms of cytokinin action and unveil an unknown code of nucleotide recognition embedded within the kinome.

To identify naturally occurring kinases with unusual ATP recognition properties, we applied tools and insights gained from engineered A*TP analog specific (*AS*) kinases.

A*TPs possess two structural permutations from the parent ATP molecule, an N^6 specificity determining element and a ^{32}P or sulfur containing γ-phosphoryl group, which enable A*TPs to serve as molecular messengers between kinase substrate pairs. For example, when *AS* Cdk utilizes N^6-benzyl [3] ATPγS (**2**), Cdk substrates are chemically differentiated from other phosphoproteins[4]. An initial indication that an endogenous kinase might recognize structurally modified nucleotides came during the course of applying *AS* kinase technology. We and others observed low levels of A*TP dependent phosphorylation even in the absence of engineered kinases[5]. In our experience with over 20 engineered kinases, A*TP analogs aren't utilized by the corresponding wild type kinases, prompting an unbiased search for the source of this activity.

We considered several potential sources of A*TP dependent background phosphorylation. One possibility is that the γ-phosphoryl label enters the nucleotide pool, producing labeled ATP which could be used by all kinases. Alternatively, one or a small subset of kinases could directly recognize A*TP. We reasoned identifying proteins which become labeled in the presence of A*TPs may help us discriminate between these possibilities. For example, if the label distributes into the ATP pool we would expect to purify an unrelated ensemble of abundant phosphoproteins. Whereas if the utilization was direct and specific we would expect to identify a select subset of substrates, which by association could lead us to the target kinase(s).

To purify proteins which become labeled in the presence of A*TPs, we applied a semi-synthetic epitope tagging approach. Cell lysate, treated with bn ATPγS, was alkylated with *p*-nitrobenzyl mesylate (PNBM) (**3**) to create the epitope for a thiophosphate ester specific antibody[3]. An abundance of labeled proteins were

visualized, purified, and identified with mass spectrometry (**Fig 1a**). Over 150 proteins were identified only in the presence of bn ATPγS (**Supplementary Table 1** online), to focus our analysis on a core set of substrates this experiment was repeated with $1/10^{th}$ the amount of input protein. Within the sub-set, transcription and splicing factors were highly enriched, and literature searches revealed 6 out of the 12 proteins were established Casein Kinase 2 (CK2) substrates, bolded in **Figure 1b**, supporting the hypothesis that a select kinase may specifically utilize bn ATPγS.

Multiple available co-crystal structures of CK2 suggest it's ATP binding pocket is unusually flexible, allowing for multiple ligand binding orientations as well as protein conformational movements[6], suggesting CK2 may be able to accommodate a bulky ATP analog. *In vitro* kinase assays confirmed the ability of CK2 to directly catalyze phosphotransfer from bn ATPγS to a protein substrate (**Fig 1c)**. CK2 also possesses the unusual property of utilizing GTP (**4**), in addition to ATP, as a phosphodonor[7]. Recently, we reported GTP suppresses A*TP utilization by non *AS* kinases[3], other strategies include ATP and kinase inhibitor addition[5]. We suspected A*TPs and GTP were targeting the same enzyme, as bn ATPγS and GTPγS yielded similar patterns of thiophosphorylated proteins (**Supplementary Figure 1** online). To further explore CK2 as the bn ATPγS utilizing enzyme in cell lysates a CK2 inhibitor, DMAT (**5**), was added in addition to bn ATPγS. DMAT strongly inhibited thiophosphorylation of the CK2 substrate, Spt5[8], (**Fig 1d**) and all cellular proteins in a dose dependant manner (**Supplementary Figure 2** online). Collectively, these experiments suggest the direct utilization of bn ATPγS by CK2 is the source of the background labeling.

We next sought to understand how CK2 may recognize A*TPs. CK2 was aligned with a number of kinases which do not utilize A*TPs unless a conserved gatekeeper residue, predicted to clash sterically with N^6 substituents, is mutated to Ala or Gly (**Fig. 2a**). Surprisingly, CK2 contains the largest gatekeeper residue found in the mammalian kinome, Phe (F113). Further, a structural alignment of CK2 and CDK2, which also contains a Phe gatekeeper but can not utilize bn ATPγS[9], illustrated the gatekeeper sidechains are superimposeable, leading us to examine additional features of the CK2 ATP binding pocket. Due to similarities among ATP binding pockets, specific kinase inhibitors are rare, the existence of relatively specific CK2 inhibitors led us to next focus on residues which pharmacologically distinguish CK2 among the kinome. Inhibitors gain selectivity for CK2 by interacting with an unusual hydrophobic groove, formed in part by V66 and I74[6], which protrude toward the ATP binding site from the β3 and β8 sheets, respectively. CDK2 contains Ala at both of these positions, and PKA, PKCδ, Src, ERK2, and GSK3β contain Ala and small residues such as Ala, Thr, and Cys at the positions corresponding to V66 and I174, respectively (**Fig 2a**).

To understand how bn ATP may discriminate between CK2 and CDK2 ATP binding pockets, we utilized molecular modeling and small molecule docking. Our model predicts bn ATP adopts a conformation that interacts favorably with the hydrophobic groove, formed in part by F113, V66, and I174, whereas this region is much less enclosed in CDK2 (**Fig 2b**). Additionally, the chemical potential of crystallographic waters in this pocket are presumably higher in CK2 than in CDK2, such that displacement of these waters by bn ATP contributes far more favorably to binding in CK2 than in CDK2. To directly test if V66 and I174 play a role in CK2-A*TP

interactions we assayed WT, V66A, and V66A/I174A CK2 with three different naturally occurring A*TP analogs. Inhibition assays were utilized because a low catalytic activity with A*TPs made it difficult to accurately determine K_m values. WT CK2 was inhibited most potently by ff ATP (**6**), less by bn ATP (**7**), and virtually insensitive to ip ATP (**8**), which is consistent with our prediction that aromatic N^6 substituents stack favorably with F113. CK2 V66A was less potently inhibited by A*TP analogs, and a double V66A/I174A mutant was completely refractive to inhibition by A*TP analogs, **Figure 2c** and data not shown. By restoring V66 and I174 to residues much more typical among the kinome we were able to significantly decrease the ability of CK2 to be inhibited by A*TP analogs.

We suspect several factors contribute to the reduced affinity CK2 mutants have for A*TPs. Most clearly, favorable hydrophobic interactions are minimized through alanine substitutions. WT CK2 has an unusual "out" hinge conformation, which helps form an enlarged purine binding plane CK2 utilizes to accommodate GTP[7]. V66 may play a role in positioning the hinge, as the hinge region in a V66A/M163L CK2 mutant aligns more closely with prototypical kinases[10], and by adopting a more typical hinge conformation CK2 mutants may less favorably accommodate A*TPs (**Fig 2d**).

The finding that CK2 recognizes A*TPs is impactful in a number of contexts. This distinguishing property could inform drug design strategies to yield more selective CK2 inhibitors. At the very least, *AS* kinase assay selectivity may be improved, as the substrates we identified, together with known CK2 substrates, represent potential false positive or dual CK2 *AS* kinase substrates. Additionally, the proteins we identified represent a rich source of potentially new CK2 substrates. For example one of our top

hits, the Paf complex subunit Ctr9, is not a reported CK2 substrate, but is known interact physically and genetically with CK2 in yeast[11], and human Ctr9 is phosphorylated *in vivo* on several CK2 consensus sites.

Our initial motivation was to discover new kinase-ATP reactions by interrogating the proteome for molecular targets of plant hormone derived cytokinin triphosphates (A*TPs). The purine bases of several of the A*TP analogs discussed in this work are naturally occurring, cell permeable, biologically active *in planta* and *in vivo*. Upon entering cells these compounds can enter general nucleotide metabolism and be converted to their ribosylated and phosphorylated forms. In the case of cytokinin induced de-differentiation of leukemic cells the biologically active form is the phosphorylated cytokinin[1]. The finding that CK2 is a target of cytokinin triphosphates may have implications for the molecular mechanisms of cytokinin action. The cytokinin kinetin (ff adenine (**9**)) rescues a splicing defect linked to the neurological disease familial dysautonomia, SAR studies indicated bn adenine (**10**) was less potent, and ip adenine (**11**) was inert[12]. This is the same trend we observed in our CK2 A*TP inhibition assays, raising the intriguing possibility that CK2 may be involved in kinetin mediated exon inclusion. CK2 can utilize A*TP analogs, albeit at a fraction of the efficiency of ATP utilization, suggesting that if a biological connection exists between A*TP analogs and CK2, inhibition may be the relevant mode of action. CK2 mutants which bind A*TPs poorly provide a unique opportunity to query this correlation

ACKNOWLEDGEMENTS

The authors are thankful to David Maltby and Aenoch Lynn for assistance collecting and analyzing mass spectrometry data, Stefania Sarno and Lorenzo Pinna for CK2 expression

constructs, Chao Zhang for assistance with alignments, Arvin Dar and Susan Slaugenhaupt for helpful conversations, and Valerie Ohman for excellent administrative assistance. This work was supported by NIH RO1 EB0001987, to K.M.S., and NIH NCRR Grants RR 01614, to ALB.

AUTHOR CONTRIBUTIONS

Jasmina Allen performed experiments and wrote the manuscript. Christopher McClendon performed modeling analysis. Beatrice Wang synthesized ff ATP. Mathew Jacobsen mentored Christopher McClendon. Robert Chalkley and Alma Burlingame provided mass spectrometry expertise. Kevan Shokat helped direct the project and write the manuscript.

COMPETING INTERESTS STATEMENT

UCSF has licensed know-how to Epitomics for commercialization of the antibody.

REFERENCES

1. Ishii, Y., Sakai, S. & Honma, Y. Cytokinin-induced differentiation of human myeloid leukemia HL-60 cells is associated with the formation of nucleotides, but not with incorporation into DNA or RNA. *Biochim Biophys Acta* **1643**, 11-24 (2003).
2. Barciszewski, J., Massino, F. & Clark, B.F. Kinetin--a multiactive molecule. *Int J Biol Macromol* **40**, 182-192 (2007).

3. Allen, J.J. et al. A semisynthetic epitope for kinase substrates. *Nat Methods* **4**, 511-516 (2007).

4. Blethrow, J.D., Glavy, J.S., Morgan, D.O. & Shokat, K.M. Covalent capture of kinase-specific phosphopeptides reveals Cdk1-cyclin B substrates. *Proc Natl Acad Sci U S A* **105**, 1442-1447 (2008).

5. Boyle, S.N. & Koleske, A.J. Use of a chemical genetic technique to identify myosin IIb as a substrate of the Abl-related gene (Arg) tyrosine kinase. *Biochemistry* **46**, 11614-11620 (2007).

6. Mazzorana, M., Pinna, L.A. & Battistutta, R. A structural insight into CK2 inhibition. *Mol Cell Biochem* (2008).

7. Niefind, K., Putter, M., Guerra, B., Issinger, O.G. & Schomburg, D. GTP plus water mimic ATP in the active site of protein kinase CK2. *Nat Struct Biol* **6**, 1100-1103 (1999).

8. Krogan, N.J. et al. RNA polymerase II elongation factors of Saccharomyces cerevisiae: a targeted proteomics approach. *Mol Cell Biol* **22**, 6979-6992 (2002).

9. Polson, A.G. et al. Kaposi's sarcoma-associated herpesvirus K-bZIP protein is phosphorylated by cyclin-dependent kinases. *J Virol* **75**, 3175-3184 (2001).

10. Yde, C.W., Ermakova, I., Issinger, O.G. & Niefind, K. Inclining the purine base binding plane in protein kinase CK2 by exchanging the flanking side-chains generates a preference for ATP as a cosubstrate. *J Mol Biol* **347**, 399-414 (2005).

11. Bandyopadhyay, S., Kelley, R., Krogan, N.J. & Ideker, T. Functional maps of protein complexes from quantitative genetic interaction data. *PLoS Comput Biol* **4**, e1000065 (2008).

12. Slaugenhaupt, S.A. et al. Rescue of a human mRNA splicing defect by the plant cytokinin kinetin. *Hum Mol Genet* **13**, 429-436 (2004).

13. Hoffman, C., Genieser, H.G., Veron, M., and Jastorff, B. Novel Synthesis of Nucleoside 5'-polyphosphates. *Bioorganic & Medicinal Chemistry Letters* **6**, 2571-2574 (1996).

Figure 1. Identification of CK2 as a bn ATPγS utilizing enzyme (**a**) HeLa lysates were assayed +/- bn ATPγS, alkylated with PNBM, and analyzed by western blot (lanes 1 and 2) and coomassie staining following immunoprecipitation (lanes 3 and 4). (**b**) Proteins identified in replicate experiments, bolded proteins are known CK2 substrates. (**c**) *in vitro* kinase assays of CK2 with ATPγS and bn ATPγS (**d**) HeLa lysates were labeled with bn ATPγS, +/- 10 μM DMAT, immunoprecipitated with α-Spt5, and visualized with α-thiophosphate ester and α-Spt5 western blot analysis.

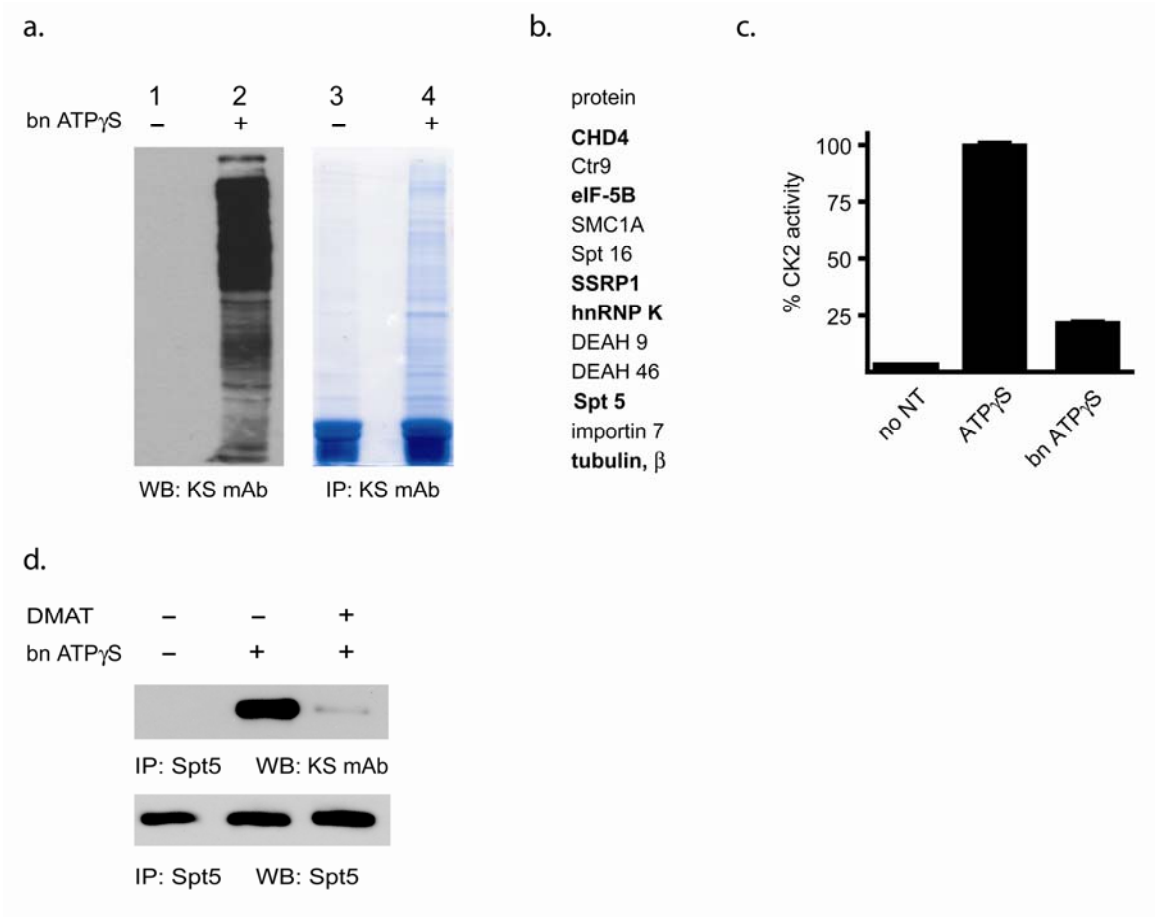

Figure 2. Features of CK2 which contribute to A*TP binding. (**a**) Alignment of CK2 with kinases that do not utilize bn ATP. Numbering indicates the residue position in CK2, residue coloring corresponds with panel **b**. (**b**) bn ATP docked to CK2. Protein atoms within 5 angstroms of the ligand are shown in surface representation. The sugar and phosphate atoms are omitted for clarity. V66, Phe113, and Ile174 are colored as in Fig. 2a. (**c**) A*TP analogs with the indicated benzyl [3], furfuryl [13], and isopentenyl (ip) N^6 moieties were assayed as inhibitors of WT and V66A CK2. IC_{50} values, with error represented as SEM, were determined by DELFIA. (**d**) Structural alignment of CK2 [8], CK2 V66A (yellow), CDK2 (purple), and Src (blue), highlighting the hinge, β-sheets, and connecting loops surrounding the ATP binding site.

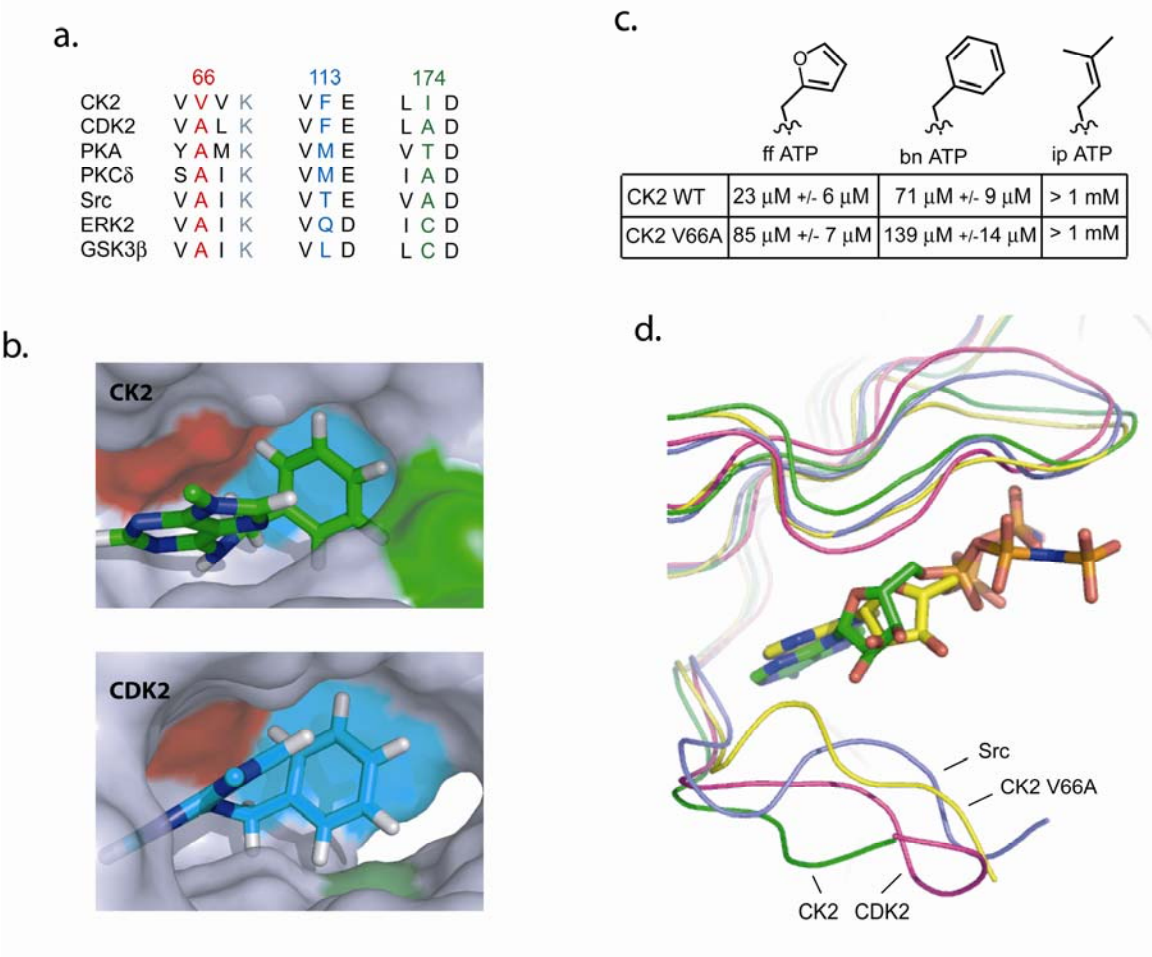

Structures of Compounds Utilized and Discussed in this Manuscript

1

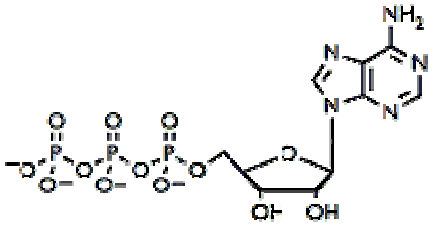

2

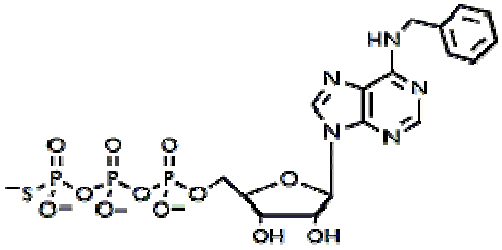

3

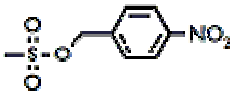

4

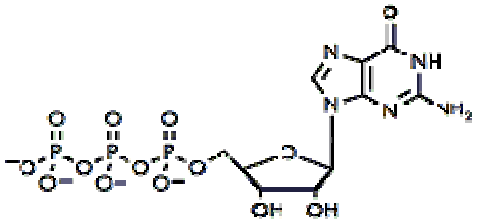

5

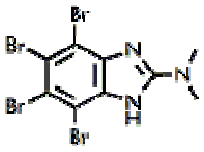

6

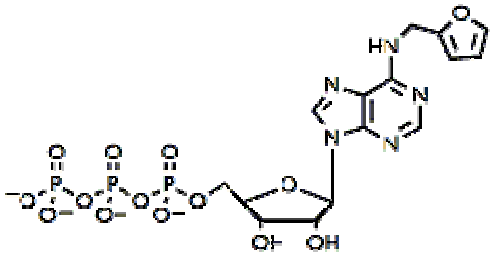

7

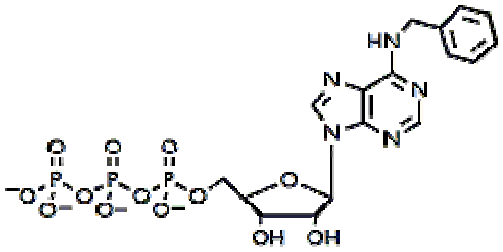

8

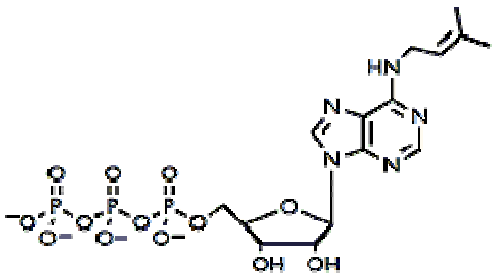

9

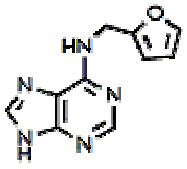

10

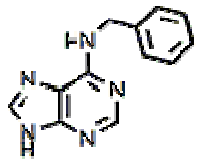

11

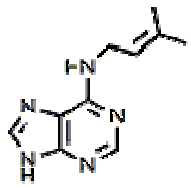

Supplementat Table 1. Proteins Identified in the Presence of bn ATPγS**.** Uniprot accession numbers, number of tandem mass spectra, and protein names are listed. Proteins are grouped by biological processes.

Acc #	# peptides	Protein Name
CHROMATIN and TRANSCRIPTION		
Q6PD62	19	RNA polymerase-associated protein CTR9
Q9NTJ3	12	Structural maintenance of chromosomes protein 4
Q9Y5B9	8	FACT complex subunit SPT16
Q13045	15	Protein flightless-1 homolog
P78347	5	general transcription factor II, i
Q9BQG0	7	Myb-binding protein 1A
Q5T626	6	nuclear autoantigenic sperm protein, histone binding
O95239	6	Chromosome-associated kinesin KIF4A
Q14683	7	SMC1A, Structural maintenance of chromosomes protein 1A
O00267	4	Transcription elongation factor SPT5
P11387	4	DNA topoisomerase 1
Q14839	3	Chromodomain-helicase-DNA-binding protein 4
A7E2E1	4	SWI/SNF related, matrix associated, actin dependent regulator of chromatin, subfamily a, member 4
Q59G16	2	SWI/SNF-related matrix-associated actin-dependent regulator of chromatin c2 isoform b variant
Q08945	2	FACT complex subunit SSRP1
Q92769	2	Histone deacetylase 2
O94776	3	MTA2, deacetylase complex
Q5UIP0	3	Telomere-associated protein RIF1
A8K281	3	cold shock domain containing E1, RNA-binding
A8KAE0	3	WD repeat and HMG-box DNA binding protein 1
P33991	5	DNA replication licensing factor MCM4
Q14566	7	DNA replication licensing factor MCM6
A8K521	3	MCM5
Q96S55	2	ATPase WRNIP1
P09874	10	Poly [ADP-ribose] polymerase 1
Q15233	8	NonO, octamer-binding
A7E2F8	3	Tankyrase 1 binding protein 1, 182kDa
P43246	2	DNA mismatch repair protein Msh2
Q4VXV9	6	Death inducer-obliterator 1
P12956	3	Lupus Ku autoantigen
A8K0Y9	2	replication protein A1, 70kDa
Q16531	2	DNA damage-binding protein 1
SPLICING and RNA METABOLISM		
Q13310	8	Polyadenylate-binding protein 4
Q2NL82	7	Pre-rRNA-processing protein TSR1 homolog
Q7L014	6	DEAD box polypeptide 46, PRP5 homolog
P52272	8	hnRNP M

Q6PKG0	5	La-related protein 1
Q15029	9	U5 snRNP-specific protein, 116 kDa
O15042	5	U2-associated protein SR140
Q9BUQ8	4	Probable ATP-dependent RNA helicase DDX23
P26599	2	Polypyrimidine tract-binding protein 1
O75400	3	Pre-mRNA-processing factor 40 homolog A
Q16630	2	cleavage and polyadenylation specific factor 6, 68kDa
A6H8W7	2	PCF11, cleavage and polyadenylation factor subunit
Q59FF0	3	EBNA-2 co-activator variant
O60231	2	Putative pre-mRNA-splicing factor ATP-dependent RNA helicase DHX16
Q92945	2	KH type-splicing regulatory protein
Q92900	3	Regulator of nonsense transcripts 1
P17844	2	Probable ATP-dependent RNA helicase DDX5
O75533	4	Splicing factor 3B subunit 1
A3RJH1	2	DEAD box polypeptide 1
Q8IYB3	2	SR-related nuclear matrix protein of 160 kDa (SSRM1)
Q15459	2	Splicing factor 3 subunit 1
Q86XP3	3	ATP-dependent RNA helicase DDX42
O43143	2	pre-mRNA-splicing factor RNA helicase DHX15
A8K964	2	similar to pinin, desmosome associated protein
A8K3W4	2	hnRNP U-like 1
A8KAQ5	2	snRNP 70kDa polypeptide
A8K6I4	2	superkiller viralicidic activity 2-like 2, helicase
A8K5W9	2	ribonuclease P/MRP subunit
A8K2E4	2	SART3

TRANSLATION

Q14152	34	eukaryotic translation initiation factor 3 subunit A
O75153	15	putative eukaryotic translation initiation factor 3 subunit
A1KYQ7	8	cell migration-inducing protein 17
Q9BY44	2	eukaryotic translation initiation factor 2A
P26640	4	valyl-tRNA synthetase
P07814	17	bifunctional aminoacyl-tRNA synthetase
P49588	4	alanyl-tRNA synthetase, cytoplasmic
A8K8I1	6	threonyl-tRNA synthetase, mRNA
P41250	4	glycyl-tRNA synthetase
P47897	5	glutaminyl-tRNA synthetase
A8K492	3	methionine-tRNA synthetase
A8KAE9	3	isoleucine-tRNA synthetase

METABOLISM

P12268	8	Inosine-5'-monophosphate dehydrogenase 2
P22102	8	Trifunctional purine biosynthetic protein adenosine-3
P23921	7	Ribonucleoside-diphosphate reductase large subunit
P17812	2	CTP synthase 1
A0AV63	5	Cytosine-specific methyltransferase
Q2TBF3	3	C-1-tetrahydrofolate synthase
A6H8Y6	2	EML4 protein
P49748	24	Very long-chain specific acyl-CoA dehydrogenase, mitochondrial precursor
Q00341	8	Vigilin, HDL-binding protein

Q01813	6	6-phosphofructokinase type C
A5PKZ6	6	Phospholipase C, beta 3
P53396	6	ATP-citrate synthase
O43175	5	D-3-phosphoglycerate dehydrogenase
A8K8L2	4	similar to tRNA methyltransferase 1
Q13085	2	Acetyl-CoA carboxylase 1
P09622	3	Dihydrolipoyl dehydrogenase, mitochondrial precursor
P11498	3	Pyruvate carboxylase, mitochondrial precursor
A6NDY6	4	Phosphorylase
PROTEIN TRANSPORT		
Q13428	11	Treacle protein TCOF1
P53621	8	Coatomer subunit alpha
P12270	8	Nucleoprotein TPR
O75694	2	Nuclear pore complex protein Nup155
O95373	3	Importin-7
Q96P70	2	Importin-9
Q14974	5	Importin subunit beta-1
Q53FR4	6	Vacuolar protein sorting 35 variant
O43747	2	AP-1 complex subunit gamma-1
O95782	2	AP-2 complex subunit alpha-1
Q15436	2	Protein transport protein Sec23A
P35606	2	Coatomer subunit beta'
A8K4K6	15	protein disulfide isomerase family A, member 4
P04843	2	dolichyl-diphosphooligosaccharide glycosyltransferase
Q14697	12	Neutral alpha-glucosidase AB precursor
P55072	7	Transitional endoplasmic reticulum ATPase
Q8IWX8	2	Calcium homeostasis endoplasmic reticulum protein
A8K6M8	4	coatomer protein complex, subunit gamma
A8K586	3	adaptor-related protein complex 3, beta 1 subunit
UBIQUITYLATION, SUMOYLATION, and PROTEOLYSIS		
A6NMY8	13	Ubiquitin carboxyl-terminal hydrolase 7
Q14694	3	Ubiquitin carboxyl-terminal hydrolase 10
Q9UBT2	2	SUMO-activating enzyme subunit 2
P49792	3	E3 SUMO-protein ligase RanBP2
O43242	4	26S proteasome non-ATPase regulatory subunit 3
Q13200	4	26S proteasome non-ATPase regulatory subunit 2
P62191	3	26S protease regulatory subunit 4
Q05CW6	2	PSMD1 protein
Q59HE3	7	Calpastatin isoform a variant
P55786	6	Puromycin-sensitive aminopeptidase
CHAPERONINS		
A1JUI8	5	Chaperonin subunit 6A
A8K402	3	TCP1, subunit 2
A8K7E6	6	TCP1, subunit 7
P50990	15	TCP1, subunit theta
A8K3C3	5	TCP1, delta subunit
P49368	7	TCP1, subunit gamma

P17987	4	TCP1, subunit alpha
A8JZY8	2	TCP1, subunit 5
CYTOSKELETON		
P52732	3	Kinesin-related motor protein Eg5
Q01082	3	Spectrin beta chain, brain 1
P27816	14	Microtubule-associated protein 4
A2BFA2	2	tubulin, beta 2C
P20700	3	Lamin-B1
Q2NKK4	2	Transforming, acidic coiled-coil containing protein 3
Q5TCU6	2	Talin 1
Q27J81	2	Inverted formin-2
A0AVD3	2	CLIP1 protein
SIGNALING ENZYMES		
Q13283	10	Ras GTPase-activating protein-binding protein 1
O15355	2	Protein phosphatase 1G
Q8TD19	2	Serine/threonine-protein kinase Nek9
A8K2V3	2	septin 9, GTP binding
Q9H2G2	4	STE20-like serine/threonine-protein kinase
P13010	6	Ku 86/80, XRCC5, DNAPK regulatory subunit
A4VCI5	2	CDC2L1 protein
OTHERS		
A8C1Z0	5	Oxigen-regulated protein 150
A4D2G6	2	Zyxin zinc binding
A8K6Y6	2	zinc finger protein 207
A4D2E6	3	Arsenate resistance protein ARS2
Q16891	2	Mitochondrial inner membrane protein
Q9BWU0	8	Kanadaptin, solute exchanger
P05023	3	Sodium/potassium-transporting ATPase subunit alpha-1 precursor
Q9NZM1	5	Myoferlin
Q4W4Y1	4	Dopamine receptor interacting protein 4
Q9BSJ8	2	Extended-synaptotagmin-1
A2BF75	2	ATP-binding cassette sub-family F
UNCHARACTERIZED		
A8MUB1	9	Uncharacterized protein TUBA4A
A6NNK5	9	Uncharacterized protein TP53BP1
A8MXP9	6	Uncharacterized protein MATR3
A8MWD3	3	Uncharacterized protein EIF3D
A8MZ70	3	Uncharacterized protein MSN
A8MQ38	2	Uncharacterized protein NOL1
A8MYX6	2	Uncharacterized protein TXNRD2
A8K008	3	cDNA FLJ78387
A6NDZ9	2	Uncharacterized protein ENSP00000269230
Q8N163	7	Protein KIAA1967, deleted in breast cancer gene 1 protein
A8K984	5	cDNA FLJ78259, ABC transporter like
Q9Y3I0	2	UPF0027 protein C22orf28
A8K559	3	cDNA FLJ76187

Supplementary Figure 1. Similar Patterns of Thiophosphorylation Result from GTPγS and bn ATPγS Treatment. Labeled proteins were visualized with α-thiophosphate ester western blot analysis.

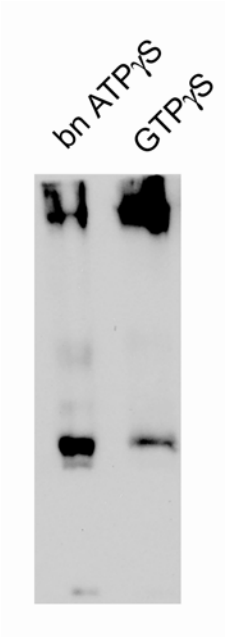

Supplementary Figure 2. A CK2 inhibitor Abolishes Labeling with bn ATPγS. HeLa lysates were labeled with 100 μM bn ATPγS, in the presence of 0, 100 nM, 1 μM, and 10 μM DMAT in lanes 1-4, respectively. Labeled proteins were visualized with α-thiophosphate ester western blot analysis.

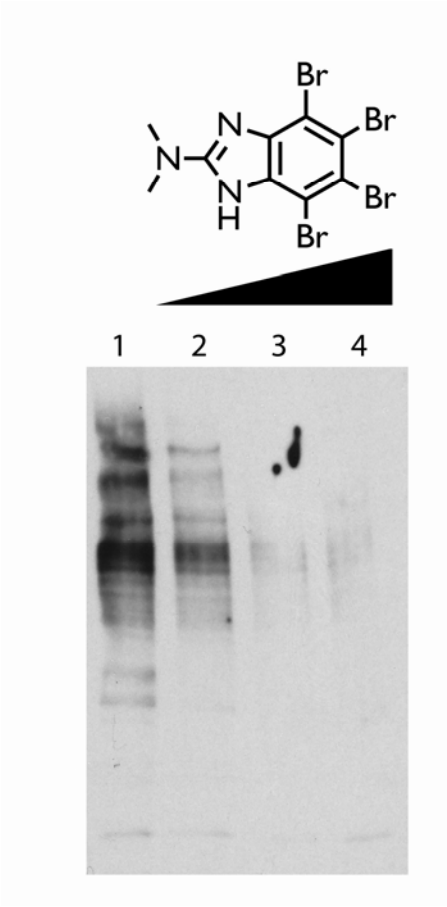

Appendix I

Supplemental Casein Kinase 2 and Cytokinin Nucleotide Data

Figure 1. CK2 Indiscriminately Utilizes a Variety of A*TPγS Analogs. Each ATPγS analog was assayed at 1 mM with recombinant wild type CK2. Phosphotransfer was measured by DELFIA, for each allele % activity with each of the analogs was scaled with respect to ATPγS. For experimental details please see Chapter 5. Each bar is labeled with the N6 moiety of the ATPγS analog used in the assay (benzyl (bn), furfuryl (ff), isopentenyl (ip), cyclopentyl (cp), and phenethyl (phe)). Error bars represent standard error about the mean.

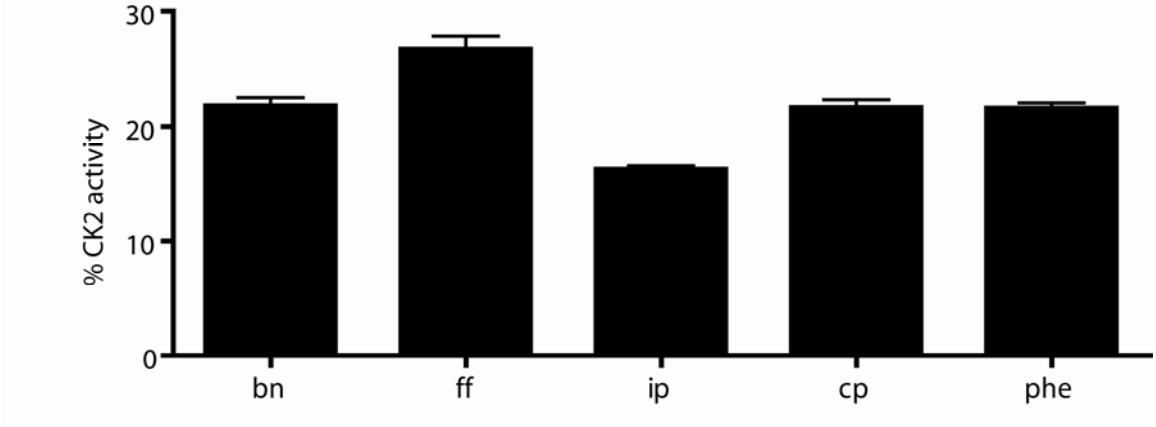

Figure 2. CK2 V66A and V66A/I17A Mutations Slightly Alter Nucleotide Utilization. Each of the CK2 alleles was assayed with ATPγS analogs containing the following N6 moieties (bn= benzyl, ff=furfuryl, ip=isopentenyl, structures are given in Supplementary Figure 2). Phosphotransfer was measured by DELFIA, for each allele % activity with each of the analogs was scaled with respect to ATPγS. For experimental details please see Chapter 5. Error bars represent standard error about the mean.

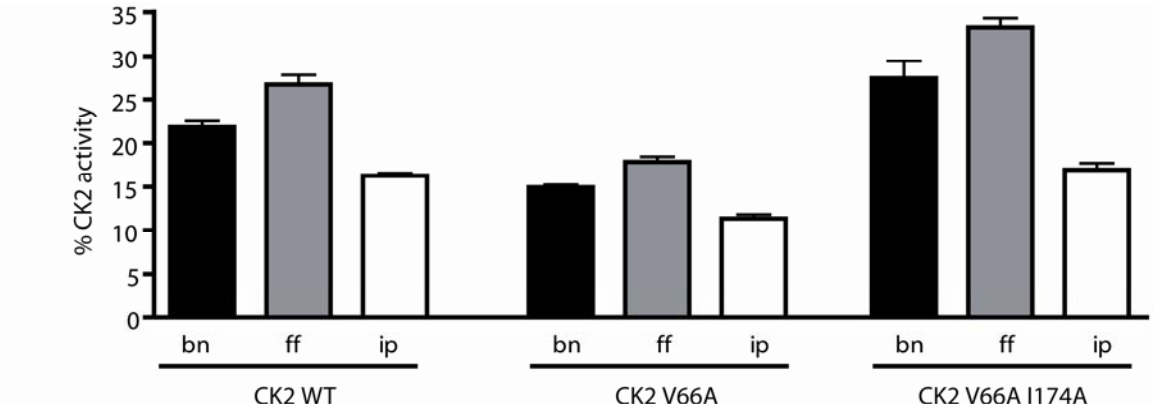

Figure 3. Immunoprecipitation of Labelled SSRM1 Peptide. CID spectra of the indicated peptide sequence. Structures indicate the observed neutral loss products. Inset, MS analysis of the isotopically labeled peptide pair. Peptides were immunoprecipitated and analyzed as described in Chapter 4.

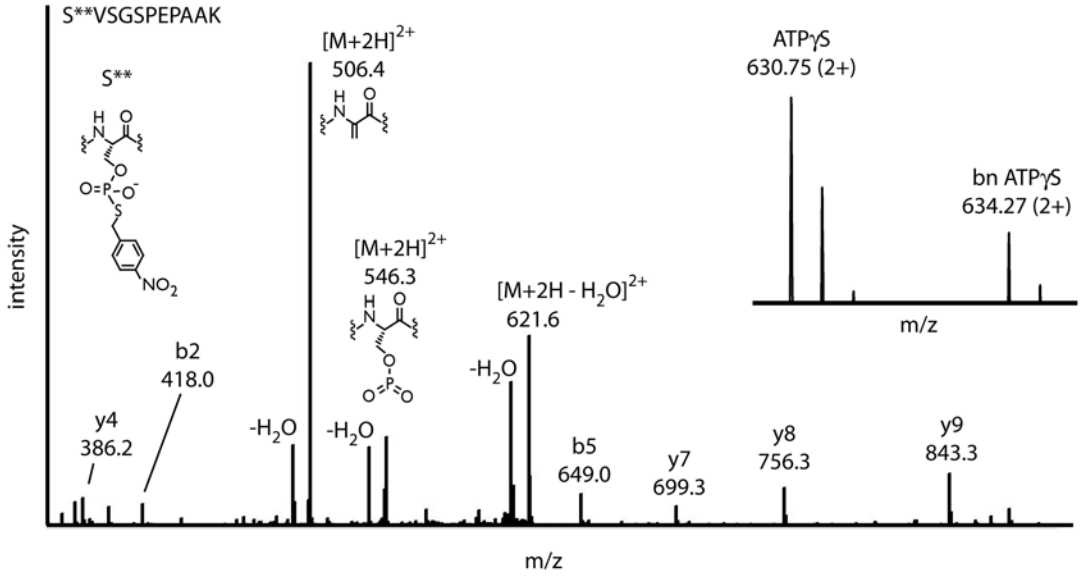

Appendix II

Protocols for Labeling Kinase Substrates in vitro and in Permeabilized Cells, Western Blot Analysis, and Immunoprecipitation

Protocol for Kinase Substrate Labeling and Western Blot Analysis

Reagents

Primary Antibody

Either rabbit polyclonal or monoclonal IgG, produced in collaboration with Epitomics. The antibody is supplied in PBS at the indicated concentration, and should be stored at 4°C after the initial thaw.

***para*–nitrobenzyl mesylate (PNBM), alkylating reagent**

The solid can be stored at 4°C. Weigh a few milligrams and add DMSO to make a 50 mM stock (MW=231 g/mol), this is a 20X stock, alkylation proceeds at 2.5 mM PNBM 5% DMSO. The 50 mM stock can be aliquoted and stored at -20°C, avoid freeze thaw cycles.

N^6 benzyl (bn)-ATPγS/ N^6 phenethyl (phe)-ATPγS/ N^6 furfuryl (ff)-ATPγS

These compounds are supplied at the concentrations indicated on the tubes. Please store the analogs at -80°C. I have noticed degradation after multiple freeze thaw cycles, so it is best to aliquot them further after the initial thaw. Shortly, they should be available from the following company.

BIOLOG Life Science Institute

Forschungslabor und Biochemica-Vertrieb GmbH

Flughafendamm 9a

D-28199 Bremen

Germany

phone: +49 421 591355

fax: +49 421 5979713

web: http://www.biolog.de

ATPγS

This can be purchased from Sigma (Catalog # A1388) as the tetralithium salt. I make a 10 mM stock and store aliquots at -80°C. Please use the same handling as for the ATPγS analogs.

Kinase Reactions Followed by Alkylation

1. Do the kinase reaction as usual. Don't include more than 0.5 mM reductant (ex DTT) in the kinase reaction buffer as it will consume the PNBM alkylating reagent. I recommend using the ATPγS analogs at 500 µM for the first set of reactions. If desired, quench reactions with EDTA (twice the concentration of metal, for example if there is 10 mM $MgCl_2$, quench with 20 mM EDTA).

2. To alkylate the proteins add 1.5 µl of the 50 mM PNBM stock directly to a 30 µl kinase reaction (or scale appropriately), to afford a final concentration of 2.5 mM, 5% DMSO. Vortex the samples after addition to mix up the buffer and DMSO and alkylate for 1-2 hours at room temperature.

*I always include a control that has PNBM but no nucleotide, tocontrol for any non-specific antibody binding.

3. After alkylation add SDS-PAGE sample buffer. At this point the samples can be stored in the freezer or analyzed immediately.

Western Blotting

1. Block for 30 minutes - 1.0 hour at room temperature with 5% Milk in TBST (Tris Buffered Saline with 0.05% Tween-20).
2. Wash the blot 1X with TBST and add the primary antibody (200-500 ng/ml in 5% Milk TBST). A couple of hours at room temperature is acceptable, but best signal is obtained after overnight incubation at 4°C. The diluted antibody may be stored in the presence of 0.01% sodium azide, stored at 4°C and utilized in several subsequent blotting applications.
3. Wash at least 3X with TBST, and add the secondary antibody (Promega goat anti-rabbit HRP (1:10,000) or other suitable anti-rabbit secondary antibody) in 5% Milk TBST.
4. Incubate with the secondary antibody at RT for 1 hour, and then wash at least 3X TBST
5. Develop with Pierce Pico Supersignal chemiluminescent detection reagent (lower level samples with Pierce Femto Supersignal) or however you typically develop blots.

Protocol for Labeling Kinase Substrates in Digitonin Permeabilized Cells

Reagent Stock Solutions

2X nuclear import buffer (1X= 20 mM Hepes pH 7.3, 100 mM KOAc, 5 mM NaOAc, 2 mM $MgOAc_2$, 1 mM EGTA)

2X RIPA (100 mM Tris pH 8, 300 mM NaCl, 2.0% NP-40, 0.2% SDS), containing 40 mM EDTA

100 mM GTP stock

100 mM ATP stock

100 mM DTT stock

10 mM N^6 derivitized ATPγS

100 mM creatine phosphate (Calbiochem Catalog # 2380)

5.7 mg/ml creatine kinase (Calbiochem Catalog # 238395)

30 mg/ml digitonin in DMSO or H_2O (1000X) (Sigma Cat#D141)

General Overview: Cells (grown in 12 well dishes for preliminary optimization labelings) are incubated in buffer that contains digitonin, an ATP regenerating system, GTP, ATP and N^6 derivitized ATPγS. After the *in situ* kinase reaction the cells are lysed, alkylated, and analyzed by western blot.

1. Grow cells to ~70-80 % confluency* in 12 well dishes. Depending on the kinase we also stimulate the cells as appropriate for the cellular phenotype we aim to measure. *The permeabilization isn't as efficient with confluent cells. If you wish to optimize the permeabilization conditions, trypan blue is an easy way to

quantify permeabilization efficiency. I found 30 µg/ml works well for mouse embryonic fibroblasts, and is consistent with literature values.

2. This is a recipe for 2.6 ml of buffer, which is sufficient for 2 x 12 well plates (100 µL per well). Scale accordingly for your desired number of reactions. If you wish to label in 10 cm plates use 500 µL per plate. I recommend optimizing nucleotide concentration, stimulation, and reaction timing in 12 well plates before scaling up, which requires the buffer to be portioned and supplemented accordingly. Add the creatine kinase, GTP, ATP, and N^6 derivitized ATPγS immediately before use.

1.3 ml	2X nuclear import buffer
26 µl	1M $MgCl_2$, final concentration is 10 mM
13 µl	100 mM DTT, final concentration is 0.5 mM
26 µl	100X Phosphatase inhibitor cocktail I (Sigma)
26 µl	100X Phosphatase inhibitor cocktail II (Sigma)
130 µl	100 mM creatine phosphate, final concentration is 5 mM
26 µl	5.7 mg/ml creatine kinase, final concentration is 57 µg/ml
138 µl	30 X (one tablet in 1.0 ml H_2O) complete protease inhibitors, EDTA free (Roche)
2.6 µl	30 mg/ml digitonin, final concentration is 30 µg/ml
78 µl	100 mM GTP, final concentration is 3 mM
2.6 µl	100 mM ATP, final concentration is 0.1 mM
26 µl	10 mM N-6-phe-ATPγS, final concentration is 0.1 mM
806 µl	ddH_20, for a final volume of 2.6 ml

3. Remove media and wash cells once with room temperature PBS.
4. Remove the PBS and add 100 µl of the above buffer.
5. Rock the plate gently, with your hands, for 1-2 minutes to disperse the buffer and let the kinase reaction proceed either at room temperature or at 37 ºC with 5% CO_2, rocking periodically.
6. Add 100 µl of 2X RIPA (100 mM Tris pH 8, 300 mM NaCl, 2.0% NP-40, 0.2% SDS) that contains, 40 mM EDTA, 5 mM PNBM, and 10% DMSO**. Therefore, the final concentration will be 1X RIPA, 20 mM EDTA, 2.5 mM PNBM, and 5% DMSO. This concurrently quenches the kinase reaction, lyses the cells, and alkylates the proteins.

**For this I make the same 50X PNBM stock as for the *in vitro* kinase reactions.

7. Place the platess on the rocker and alkylate at room temperature 1-2 hours
8. Add sample buffer (I add 50 µl of 5X), transfer into eppendorf tubes. At this point the samples may be frozen for later analysis. I usually spin the samples at 14,000 g before loading the gel, alternatively the samples may be spun before adding sample buffer.
9. Analyze by western blot as described for the *in vitro* kinase reactions.

Note: If analyzing substrates in a candidate based approach I recommend alkylating with PNBM after immunoprecipitating the candidate to avoid any interference from alkylating the antibody and/or masking the epitope.

Immunoprecipitation with the Thiophosphate Ester Specific Antibody

1. Perform kinase reactions* and alkylate with 2.5 mM PNBM, 5% DMSO. The PNBM should first be prepared as a 50 mM DMSO stock. Typical volumes for kinase reactions followed by immunoprecipitation are 1- 2 ml, containing 5-15 mg of protein. *Perform a control reaction that doesn't contain either the the kinase of interest or the ATPγS analog, the choice of control depends on the experiment.
2. After alkylation spin the lysate at 14,000 Xg, max speed on a benchtop microcentrifuge, for 5-10 minutes and discard any precipitate.
3. Remove PNBM with a PD-10 size exclusion column (Amersham) using RIPA (50 mM Tris pH 8, 150 mM NaCl, 1.0% NP-40, 0.1% SDS, and protease inhibitors (Roche, complete)) as the eluent. Collect 0.5 ml fractions.
4. Assay each fraction for protein content with a Bradford Assay. Pool peak protein containing fractions, generally fractions 7-9. Discard the final protein containing fraction as it may contain PNBM, which inhibits immunoprecipitation.
5. Bind ~ 50-100 µg 51-8 antibody to 100 µl of a 50% slurry of rProtG agarose beads (Invitrogen). Perform this binding step in 1.0 ml of PBS or RIPA for 2-5 hours at 4º C. This is for two samples, such that each will have 50 µl of beads and ~25-50 µg of antibody.
6. Meanwhile, pre-clear each sample with 100 µl of rProt G agarose for 2-5 hours at 4ºC.

7. Spin down the beads from step 6 and transfer the supernatants to a fresh tube. Save 30 μL for western blot analysis of the input samples.
8. Spin down the antibody conjugated beads from step 5, wash with 1.0 ml RIPA, and resuspend the beads in 90 μL RIPA. Add 50 μL of this 50 % slurry to each sample, affording ~ 25-50 μg of antibody per IP.
9. IP for a minimum of 2 hours and a maximum of overnight at 4ºC.
10. Wash each sample 3-5 times with 1.0 ml RIPA. Remove residual RIPA from the final wash with a gel loading pipette tip.
11. Elute immunoprecipitated proteins by boiling for 3 minutes in 30 μL sample buffer that contains reductant (ex. DTT) and analyze the immunoprecipitated proteins by SDS-PAGE.
12. Load 1 μL of the eluted samples and the input samples to determine the immunoprecipitation efficiency by western blot analysis using the thiophosphate ester specific antibody.
13. Load the remainder of the immunoprecipiatated samples and visualize with Invitrogen colloidal Coomassie, or another protein stain.

Immunoprecipitation of Candidate Protein Substrates Followed by Detection with the Thiophosphate Ester Specific

Note: This technique is useful for assaying candidate proteins as kinase substrates, whereas the protocol above is a hypothesis free method for purifying kinase substrates.

1. Perform the kinase reaction as usual, utilizing ATPγS or N^6 alkylated ATPγS as the phosphodonor.
2. Dillute the kinase reaction by adding an equal volume of 2X RIPA.
3. Immunoprecipitate with an antibody that recognizes the candidate protein of interest.
4. After washing the beads, resuspend them in 30 µL of 50 mM HEPES pH 7.5, 150 mM NaCl, 2.5 mM PNBM, 5% DMSO. The PNBM should first be prepared as a 50 mM DMSO stock.
5. Alkylate the proteins 1-2 hours at room temperature.
6. Add SDS-PAGE sample buffer and perform wester blot analysis for the candidate and for thiophosphorylation.

I hereby grant permission to the Graduate Division of the University of California, San Francisco to release copies of my thesis or dissertation to the Campus Library to provide access and preservation, in whole or in part, in perpetuity.

Author Signature

9/3/08

Date